

AD A 132078

NSWC MP 82-572

12

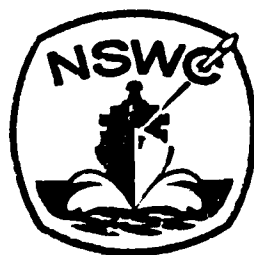
## HIGH ALTITUDE AERODYNAMIC TESTS WITH SIMULATED HEAT-SHIELD OUTGASSING

BY C. FISCINA R. VOISINET E. HEDLUND M. ROBERTS  
STRATEGIC SYSTEMS DEPARTMENT

1 DECEMBER 1982

Approved for public release, distribution unlimited.

DTIC  
ELECTE  
SEP 6 1983  
S D  
B



NAVAL SURFACE WEAPONS CENTER

Dahlgren, Virginia 22448 • Silver Spring, Maryland 20910

DTIC FILE COPY

83 08 31 01

UNCLASSIFIED

SECURITY CLASSIFICATION OF THIS PAGE (When Data Entered)

REPORT DOCUMENTATION PAGE		READ INSTRUCTIONS BEFORE COMPLETING FORM
1. REPORT NUMBER NSWC MP 82-572	2. GOVT ACCESSION NO. DND 1132075	3. RECIPIENT'S CATALOG NUMBER
4. TITLE (and Subtitle) HIGH ALTITUDE AERODYNAMIC TESTS WITH SIMULATED HEATSHIELD OUTGASSING		5. TYPE OF REPORT & PERIOD COVERED Final Report January 1982 - October 1982
		6. PERFORMING ORG. REPORT NUMBER
7. AUTHOR(s) CHARLES FISCINA, ROBERT L. P. VOISINET, ERIC R. HEDLUND, MARK M. ROBERTS		8. CONTRACT OR GRANT NUMBER(s)
9. PERFORMING ORGANIZATION NAME AND ADDRESS Naval Surface Weapons Center (Code K24) White Oak Silver Spring, MD 20910		10. PROGRAM ELEMENT, PROJECT, TASK AREA & WORK UNIT NUMBERS 11221N; J0094-SB 2K25BB
11. CONTROLLING OFFICE NAME AND ADDRESS		12. REPORT DATE 1 December 1982
		13. NUMBER OF PAGES 144
14. MONITORING AGENCY NAME & ADDRESS (if different from Controlling Office)		15. SECURITY CLASS. (of this report)  UNCLASSIFIED
		15a. DECLASSIFICATION/DOWNGRADING SCHEDULE
16. DISTRIBUTION STATEMENT (of this Report)  Approved for Public Release; Distribution Unlimited		
17. DISTRIBUTION STATEMENT (of the abstract entered in Block 20, if different from Report)		
18. SUPPLEMENTARY NOTES		
19. KEY WORDS (Continue on reverse side if necessary and identify by block number)  Heatshield outgassing High altitude simulation Side force generation Asymmetric outgassing		
20. ABSTRACT (Continue on reverse side if necessary and identify by block number) This report presents the results from the High Altitude Side Force Test conducted in the NSWC Hypervelocity Wind Tunnel at Mach 14. The objectives of the test were to provide static force and moment data as well as pressure and heat transfer distributions on typical reentry configurations with asymmetric boundary layer outgassing. The results presented herein include normal force and moment, yaw force and moment, surface pressures and surface heat transfer rate on both 7 degree and 9 degree blunt cone models. These models incorporated a circumferentially asymmetric outgassing distribution.		

UNCLASSIFIED

SECURITY CLASSIFICATION OF THIS PAGE (When Data Entered)

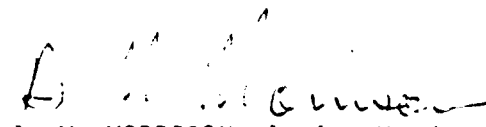
**BLANK PAGES  
IN THIS  
DOCUMENT  
WERE NOT  
FILMED**

## FOREWORD

This report presents the results from the High Altitude Side Force Test conducted in the NSWC Hypervelocity Wind Tunnel at Mach 14. The objectives of the test were to provide static force and moment data as well as pressure and heat transfer distributions on typical reentry configurations with asymmetric boundary layer outgassing. This data is to be used as a data base to aid in the development and validation of new aerodynamic computer models.

The results presented herein include normal force, pitching moment, yaw force, yaw moment, surface pressures and surface heat transfer rate on both 7-degree and 9-degree blunt cone models. These models incorporated a circumferentially asymmetric outgassing distribution.

Approved by:

  
A. M. MORRISON, Acting Head  
Weapon Dynamics Division

✓

By		
Distribution		
Availability		
Dist	Avail	Spec
A		

## CONTENTS

<u>Chapter</u>		<u>Page</u>
1	INTRODUCTION . . . . .	1
2	MODEL DESIGN . . . . .	5
	SHELL DESIGNS . . . . .	7
	SHELL CALIBRATION TECHNIQUE . . . . .	7
	DESIGN VS. ACTUAL DISTRIBUTIONS . . . . .	8
	CHARACTERIZATIONS OF ASYMMETRIC BLOWING SHELLS . . . . .	8
3	EXPERIMENTAL APPARATUS . . . . .	9
	PRESSURE INSTRUMENTATION AND CALIBRATION . . . . .	9
	HEAT TRANSFER INSTRUMENTATION AND CALIBRATION . . . . .	10
	FORCE AND MOMENT BALANCE . . . . .	10
	NITROGEN SUPPLY SYSTEM . . . . .	11
4	TESTING . . . . .	13
	TUNNEL CONDITIONS . . . . .	13
	PHASE ONE . . . . .	14
	PHASE TWO . . . . .	16
5	SUMMARY. . . . .	19
	REFERENCES . . . . .	93
	NOMENCLATURE . . . . .	95
<u>Appendix</u>		
A	TABULAR LISTING OF TEST DATA . . . . .	A-1

## ILLUSTRATIONS

<u>Figure</u>		<u>Page</u>
1	SIDE FORCE AND MOMENT DEVELOPMENT . . . . .	20
2	MACH 18 CAMPHOR MODEL . . . . .	21
3	PROOF-OF-PRINCIPLE EXPERIMENTAL RESULTS . . . . .	22
4	SCHEMATIC OF BLOWING MODEL DESIGN . . . . .	23
5	3M MATERIAL CHARACTERIZATION SETUP . . . . .	24
6	CALIBRATION CURVES FOR 3M DISKS . . . . .	25
7	RADIUS OF CURVATURE EFFECT . . . . .	26
8	UNIFORM DISTRIBUTION SHELL DESIGN (3M) . . . . .	27
9	REQUESTED DISTRIBUTION - TYPE 3 . . . . .	28
10	TYPE 3 DESIGN . . . . .	29
11	REQUESTED DISTRIBUTION - TYPE NOMINAL . . . . .	30
12	TYPE NOMINAL DESIGN . . . . .	31
13	REQUESTED DISTRIBUTION - TYPE 2 . . . . .	32
14	TYPE 2 DESIGN . . . . .	33
15	REQUESTED DISTRIBUTION - TYPE 4 . . . . .	34
16	TYPE 4 DESIGN . . . . .	35
17	PROBE SETUP . . . . .	36
18	PROBE CONFIGURATION . . . . .	37
19	EFFECT OF PROBE PRESSURE ON MEASUREMENT TECHNIQUE . . . . .	38
20	PLOT OF FLOW EFFICIENCY FACTOR . . . . .	39
21	UNIFORM MODEL - MEASURED BLOWING RATES ( $m_{TOT} = 0.466$ SCFM) . . . . .	40
22	UNIFORM MODEL - MEASURED BLOWING RATES ( $m_{TOT} = 0.7$ SCFM) . . . . .	41
23	UNIFORM MODEL - MEASURED BLOWING RATES ( $m_{TOT} = 1.4$ SCFM) . . . . .	42
24A	MEASURED BLOWING DISTRIBUTION - TYPE 3 . . . . .	43
24B	MEASURED BLOWING DISTRIBUTION - TYPE 3 . . . . .	44
24C	MEASURED BLOWING DISTRIBUTION - TYPE 3 . . . . .	45
24D	MEASURED BLOWING DISTRIBUTION - TYPE 3 . . . . .	46
24E	MEASURED BLOWING DISTRIBUTION - TYPE 3 . . . . .	47
25A	MEASURED BLOWING DISTRIBUTION - TYPE NOMINAL . . . . .	48
25B	MEASURED BLOWING DISTRIBUTION - TYPE NOMINAL . . . . .	49
25C	MEASURED BLOWING RATES - TYPE NOMINAL . . . . .	50
25D	MEASURED BLOWING DISTRIBUTION - TYPE NOMINAL . . . . .	51
25E	MEASURED BLOWING DISTRIBUTION - TYPE NOMINAL . . . . .	52
26A	MEASURED BLOWING DISTRIBUTION - TYPE 2 . . . . .	53
26B	MEASURED BLOWING DISTRIBUTION - TYPE 2 . . . . .	54
26C	MEASURED BLOWING DISTRIBUTION - TYPE 2 . . . . .	55
26D	MEASURED BLOWING DISTRIBUTION - TYPE 2 . . . . .	56
26E	MEASURED BLOWING DISTRIBUTION - TYPE 2 . . . . .	57
27A	MEASURED BLOWING DISTRIBUTION - TYPE 4 . . . . .	58

## ILLUSTRATIONS (CONT.)

<u>Figure</u>		<u>Page</u>
27B	MEASURED BLOWING DISTRIBUTION - TYPE 4 . . . . .	59
27C	MEASURED BLOWING DISTRIBUTION - TYPE 4 . . . . .	60
27D	MEASURED BLOWING DISTRIBUTION - TYPE 4 . . . . .	61
27E	MEASURED BLOWING DISTRIBUTION - TYPE 4 . . . . .	62
28	CALIBRATION SETUP . . . . .	63
29	CALIBRATION OF TYPICAL TRANSDUCER . . . . .	64
30	REPEATABILITY OF CALIBRATION . . . . .	65
31	EXTRAPOLATED CALIBRATION CURVE . . . . .	66
32	COMPARISON OF EXTRAPOLATED TO ACTUAL CALIBRATION . . . . .	67
33	SCHEMATIC OF GARDON GAGE INSTALLATION . . . . .	68
34	SCHEMATIC OF GARDON GAGE CALIBRATION SETUP . . . . .	69
35	FORCE BALANCE . . . . .	70
36	NITROGEN SUPPLY SYSTEM . . . . .	71
37	TIMING FOR CHANGING MASS FLOW RATES . . . . .	72
38	INSTRUMENTATION LOCATIONS . . . . .	73
39	PRESSURE VS S/RN . . . . .	74
40	INDUCED PRESSURE VS AXIAL STATION . . . . .	75
41	ST/ST <sub>0</sub> VS S/RN - UNIFORM DISTRIBUTION . . . . .	76
42	COMPARISON OF EXPERIMENT TO THEORY (SYMMETRIC BLOWING) . . . . .	77
43	COMPARISON OF EXPERIMENT TO THEORY (SYMMETRIC BLOWING) . . . . .	78
44	NFC VS $\alpha$ - 70° CONE . . . . .	79
45	PMC VS $\alpha$ - 70° CONE . . . . .	80
46	X <sub>cp/l</sub> VS $\alpha$ - 70° CONE . . . . .	81
47	NFC VS $\alpha$ - 90° CONE . . . . .	82
48	PMC VS $\alpha$ - 90° CONE . . . . .	83
49	X <sub>cp/l</sub> - 90° CONE . . . . .	84
50	SIDE FORCE COMPARISON . . . . .	85
51	SIDE MOMENT COMPARISON . . . . .	86
52	INDUCED PRESSURE VARIATION . . . . .	87
53	ST/ST <sub>0</sub> VS PHI - TYPE 4 . . . . .	88
54	COMPARISON OF EXPERIMENT TO THEORY (ASYMMETRIC BLOWING). . . . .	89

## TABLES

<u>Table</u>		<u>Page</u>
1	TEST MATRIX . . . . .	90
2	ACTUAL OUTGASSING RATES . . . . .	91

## CHAPTER 1

## INTRODUCTION

Understanding, modeling and predicting the accuracy of high performance reentry systems have been the goals of a number of recent programs throughout the strategic community. One area which has been identified as a result of such studies is the ability to predict with confidence, the high angle-of-attack performance of vehicles reentering the earth's atmosphere in the altitude regime between 400,000 and 100,000 feet. The earliest investigators applied the method of Newton<sup>1</sup> in order to predict the aerodynamics of meteorites and man-made vehicles as they passed through the high altitude regime. The requirement for increased accuracy in predicting high altitude performance led to the development of more complex techniques.<sup>2,3,4</sup> Investigators also noticed anomalous aerodynamic effects in ground and flight experiments.<sup>5,6</sup> The referenced flight test experience involved two tests of the English Black Knight Reentry Vehicle. These were the RVs of BK09 and BK18. Both vehicles were  $12\frac{1}{2}^\circ$  half-angle blunted cones with 15.4-inch diameter bases and 2-inch radius noses and nominal hypersonic static margins of 1.5 inches. The heatshield was composed of phenolic resin reinforced with asbestos flock. RV-BK09 was also painted with Araldite to prevent outgassing affecting a sensitive pressure gage used to initiate the reentry boost motor. RV-BK09, flown in 1960, reentered at a speed of 15,000 fPS, experienced a dynamic instability at 140,000 feet which grew until the vehicle became dynamically unstable and subsequently broke up at 70,000 feet. The reentry vehicle also experienced windward meridian temperatures that would cause

<sup>1</sup>Zahm, A. F., "Superaerodynamics," Journal of the Franklin Institute, Vol. 217, 1934, pp. 153-166.

<sup>2</sup>Tsien, H. S., "Superaerodynamics, Mechanics of Rarefied Gases," Journal of the Aeronautical Sciences, Vol. 13, 1946, pp. 653-664.

<sup>3</sup>Adams, M. C., and Probst, R. F., "On the Validity of Continuum Theory for Satellite and Hypersonic Flight Problems at High Altitudes," Jet Propulsion, Feb 1958, pp. 86-89.

<sup>4</sup>Tan, H. S., "Nose Drag in Free-Molecular Flow and Its Minimization," Journal of the Aerospace Sciences, Jun 1959, pp. 360-365.

<sup>5</sup>Ericsson, L. E., "Effect of Nose Bluntness on the Hypersonic Unsteady Aerodynamics of an Ablating Reentry Body," J. Spacecraft and Rockets, Vol. 4, No. 6, Jun 1967, pp. 811-813.

<sup>6</sup>Waterfall, A. P., "Effect of Ablation on the Dynamics of Spinning Reentry Vehicles," J. Spacecraft and Rockets, Vol. 6, No. 9, Sep 1969, pp. 1038-1044.



the Araldite paint to char and inject mass into the vehicle boundary layer at an altitude of 140,000 feet. The RV-BK18 was flown to check some of the problems raised by RV-BK09. It was instrumented extensively and excellent quality data was obtained. The BK18 was not painted with Araldite. No dynamic effects were exhibited in the region where BK09 experienced dynamic instabilities. At about 85,000 feet vehicle dynamics caused a divergence in the angle-of-attack. The altitude where ablation of the phenolic afterbody heatshield was expected is at 85,000 feet. Six-degree-of-freedom trajectory simulation of BK18 and BK09 was attempted post flight. Agreement with flight-observed performance could be obtained in the regions of observed dynamic instability only when a Magnus-like term was included in the equations of motion. The size of the required Magnus term was much too large to be physically explained as a classical Magnus phenomena. It was, therefore, proposed that the source of the Magnus-like term was an out-of-plane pitching moment associated with the charring or ablation of the Araldite phenolic heatshield.

The injection of mass into the boundary layer of a reentry vehicle traveling at high speed can influence aerodynamic forces by altering both the skin friction and boundary layer displacement induced pressure effects. The combined effects of mass addition, spin and angle of attack can produce a mechanism which can lead to out-of-plane forces and moments as illustrated in Figure 1. The windward side of the reentry vehicle would first experience the temperature and pressure necessary to induce mass addition. Once the reentry vehicle heatshield experienced these conditions, a finite period of time would be required for the material to respond and eject mass. In the case of a spinning reentry vehicle this material lag would cause the rate of mass addition to be higher on one side of the vehicle than the other, in that, as an outgassing ray moves to the lee ray, the temperature and pressure decrease, as does the rate and magnitude of mass addition. The differential mass addition rate and magnitude causes the side with the higher mass addition to have a thicker boundary layer. The boundary layer asymmetry leads to an induced pressure force and moment. The resultant force acts in a direction opposite to that of a classical Magnus force.

In general, the aerodynamic shear associated with a thin boundary layer is larger than associated with a thicker boundary layer. A shear couple, therefore, also results due to the longitudinal shear differential associated with the high and low mass addition sides of the vehicle. Radial shear differential would also create a couple opposing roll.

Early tests of ablating and nonablating spherically-blunted cone models were conducted at Mach 18 in the Naval Surface Weapons Center Hypervelocity Research Tunnel.<sup>7</sup> Details of the configuration tested are shown in Figure 2. Camphor was used as an ablating material and model shells were fabricated with a 0.32-cm layer of camphor covering 86.9 percent of the body length. An aluminum shell was fabricated for the nonablating model. A steel nosetip was

<sup>7</sup>Ragsdale, W. C., and Horanoff, E. V., "Investigation of a Side Force Due to Ablation," J. Spacecraft and Rockets, Vol. 16, No. 9, Sep 1978, pp. 1010-1011.

used for the ablating models as well as the nonablating model to avoid shape change effects in the region of highest aerodynamic heating. Static force measurements were made with a four-component strain gage force balance which was designed for the test program and incorporated a mechanism for spinning the models.

The test procedure was to spin the model to the desired rate while bringing the wind tunnel supply pressure and temperature to the run condition. During this start-up period, the model was kept in a retracted position in the test cell of the open-jet wind tunnel. When the run conditions were achieved, the model was injected into the tunnel flow and force data were recorded, while the angle of attack was swept at a rate of roughly 1.5 deg/s up to a maximum value which depended on the tunnel supply pressure. During most of the ablating model tests, the sweep was halted for a few seconds at 10 and 25 deg angle of attack to look for possible transient effects. After completing the data sweep, it was necessary to return the model to a small angle of attack before retracting it from the tunnel flow. As a result, the amount of camphor ablated during the data sweep could not be determined. Usually, all the camphor was ablated during the wind tunnel run and shutdown process. Observation via a television monitor indicated that the camphor-coated portion of the models remained fully coated throughout the data sweep. Models examined after two aborted runs indicated that roughly 20-30 percent of the camphor could have ablated prior to the data sweep as a result of exposure to the low-pressure test cell environment.

The side force data obtained from the wind tunnel experiments are given in Figure 3, as plots of yaw force coefficient  $C_y$  vs. angle of attack. Data taken during the pauses in the angle-of-attack sweeps at 10 and 25 deg agreed very well with the data taken during the continuous pitch sweeps, thereby verifying the sweeping technique. Comparisons made among data from ablating and nonablating model experiments clearly indicated a significant side force due to ablation. The ablating model data also indicated that the side force is a strong function of the angle-of-attack, nonlinear up to about 10 deg and linear at higher angles. Data was gathered at spin rates between 1 and 7 rps. For camphor ablation at the test conditions reported here, the side force due to ablation was independent of spin rate at speeds greater than 1-2 rps for angles of attack up to 25 deg.

The shape change effects and the inability to characterize the mass addition parameters of the camphor during the experiment classify these results as qualitative. They do, however, provide a proof-of-principle demonstration of the ablation lag effect.

The purpose of the current test program was to test models with which the heatshield outgassing could be correctly modeled and accurately characterized. In addition to making measurements of static forces and moments; surface pressure and heat transfer distributions would also be obtained.

## CHAPTER 2

## MODEL DESIGN

Two different nonspinning model bodies were used in this test program. One model body was used for the pressure/heat transfer portion of the test and had provisions for holding the necessary pressure transducers and Gardon gages. The second model body was used for the portion of the test where aerodynamic forces and moments were measured and incorporated an internally mounted strain gage balance. Both models were designed with an internal passageway through which pressurized nitrogen was fed and then used for heatshield outgassing.

Six porous model shells were built which would fit over either of the two model bodies. Two of these had a uniform outgassing distribution, both axially and circumferentially, while the other four shells had asymmetric outgassing distributions. The exact distributions will be discussed later.

Of the two shells with uniform distributions, one was constructed from a sheet of KenDan Varaperf.<sup>8</sup> This is simply a sheet of stainless steel of 0.024-inch thickness with 450 evenly spaced 0.005 inch-diameter holes per inch. The sheet was rolled into a conical shape, thus providing a uniform outgassing distribution when internally pressurized to a valve that ensures that the orifices are choked. The magnitude of this outgassing can be described by the following equation, which defines the flow through a choked orifice:

$$\dot{m} \text{ (lbm/sec)} = \frac{0.532 P_o A_*}{\sqrt{T_o}} \quad (1)$$

where:

$P_o$  = upstream pressure (psia)

$A_*$  = orifice area (in<sup>2</sup>)

$T_o$  = upstream temperature (°R).

The second uniform shell and the four with asymmetric outgassing were constructed from 3M Porous Structures Grade 15. This material is supplied in large sheets from which a number of disks were cut, epoxied together and machined to yield a conical shaped shell with a hollow interior. Figure 4 shows a schematic of the structure of a typical porous shell.

<sup>8</sup>Dannenberg, R. E., Weiberg, J. A., and Gambucci, B. J., Perforated Sheets as the Porous Material for a Suction-Flap Application, NACA TN 4038, May 1957.

Instead of a spinning body producing the asymmetric heating, the outgassing distribution was modeled by varying the shell wall thickness both circumferentially and axially. In order to determine what wall thicknesses were required, it was first necessary to characterize the material. This characterization consisted of determining the relationship between outgassing magnitude and pressure drop through the material.

The material characterization was accomplished by mounting a disk of the material in a holder as shown in Figure 5. The sample holder was placed in a vacuum chamber to simulate the lower external pressures which would be experienced in the wind tunnel tests. An air line fed the sample holder through a mass flow meter. In the side of the sample holder was a pressure tap used to measure the internal pressure. By measuring the mass flow into the sample holder at various internal pressures, it was found that the material response could be described by equation (2)

$$\Delta P^2 = C \left( \frac{\dot{m}}{A} \right)^s t \quad (2)$$

where:

$$\Delta P^2 = (P_{\text{internal}})^2 - (P_{\text{external}})^2$$

$$\frac{\dot{m}}{A} = \text{mass flow rate per unit area (lbm/ft}^2\text{-sec)}$$

$$t = \text{sample thickness}$$

$$s = \text{exponent (equal to 1.0)}$$

$$c = \text{constant.}$$

Figure 6 shows the results of this calibration for samples of two different porosities.

The next step in the material characterization was to account for the curvature of the shell walls in the thickness calculations. Figure 7 is a diagram of a portion of the shell showing that the internal pressure acts over a smaller inside surface area than the external surface area. This effect can be described by equation (3)

$$A_1/A_2 = \frac{(R - t) d\theta}{R d\theta} = \frac{(R - t)}{R} \quad (3)$$

From continuity we know:

$$\dot{m}_1/A_1 = \dot{m}_2/A_2 \left( \frac{R}{R - t} \right) \quad (4)$$

Combining equations (4) and (2):

$$\Delta P^2 = C \left( \frac{\dot{m}}{A_2} \cdot \frac{R}{R - t} \right)^s t \quad (5)$$

For this test program it was desired to calculate wall thicknesses for a given  $\Delta P^2$  and mass flow rate. This was accomplished by using the following relations:

$$\frac{t}{R - t} = \left( \frac{\Delta P^2}{(C) \left( \frac{m}{A} \right) (R)} \right) = A \quad (6)$$

$$t = \frac{AR}{1 + A} \quad (7)$$

## SHELL DESIGNS

The first two model shells were designed to have a uniform outgassing distribution of 0.00115 lbm/ft<sup>2</sup>-sec. For the Varaperf model shell, equation (1) was applied to calculate the required internal pressure to produce this mass flow rate with sonic conditions in the orifices. For the shell constructed from the 3M material, a more complex procedure was required. First, it was necessary to select a value for  $\Delta P^2$  which was high enough so that small variations in external pressure would not affect the mass flow through the shell significantly. Then, using this value of  $\Delta P^2$ , the desired mass flow rate and the local radius, the shell could be designed to give a uniform outgassing rate.

Figure 8 shows the resulting design for a  $\Delta P^2$  of 30 (psia)<sup>2</sup>. As can be seen, even though a uniform axial distribution is desired, the wall thickness must increase with axial distance to compensate for the increasing radius of the cone as described above by equation (4).

The requested distributions and resulting designs for the asymmetrically outgassing shells are shown in Figures 9 through 16. These shells were designated as Type 3, Type Nominal, Type 2 and Type 4. The first three were for sphere-cone shells with a 7° half-angle and 0.22 bluntness ratio ( $R_n/R_b$ ) and the type 4 shell was a 9° cone with a bluntness ratio of 0.08.

## SHELL CALIBRATION TECHNIQUE

After the model shells were designed and constructed it was necessary to measure the actual outgassing rates to insure an accurate simulation of the required distributions. This task was complicated by the extremely small magnitudes of outgassing that it was necessary to measure (on the order of 10<sup>-4</sup> lbm/ft<sup>2</sup>-sec).

The technique that was finally used was developed specifically for this test but could be used for any task where measurements of small mass flow rates were required. First, the model shell to be calibrated was placed in a vacuum chamber so that the external pressure could be reduced to values that would be expected in the actual testing. Figure 17 shows a schematic of the calibration setup.

Three probes were designed which would be used to measure the outgassing at specific axial locations on the model surface and a schematic of this probe is shown in Figure 18. One side of a differential pressure transducer was connected to the side of the probe and the other side of the transducer was open

to the vacuum chamber pressure. The top of the probe was connected to a vacuum pump through a calibrated sonic orifice, used as a mass flow measuring device, and a needle valve. By adjusting this needle valve, the pressure inside the probe could be made equal to the test cell pressure as indicated when the output of the differential transducer was zero. Matching these pressures eliminates the need for a seal around the probe because with no pressure differential there is no leakage into or out of the probe and the probe can just rest on the model surface (see Figure 19). The flow rate of the air passing through the area covered by the probe is subsequently determined by measuring the pressure upstream of the calibrated sonic orifice and using equation (1). A calibration coefficient,  $C_f$ , was determined for the probe by comparing the mass flow per unit area measured by the probe to the total mass flow into the model divided by the model surface area. This was done at several different values of total mass flow and a calibration curve was developed for the probe system and is shown in Figure 20. A curve fit through this data was used to correct the mass flow measurements from the probes. Therefore, for a given measurement of the upstream orifice pressure, a correction factor is determined and the actual mass flow rate per unit area can be calculated by the following equation:

$$\frac{\dot{m}}{A} \left( \frac{\text{lbm}}{\text{ft}^2 \cdot \text{sec}} \right) = \frac{.532(P_0)(A^*)}{\sqrt{T_0} (A \text{ probe})} C_f. \quad (8)$$

#### DESIGN VS. ACTUAL DISTRIBUTIONS

Figure 21 illustrates the characterization of the mass flow rates along the 3M model shell designed to have a uniform blowing distribution. The total mass flow into the model was measured by the flow meter as a 0.466 standard cubic feet per minute (SCFM). Dividing by the surface area of the model, this measurement corresponded to a mass flow per unit area of  $4.25 \times 10^{-3} \text{ lbm/ft}^2 \cdot \text{sec}$ . Figure 21 shows the locally measured mass flow rates for three axial stations along four circumferential rays. Figure 22 and 23 show the same type of plot for total mass flows of 0.7 SCFM and 1.4 SCFM, respectively. As can be seen, there is very good agreement between the measurement derived from the probes and that of the mass flow meter. The maximum difference was approximately  $\pm 10$  percent.

#### CHARACTERIZATIONS OF ASYMMETRIC BLOWING SHELLS

After successfully demonstrating the probe technique on the uniform blowing models, measurements were then taken on the models designed to produce asymmetric blowing distributions. The same probes used for the uniform blowing shells were used here. In addition, a fourth probe was constructed to make measurements at an axial station closer to the nose of the model. The four probes were all designed to fit the  $7^\circ$  cone shells but there was no difficulty in using them to calibrate the one  $9^\circ$  cone shell used here also.

Figures 24 through 27 illustrate the predicted and measured blowing characterizations for the four asymmetric blowing models, respectively. The figures show the high and low blowing rays of each model as well as the circumferential distributions at the four axial stations. There was excellent agreement between the measured rates and the design rates, with an error of no more than  $\pm 10$  percent.

## CHAPTER 3

## EXPERIMENTAL APPARATUS

## PRESSURE INSTRUMENTATION AND CALIBRATION

As was described earlier, one of the major objectives of this test program was to measure the surface pressures on the models under simulated high altitude conditions. Due to this simulation of high altitudes, the surface pressures were expected to be extremely small. Lee-side pressures were expected to be as low as 0.001 psia.

The pressure transducers selected for this test were Microswitch model 130 PC which were solid state, piezoresistive transducers with a 0.625-inch square base and a height of 0.8125 inches. The sensing element is a 0.1-inch square silicon chip with a sensing diaphragm and four piezoresistors. When a pressure is applied, the diaphragm flexes, changing the resistance. This results in an output voltage proportional to the applied pressure. This transducer had a range of 0-15 psia.

Because the expected pressures were so low and the Microswitch transducers have a much higher rated pressure, a calibration setup was utilized to check the transducers for linearity and repeatability in the low pressure regime, below 0.2 psia. This setup, shown in Figure 28, incorporated a vacuum pump, bell jar and two low pressure standards (a Universal mercury manometer and a McLeod gage).

The pressure range of greatest importance in this test was from 0.001 psi to 0.067 psi. Figure 29 shows the initial linearity check of a random Microswitch transducer versus data acquisition system counts (DARE counts). DARE counts are an artificial measurement of the transducer voltage output. During the calibration, the system was pumped down and measurements were taken. The system was then vented to atmospheric pressure and the procedure was repeated to assure no transducer hysteresis. A more detailed calibration at lower pressures (Figure 30) showed the good repeatability and linearity of this Microswitch transducer.

The Microswitch transducers were also linear over the range 0.001 psi to 0.4 psi (Figure 31). The impact of this fact was two-fold. First, a wide range of pressures could be measured accurately during one test. More importantly, an accurate calibration could be accomplished immediately prior to a wind tunnel run. Traditionally, an in-site calibration of each transducer is performed prior to a run by taking discrete measurements as the wind tunnel is being evacuated. In certain cases, however, the pressure to be measured during a test is lower than the lowest pressure attained during tunnel evacuation. For a low-pressure case, an accurate calibration can be made down to the minimum evacuation pressure and the slope must be extrapolated to the low pressure range

of interest. The extrapolation of the slope of a Microswitch transducer compared very favorably with test measurements (Figure 32).

In this test, the excitation voltage was limited to seven volts during a run. The sensitivity of the transducer with seven volts excitation is 0.0003 psia per DARE count. Standard deviations obtained during calibration were  $\pm 3$  DARE counts (0.001 psia). Therefore, the uncertainty in the measurement of pressures in the 0.001 psia range was high, but higher pressures, as on the windward side of a model, can be measured quite accurately.

#### HEAT TRANSFER INSTRUMENTATION AND CALIBRATION

Gardon gages were used to measure the heat transfer rates on the model surface in this test. Figure 33 shows a typical Gardon gage and how it is installed in a standard model. For use in the 3M porous models, another copper sleeve was press fit in the model. A wire was then soldered to the extra sleeve to allow for the gage to be grounded.

Figure 34 shows the calibration setup for the Gardon gages. A quartz lamp is placed over the gage at a precise distance. The lamp has been calibrated so that the heat transfer rate is known for that distance above the gage. The output of the gage is amplified and used to generate a sensitivity coefficient for the gage in BTU/ft<sup>2</sup> -sec per m.v.

#### FORCE AND MOMENT BALANCE

Another of the major objectives of this test program was to measure the side forces developed due to asymmetric heatshield outgassing. Pre-test predictions indicated that these side forces would be extremely small, as small as 0.005 lbs. In order to be able to accurately measure forces of this magnitude, it was necessary to construct a special force balance. Not only would this balance need to be extremely sensitive but an additional requirement was that it be made with a hollow center to allow the nitrogen to be used to simulate the heatshield outgassing to pass through it. Figure 35 shows a diagram of the balance constructed for this test.

The balance was made to measure four components of the aerodynamic loads. These were normal force, pitching moment, side or yaw force and yaw moment. As can be seen, the gage sections were very thin, as the thickness determined the sensitivity of the balance. Additionally, the gages intended to measure the yaw forces and moments were placed on sections that are much thinner than those for the normal forces. This was done since the normal forces were expected to be two orders of magnitude greater than the yaw forces.

In addition, very sensitive semi-conductor gages were used. These gages have approximately 60 times more output than the commonly-used foil gages for the same loads.



## NITROGEN SUPPLY SYSTEM

In order to simulate heatshield outgassing, nitrogen gas was fed to the model through the sting and then out through the porous model shell. The gas supply system was not only required to supply a specified mass flow rate, but to supply three different rates to the model during each run. Figure 36 shows a schematic of the system used for this test. Two individually adjustable supply lines were connected to the model through a manifold. Each line could be shut-off separately through a solenoid operated valve.

Prior to a tunnel run, each line would be opened separately and adjusted to a specific mass flow rate. A pressure transducer inside the model shell was used to determine the mass flow rate through the model based on the shell calibrations described earlier.

The solenoid valves were connected to the tunnel sequencer which was programmed to open each valve at a pre-determined time during a tunnel run.

After the tunnel was started, the data system was started. After 2 seconds, the first valve was opened feeding the model with the first mass flow rate. Five seconds later the first valve was closed and the second valve was opened, thus supplying the model with a second, higher blowing rate. Data was recorded for 12.5 seconds, after which the second valve was closed and the tunnel shut down.

This technique was used so that both the blowing and non-blowing data were recorded in one tunnel run for each angle-of-attack. This eliminated the effects of run-to-run differences in tunnel operating conditions.

Figure 37 shows a typical plot of the output of the internal pressure transducer. Not only does it indicate when blowing rates were changed, but it also shows when steady conditions were reached. This information was later used in the data reduction so that only data recorded during steady conditions was examined.

## CHAPTER 4

## TESTING

## TUNNEL CONDITIONS

The Hypervelocity Wind Tunnel (HWT) is a blow-down facility that is designed to generate flows at either Mach 10 or Mach 14. It has a 5-foot diameter test cell which facilitates the use of relatively large models. Traditionally, the tunnel is operated with supply pressures of 3000 psia to 20,000 psia which produces altitude simulations of approximately 50,000 feet. As the purpose of this test was to investigate effects that occur at altitudes above 200,000 feet, the tunnel was adapted to run at much lower supply pressures (100 to 300 psia). This reduction in supply pressure produced conditions equivalent to approximately 200,000 feet.

In general, the tunnel operates by heating and pressurizing a fixed volume of gas, nitrogen, and then blowing this gas down through either a Mach 10 or Mach 14 nozzle. Therefore, in addition to increasing the altitude simulated, the reduction in supply pressure also lengthened the run time of the tunnel from approximately 1 second to about 28 seconds at the 300 psia supply pressure.

For all but one of the runs in the test program, the tunnel was operated with the following conditions:

Supply pressure	: 300 psia
Supply temperature	: 2000° F
Mach number	: 13
Dynamic pressure	: 0.14 psia
Free-stream velocity	: 5500 ft/sec
Re/ft	: 120,000
Knudsen number	: 0.032
Run time	: 28 seconds

The other run was made at the following tunnel conditions:

Supply pressure	: 100 psia
Supply temperature	: 1500° F
Mach number	: 13
Dynamic pressure	: 0.065 psia
Free-stream velocity	: 4600 ft/sec
Re/ft	: 90,000
Knudsen number	: 0.035
Run time	: 15 seconds

The testing was divided into two phases. Phase 1 consisted of measuring surface pressure and heat transfer rates on the two uniform outgassing model shells. Phase 2 included force and moment measurements as well as pressure and heat transfer measurements on the four asymmetric outgassing shells. Table 1 shows the test matrix and Table 2 shows the actual blowing rates used in both phases.

#### PHASE ONE

This phase of the test consisted of six runs on the two shells with uniform outgassing distributions discussed earlier, four runs with the 3M shell and two runs with the Varaperf shell. All six runs here were made with the model at zero angle of attack. Measurements were made of surface pressures at 24 locations around the body. Figure 38 shows the locations of the pressure instrumentation. The models were also instrumented with 8 Gardon gages, 4 on the windward ray and 4 on the leeward ray.

The use of two model shells made of different materials allowed a comparison to be made of the effect that the manner of outgassing has on the resulting induced pressures and heat transfer rates. For the same magnitude of outgassing on each shell, the Varaperf shell was expected to have a higher injection velocity than that of the 3M shell. This higher injection velocity is due to the Varaperf material having individual holes acting as sonic orifices while the 3M material is a porous structure with a large number of micropores.

The secondary objective of this phase of the testing was to evaluate the effectiveness of the pressure and heat transfer instrumentation. To this end, one run was made at a supply pressure of 100 psia to determine if the extremely low values of pressure and heat transfer expected could be measured accurately. The remaining five runs were conducted at the 300 psia supply pressure conditions. Results from this comparison indicated that measurements could be made at the 100 psia conditions but that better data accuracy could be obtained at the slightly higher supply conditions. As a result, the remainder of the testing, both in phase one and phase two, was conducted at the 300 psia conditions.

Figure 39 shows the results of pressure measurements made before turning on the model blowing. A comparison is made between measurements on the Varaperf and 3M shells and two computer predictions. As can be seen, the data agrees very well with the LMSC code. This is the code currently under development that this data will be used to validate. In addition to the agreement with the code, the data indicates very good repeatability between runs. This result shows that the pressure instrumentation is suitable for making measurements in this high altitude simulation regime.

Figure 40 shows the effect that different outgassing rates have on the pressure distribution along the body. Shown here is the change in surface pressure,  $\Delta P$ , between the no-blowing and blowing cases for both the Varaperf and 3M shells. The blowing rates listed at the right indicate the blowing magnitude as a percentage of the tunnel freestream mass flow rate. As can be seen at low blowing rates, under 1 percent, the induced pressure is constant along the length of the body and there seems to be no difference between the two model shells.

As the blowing rates become larger, we see a trend towards a higher induced pressure at the front of the model than that at the rear of the model. This indicates that the blowing has become high enough to begin blowing the boundary layer off at the rear of the body.

In addition, we now see a large difference in induced pressures on the two shells at the same blowing magnitudes, i.e., the 3M shell at 2.8 percent compared to the Varaperf shell at 2.7 percent. The 3M shell, in general, tends to exhibit a much higher induced pressure for the same blowing rates. Much more analysis is required at this time to understand the causes of this difference but it is believed that the difference in injection velocity is a contributing factor.

Figure 41 shows some of the results of the heat transfer measurements made on the two model shells. Plotted is the Stanton number,  $ST$ , normalized by the Stanton number without blowing,  $ST_0$ , versus  $S/RN$ . As is expected, the heat transfer rates decrease as the blowing rates increase. The condition described earlier of boundary layer blow-off is defined by where the heat transfer rate goes to zero. It can be seen that this occurs at a blowing rate around 1 percent. This agrees well with the results of the induced pressure measurements described earlier.

In the case of the heat transfer rates there again seems to be little difference between the two shell materials at low blowing rates. This is shown by comparing the 3M shell at .58 percent to the Varaperf shell at .68 percent. As can be seen the data for the two shells are almost identical. A comparison at higher blowing rates is impossible since the heat transfer rates go to zero due to boundary layer blow-off.

Figure 42 shows a comparison of the experimental results to several theoretical correlations.<sup>9,10</sup> As can be seen the data correlates very well with the theoretical values given for flow over cones. Some of the scatter in the data can be attributed to the fact that the correlation is based on free-stream properties and does not take into account the variation in conditions over the surface of a cone.

Figure 43 shows a similar correlation, but in this case the model blowing rates are normalized by the properties at the edge of the boundary layer.<sup>11</sup> This then takes into account any variation in flow field properties over the cone surface.

<sup>9</sup>Laganelli, A. L., Foganoli, R. P., and Martillucci, A., The Effects of Mass Transfer and Angle of Attack on Hypersonic Turbulent Boundary Layer Characteristics, AFFDL-TR-75-35, Apr 1975.

<sup>10</sup>Walker, G. K., Turbulent Boundary Layers with Mass Addition, G. E. Document No. TFM-8151-021, Nov 1963.

<sup>11</sup>Libby, P. A., "The Homogeneous Boundary Layer at an Axisymmetric Stagnation Point with Large Rates of Injection," J. Aeronautical Sciences, Jan 1962.

In summary, the results from phase one indicated that the instrumentation had adequate sensitivity to make the required measurements. The data also points to a difference in the induced pressures at higher blowing rates between the two shells, while a comparison of heat transfer rates is not possible due to the effect of boundary layer blow-off. Finally, the heat transfer data at low blowing rates correlates very well with theoretical values for both the 3M and Varaperf shells.

## PHASE TWO

This phase of the test consisted of 28 runs, 14 dedicated to force and moment measurements and 14 dedicated to measuring surface pressure and heat transfer rates. All the runs made in this phase were with the shells designed to produce an asymmetric outgassing distribution. The runs were made at various angles of attack between  $0^\circ$  and  $35^\circ$ . In all the data to be presented for phase two, the blowing magnitude listed is the maximum rate. This maximum with only a few exceptions was located at a circumferential location,  $\theta$ ,  $60^\circ$  from the windward ray. Two runs were made with the maximum located at a value of  $\theta = -60^\circ$  from the windward ray.

Figures 44 through 46 show the effect of blowing on the normal force coefficient, pitching moment coefficient and center-of-pressure location, respectively, for the  $7^\circ$  conical models. The normal force and pitching moment coefficients are seen to be only slightly reduced due to the blowing. At higher angles of attack ( $>10^\circ$ ) there is also only a slight effect on center-of-pressure location ( $X_{cp}/l$ ) but at  $\alpha = 5^\circ$  there is a very large change in  $X_{cp}/l$ . Since the normal force and pitching moment are both very small at this angle, a very small change in them causes a very large shift in  $X_{cp}/l$ .

A comparison can be made between these parameters for the  $7^\circ$  cone to those for the  $9^\circ$  cone using Figures 47 through 49. Here we see that the changes in normal force and pitching moment coefficients are even smaller than those of the  $7^\circ$  cone. This results, therefore, in a much smaller shift in  $X_{cp}/l$  for the  $9^\circ$  cone. One thing that is evident is that the  $X_{cp}/l$  shift on the  $9^\circ$  cone tends to make the body more stable while on the  $7^\circ$  cone it has a destabilizing effect.

A comparison of the out-of-plane forces and moments on the two cones is shown in Figures 50 and 51. The values for the  $7^\circ$  cone are taken from the shell designated as type "nominal" which corresponds to the blowing distribution used on the  $9^\circ$  cone. From Figure 50 it can be seen that the side force generated for the same blowing magnitude on the  $9^\circ$  cone is, on the average, about one-half that for the  $7^\circ$  cone. Similarly, Figure 51 shows that the side moments are generally higher on the  $7^\circ$  cone also.

This difference in side force on the two bodies is a result of the induced pressure variation shown in Figure 52. Shown here are the circumferential variations of induced pressure measured on the type "nominal" ( $7^\circ$  cone) and type 4 ( $9^\circ$  cone) at one axial station. It can be seen that the change in pressure on the left side of the  $7^\circ$  cone is larger than the change in pressure on the right side. This difference in induced pressure causes a force to the right. On the  $9^\circ$  cone the changes in pressure on the left side are only slightly larger than those on the right side, resulting in the much smaller side forces seen in the force and moment results described earlier.

Figure 53 shows the results of the heat transfer measurements made during a typical run, in particular, the first station of the type "4" shell at two blowing magnitudes and zero angle of attack. Shown is the Stanton number normalized by the non-blowing Stanton number. Again, as in phase one, the heat transfer rates are reduced due to the blowing. Here the heat transfer distribution varies circumferentially as the blowing rates vary circumferentially, the maximum reduction corresponding to the maximum blowing rate.

Figure 54 shows the heat transfer data for all four asymmetric blowing shells tested. Here the data are plotted against the same correlation described in Reference 11. Again we see very good agreement between the data taken here and the theoretical values.

## CHAPTER 5

### SUMMARY

The heat transfer data has been correlated very well with known theories for the flow over conical bodies. Inspection of the induced pressure data indicates agreement with the side force and moment data.

As described earlier, one of the objectives of this test program was to provide data with which to validate computer models now under development. Preliminary calculations made with these new computer models have not shown very good agreement with experimental results. This, it is believed, is due to the inability of the computer models to correctly simulate the manner in which the outgassing occurs at the model surface. Much more analysis is required in this area before the computer models can be finalized and this work is now underway.

The successful completion of this test has demonstrated several new capabilities that can be very useful in future testing. One new capability is the ability to simulate very high altitude conditions at a nominal Mach number of 13. With the increasing interest in high altitude aerodynamics, this can become a very valuable tool. Also demonstrated was the ability to accurately simulate the asymmetric outgassing distributions of typical reentry vehicle configurations.

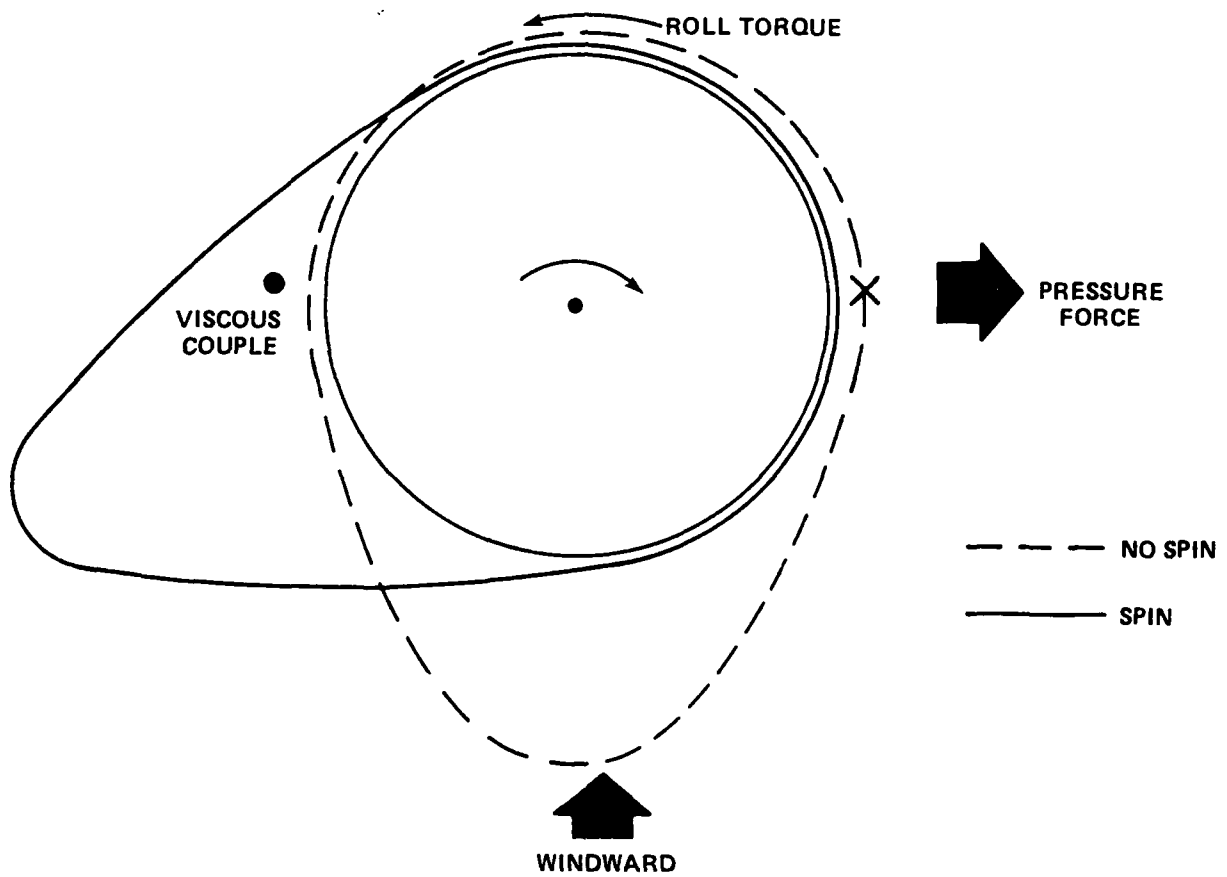


FIGURE 1. SIDE FORCE AND MOMENT DEVELOPMENT



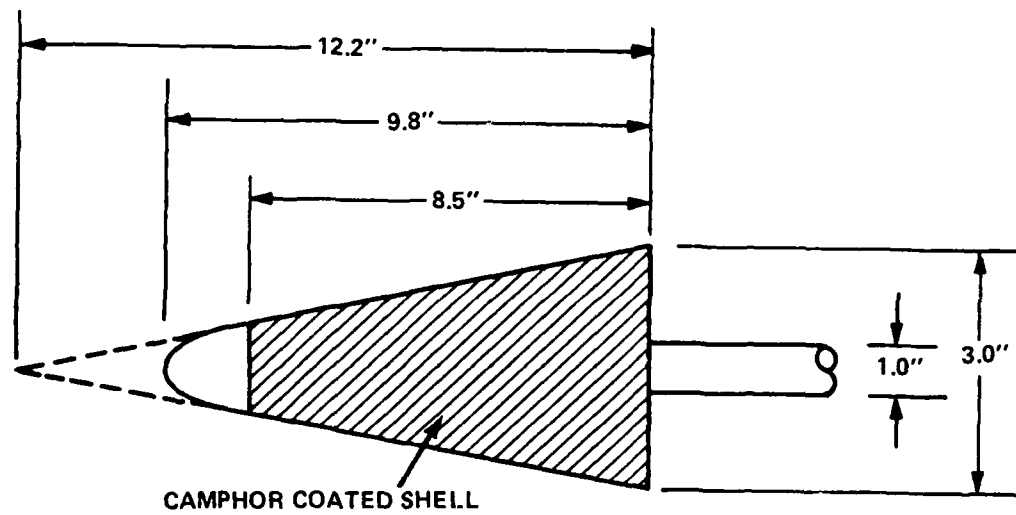


FIGURE 2. MACH 18 CAMPHOR MODEL

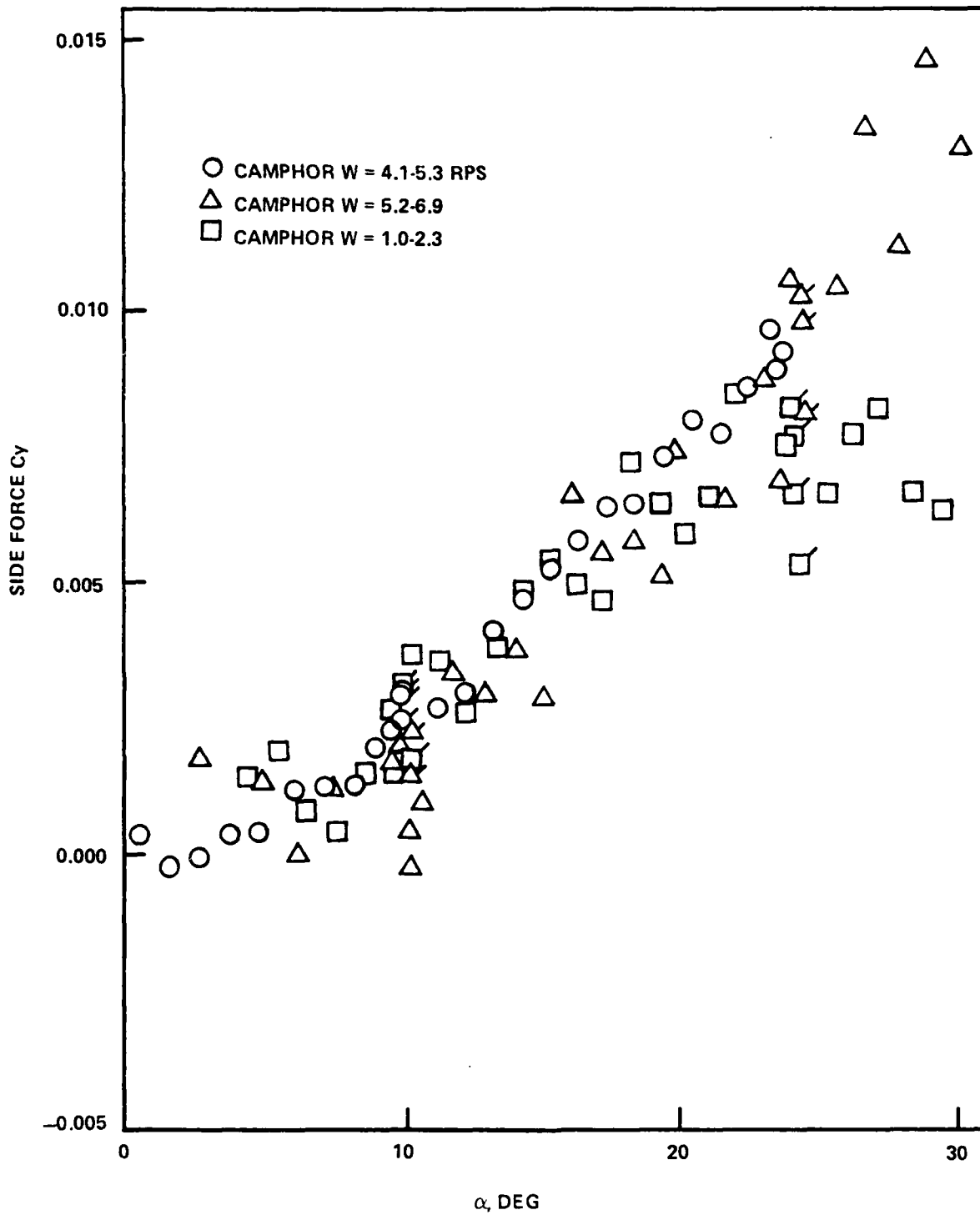


FIGURE 3. PROOF-OF-PRINCIPLE EXPERIMENTAL RESULTS

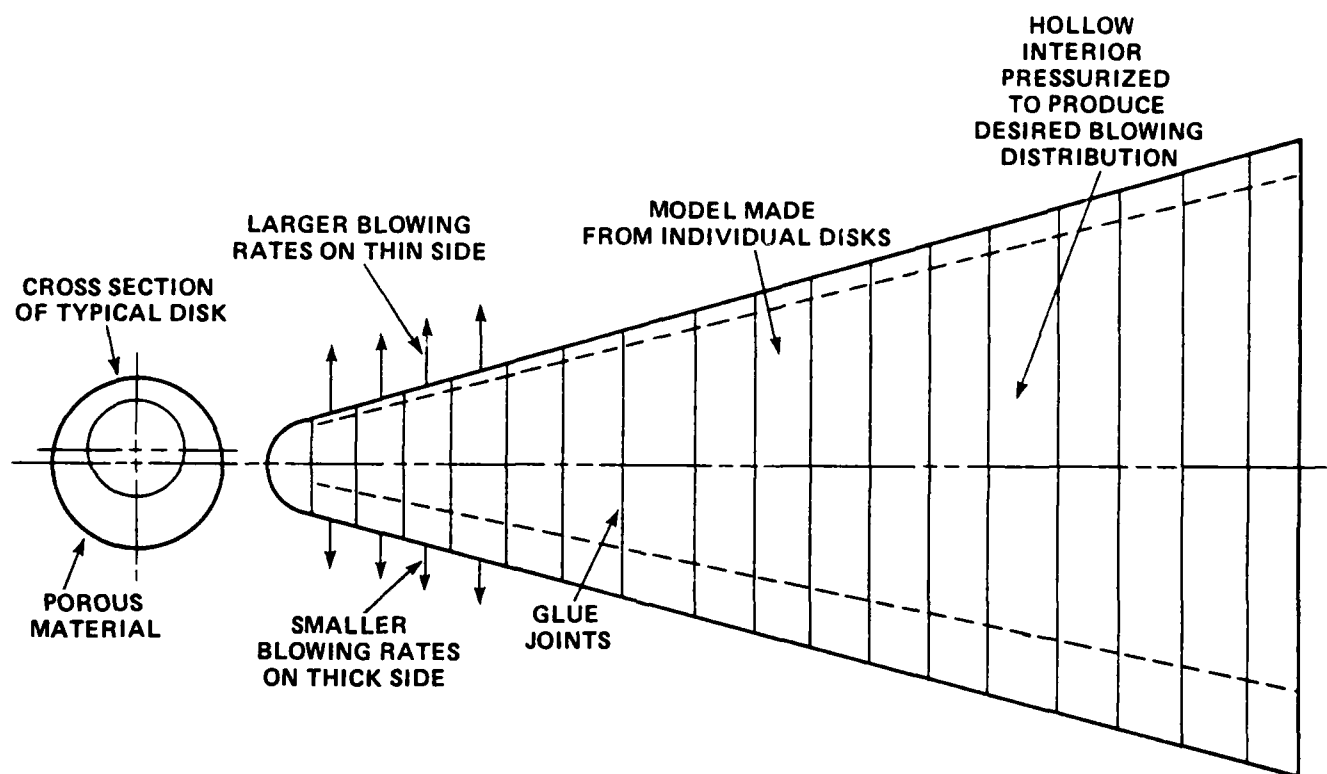


FIGURE 4. SCHEMATIC OF BLOWING MODEL DESIGN

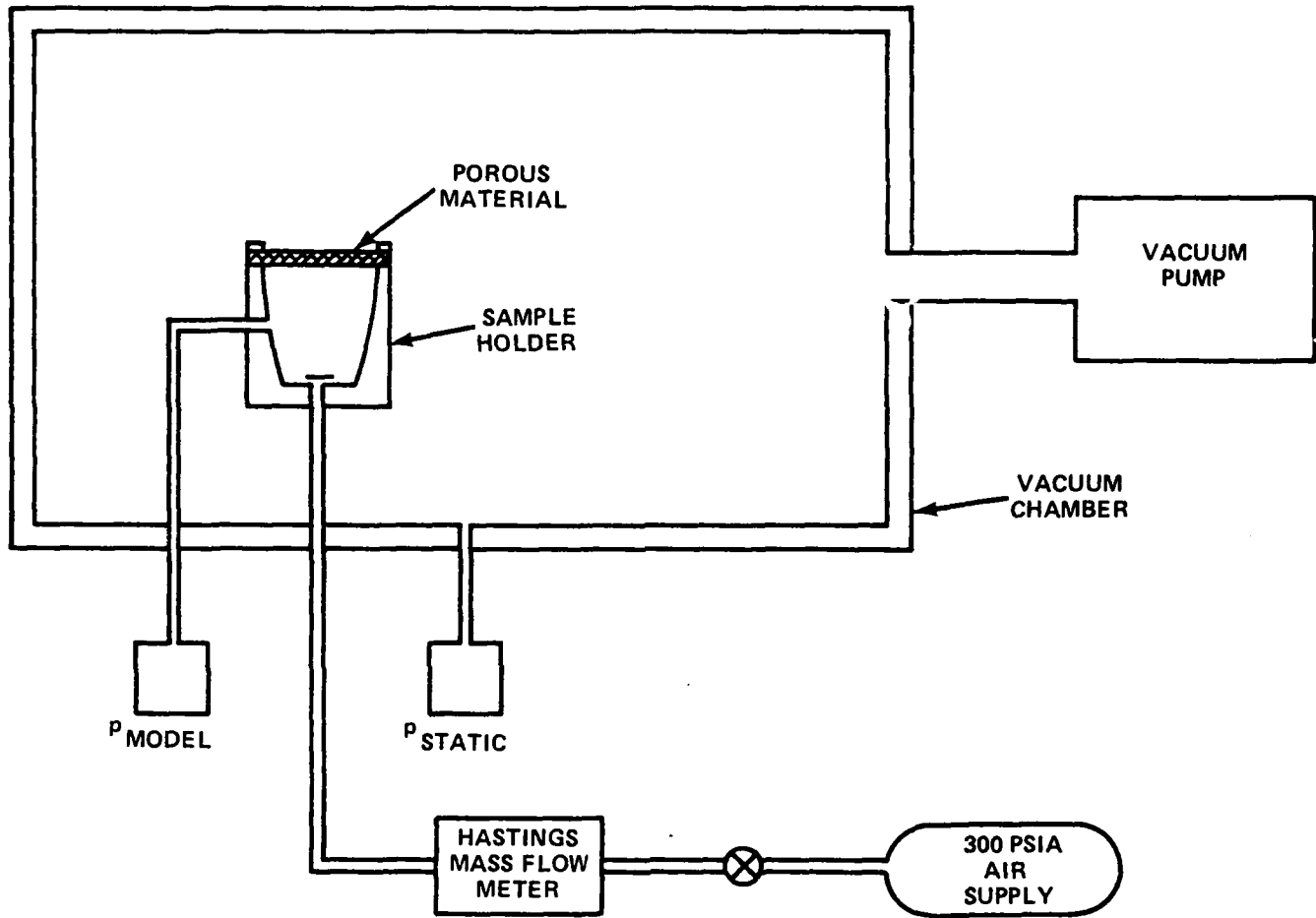


FIGURE 5. 3M MATERIAL CHARACTERIZATION SETUP

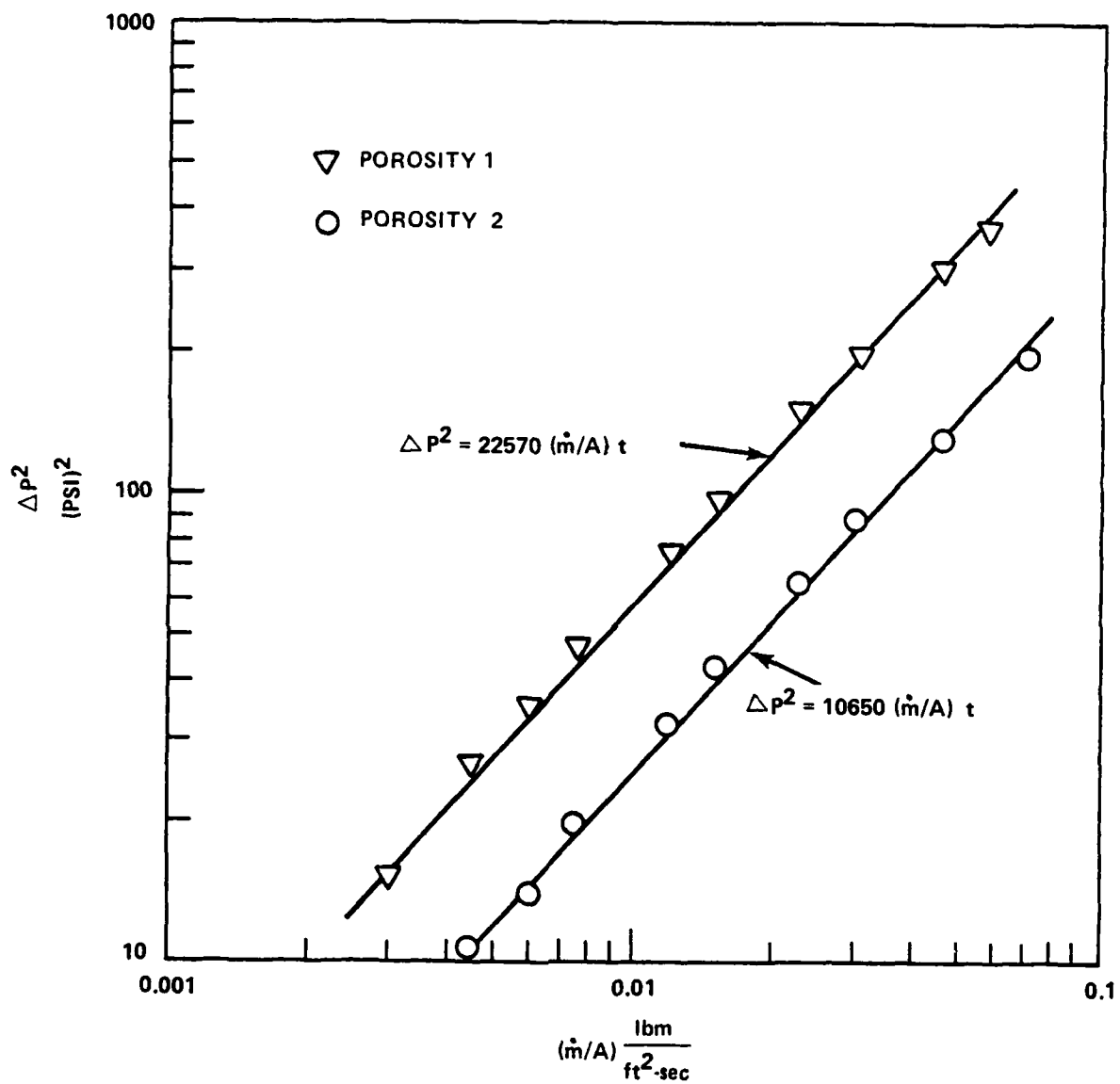


FIGURE 6. CALIBRATION CURVES FOR 3M DISKS

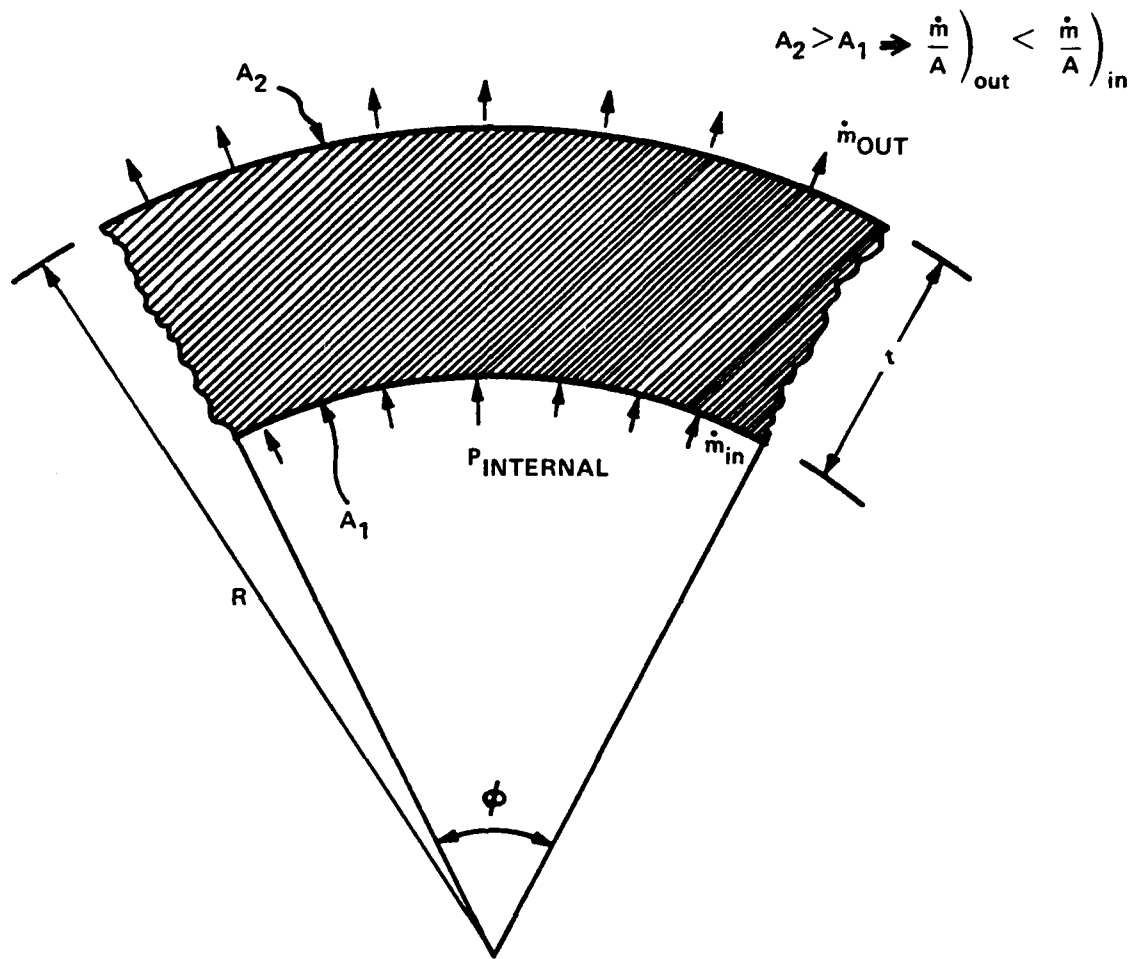


FIGURE 7. RADIUS OF CURVATURE EFFECT

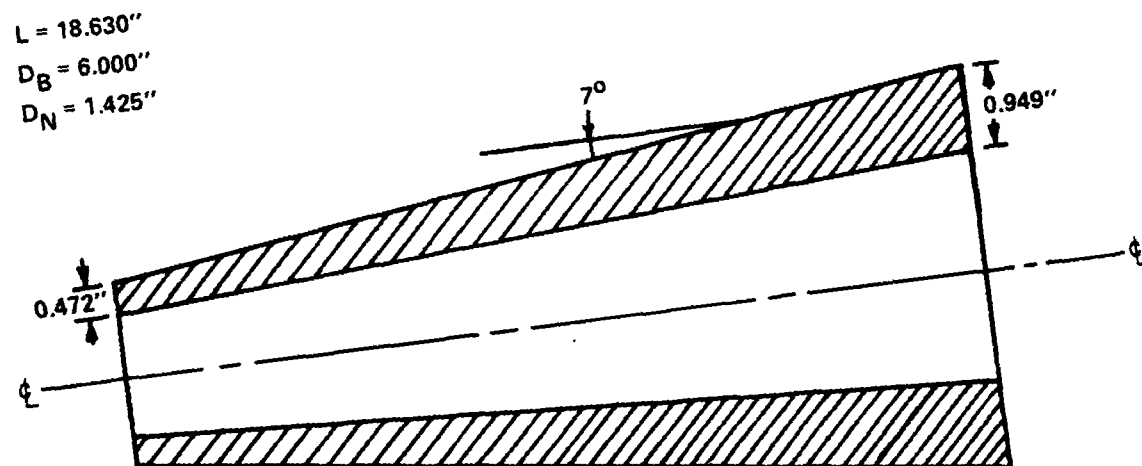


FIGURE 8. UNIFORM DISTRIBUTION SHELL DESIGN (3M)

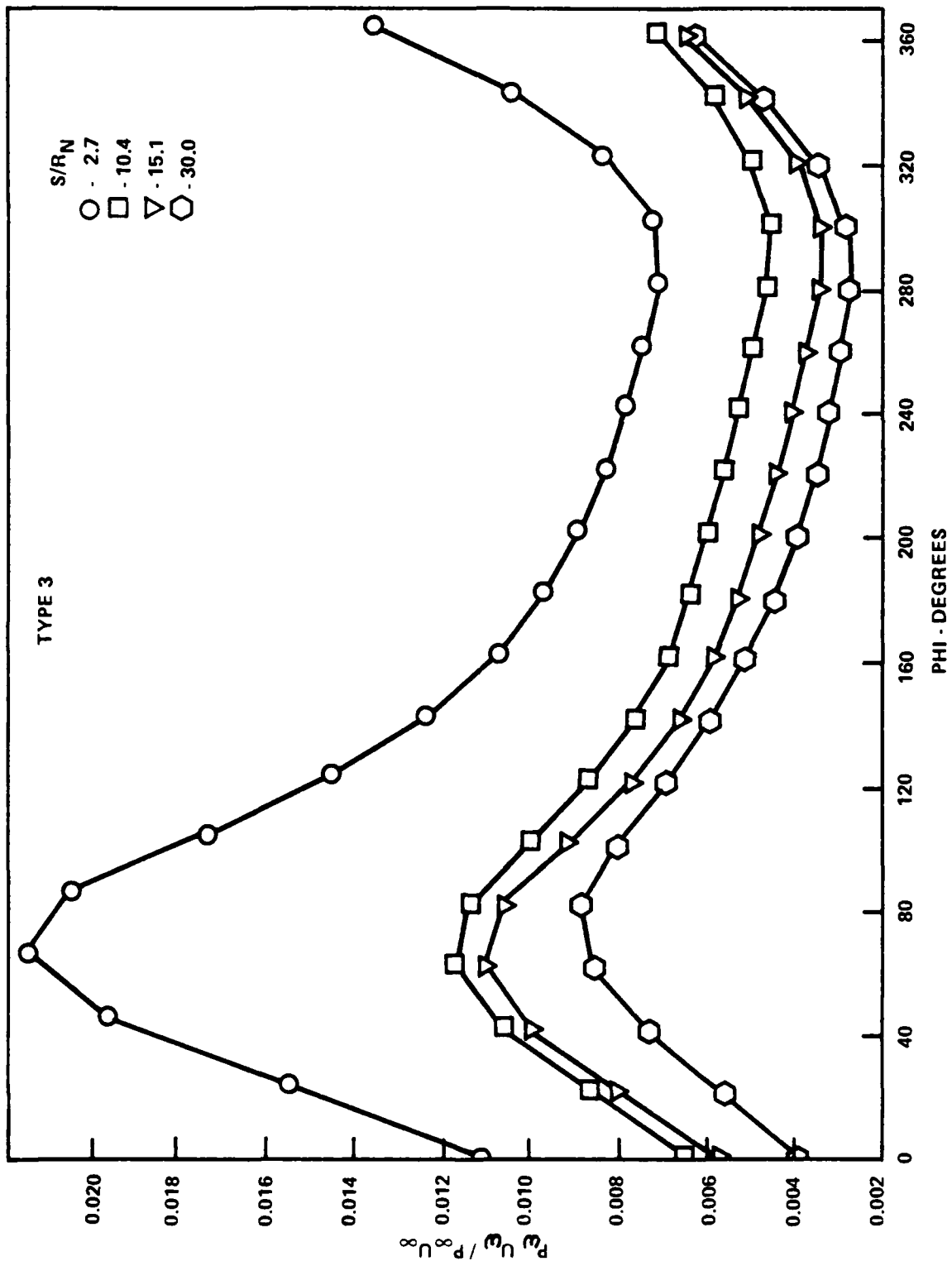


FIGURE 9. REQUESTED DISTRIBUTION - TYPE 3



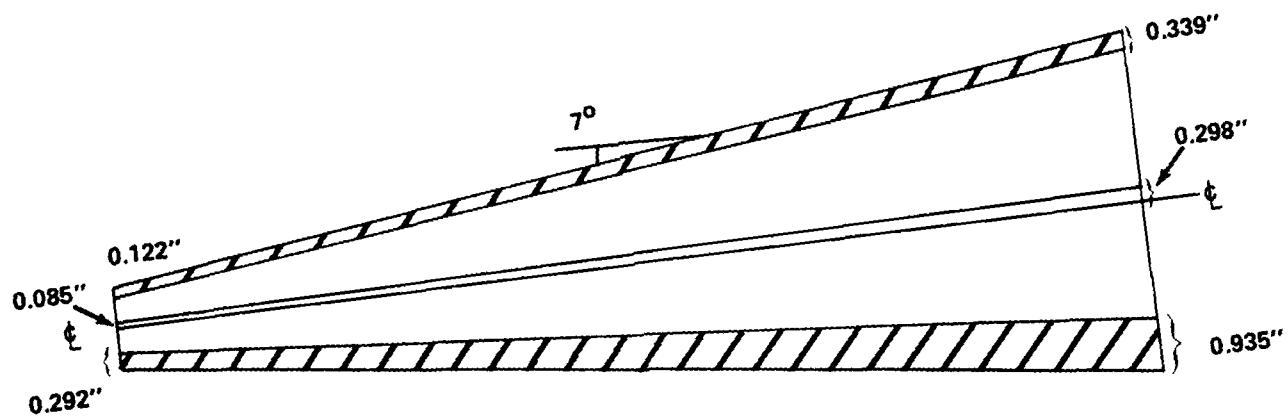


FIGURE 10. TYPE 3 DESIGN

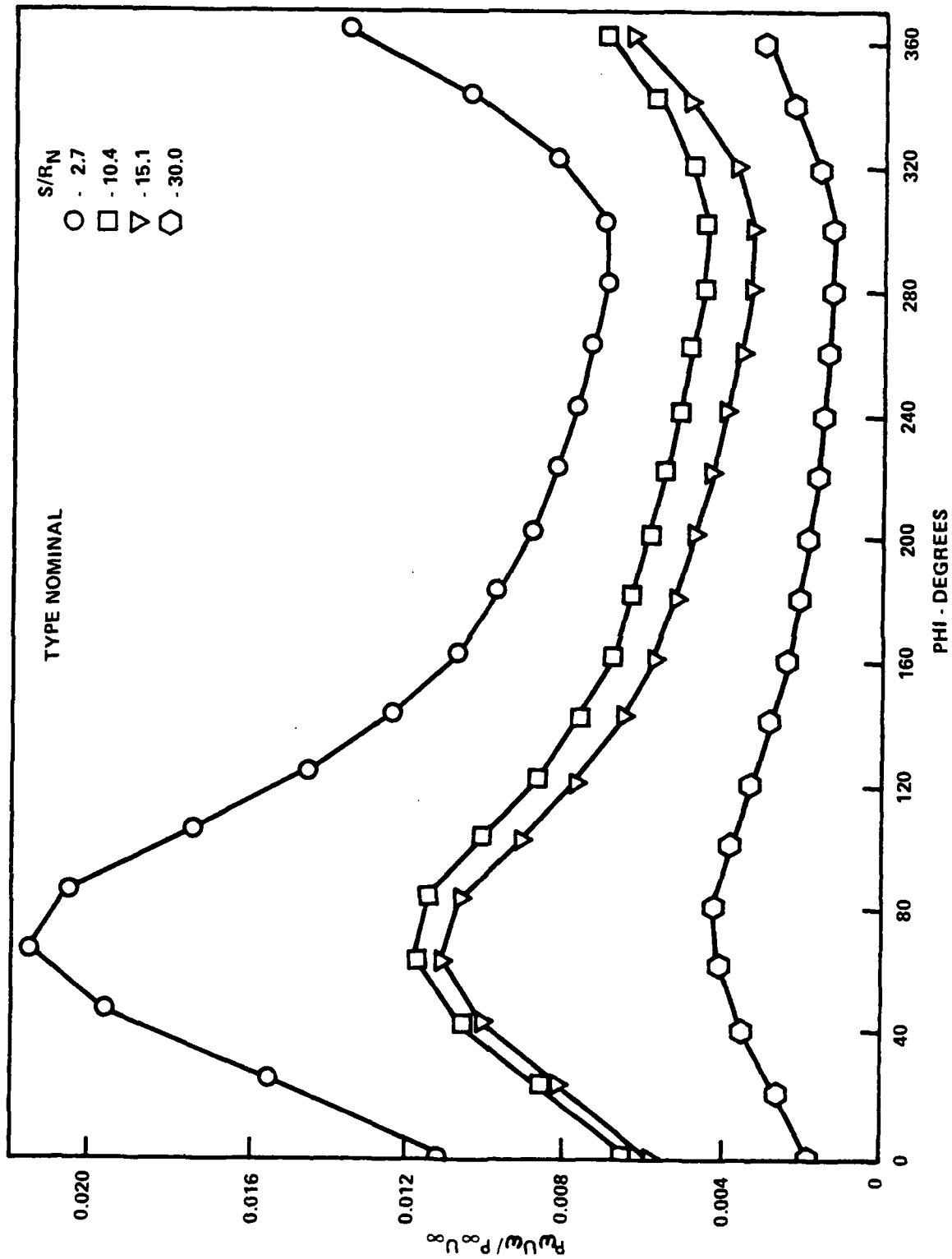


FIGURE 11. REQUESTED DISTRIBUTION - TYPE NOMINAL

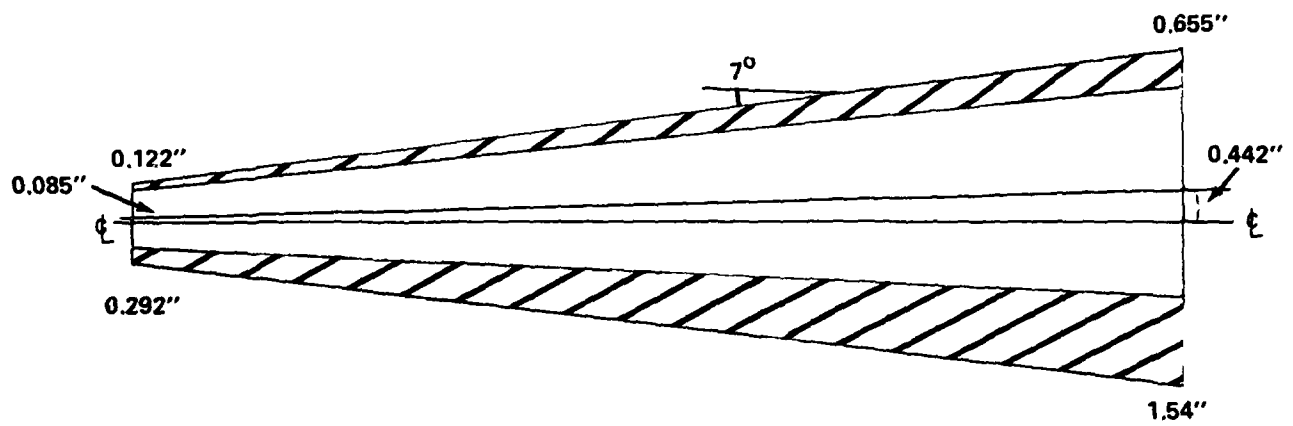


FIGURE 12. TYPE NOMINAL DESIGN

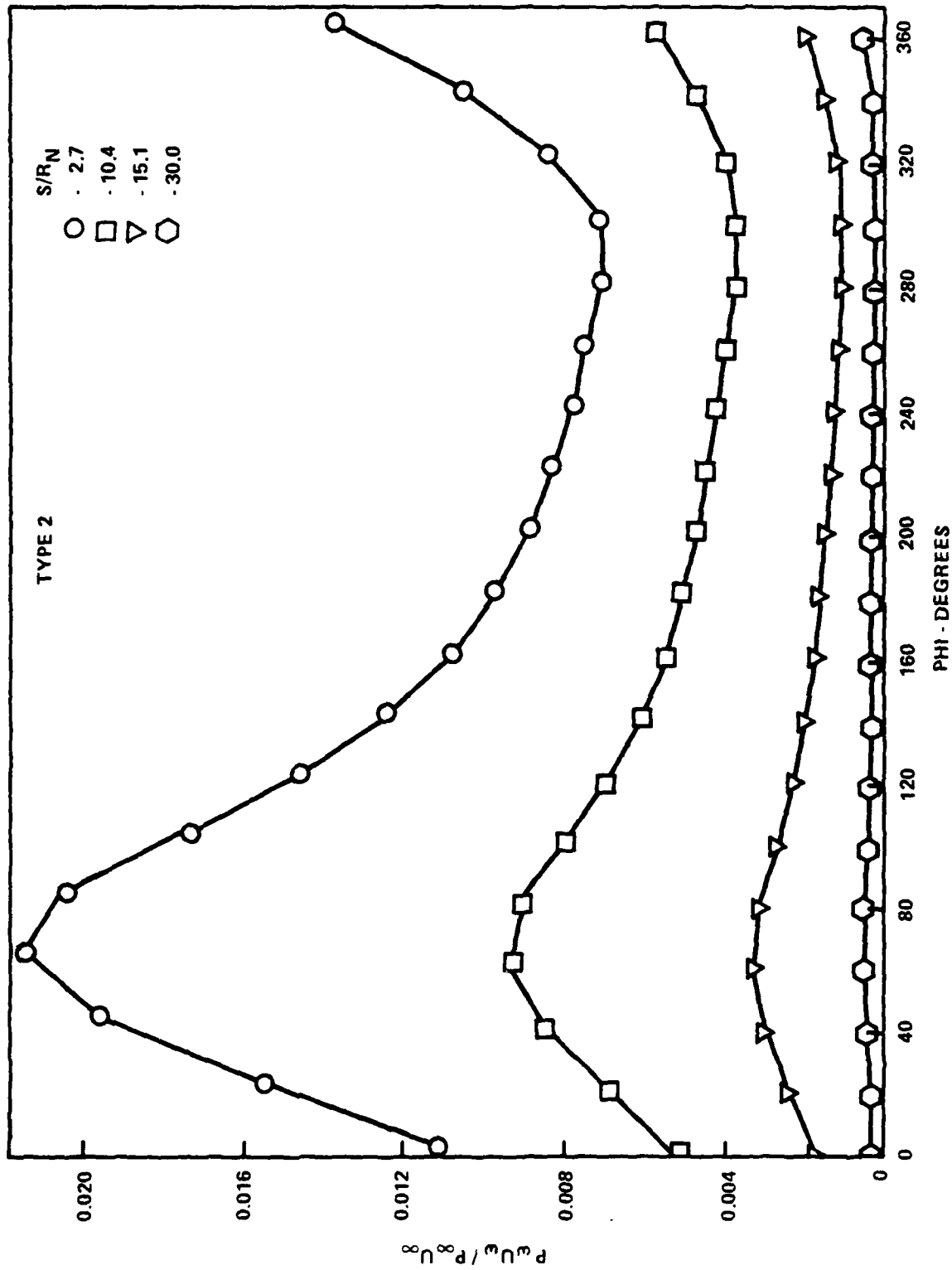


FIGURE 13. REQUESTED DISTRIBUTION - TYPE 2

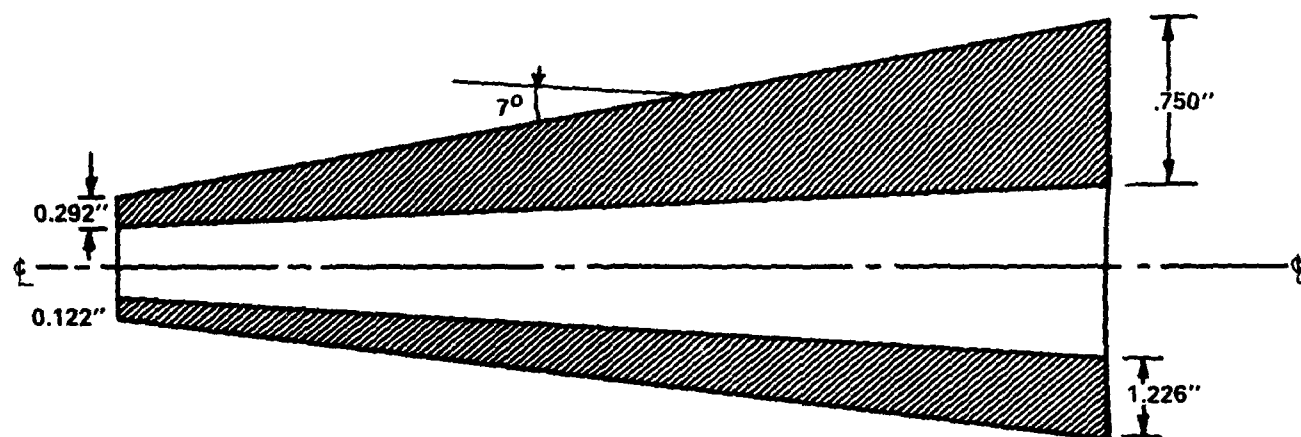


FIGURE 14. TYPE 2 DESIGN

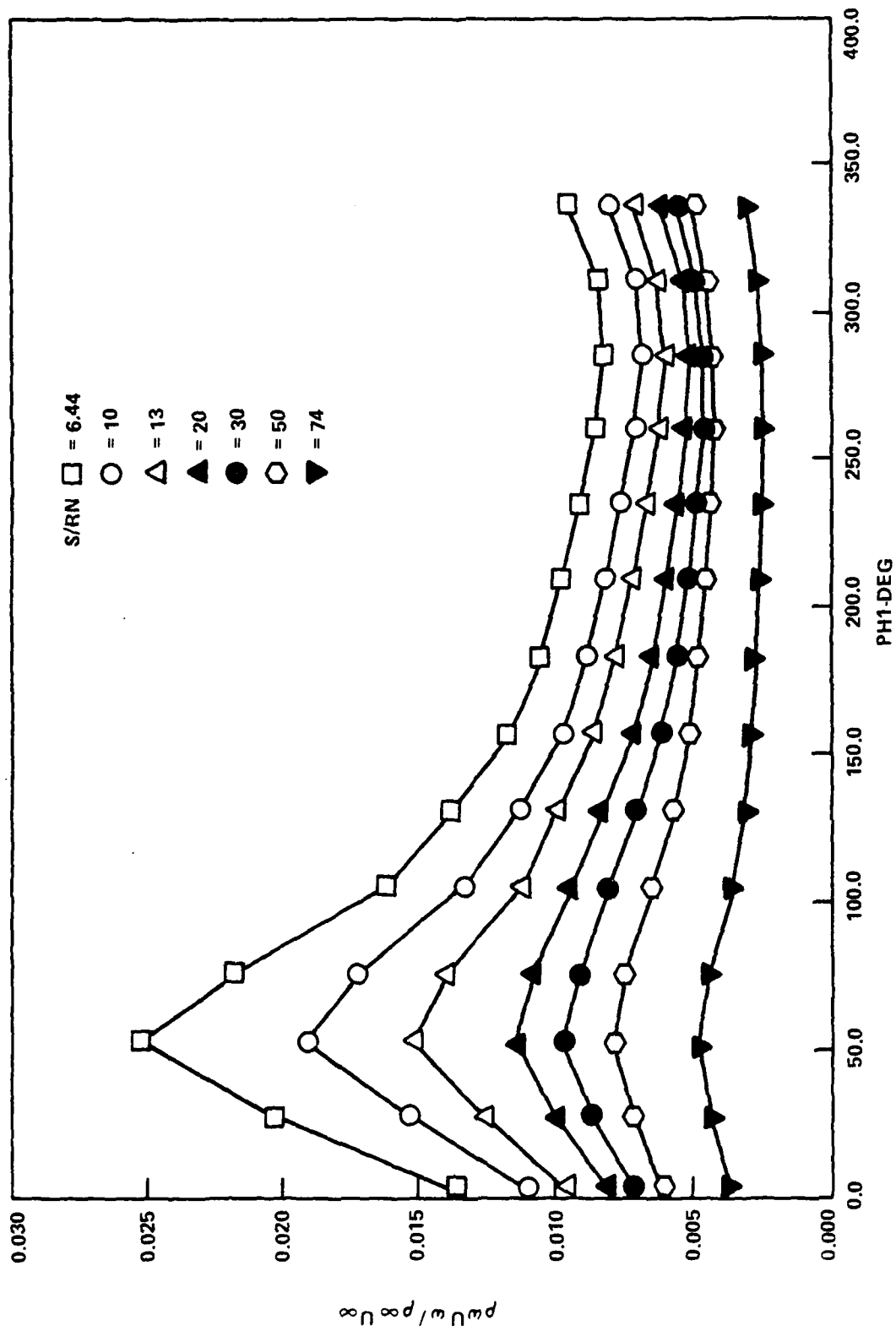


FIGURE 15. REQUESTED DISTRIBUTION - TYPE 4

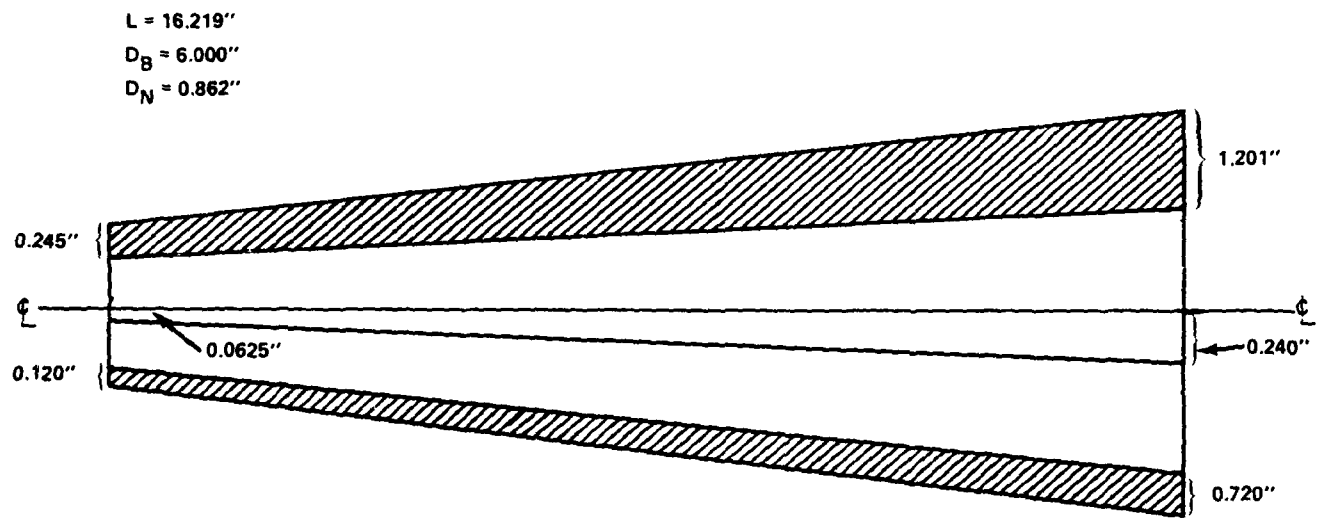


FIGURE 16. TYPE 4 DESIGN

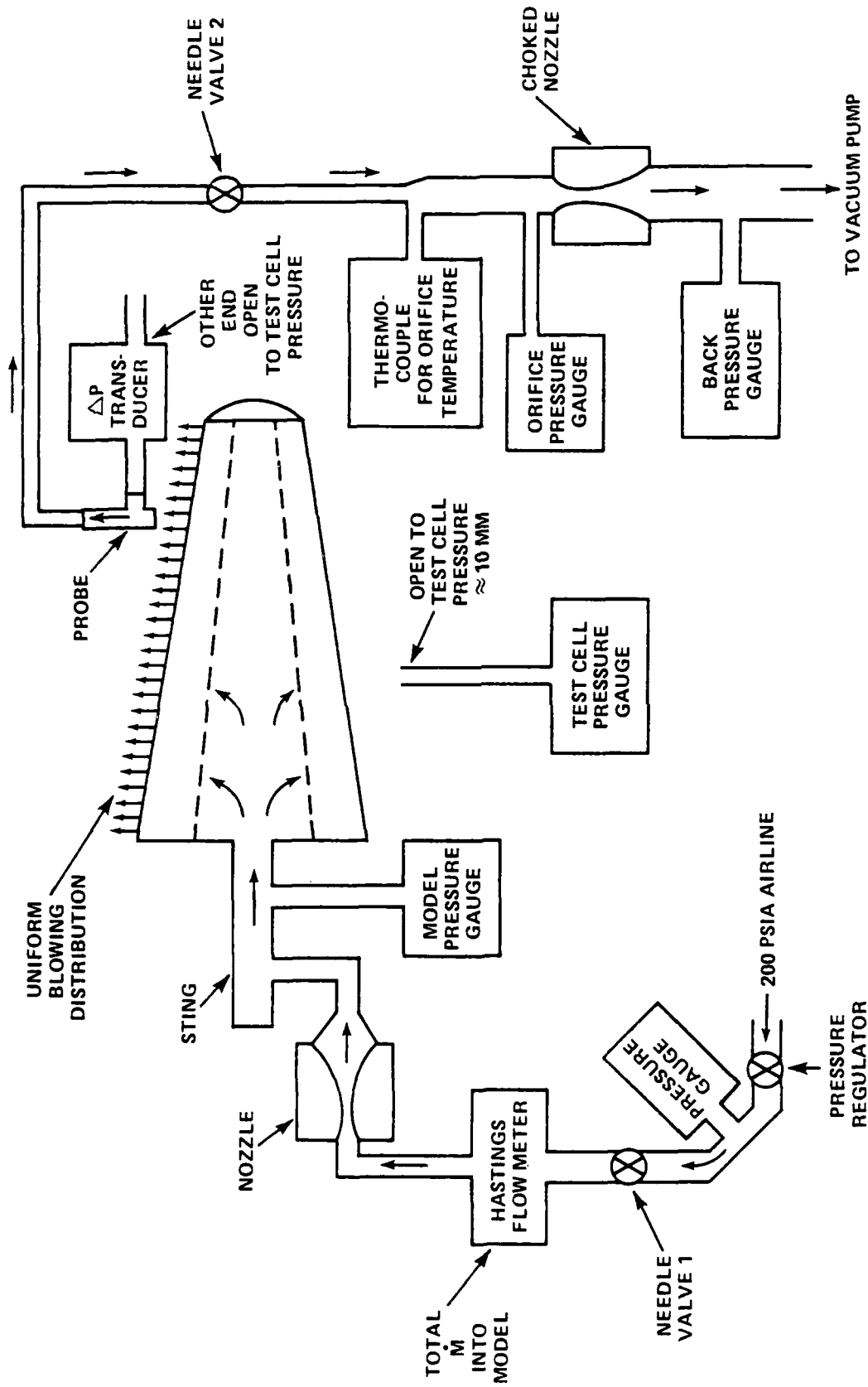


FIGURE 17. PROBE SETUP



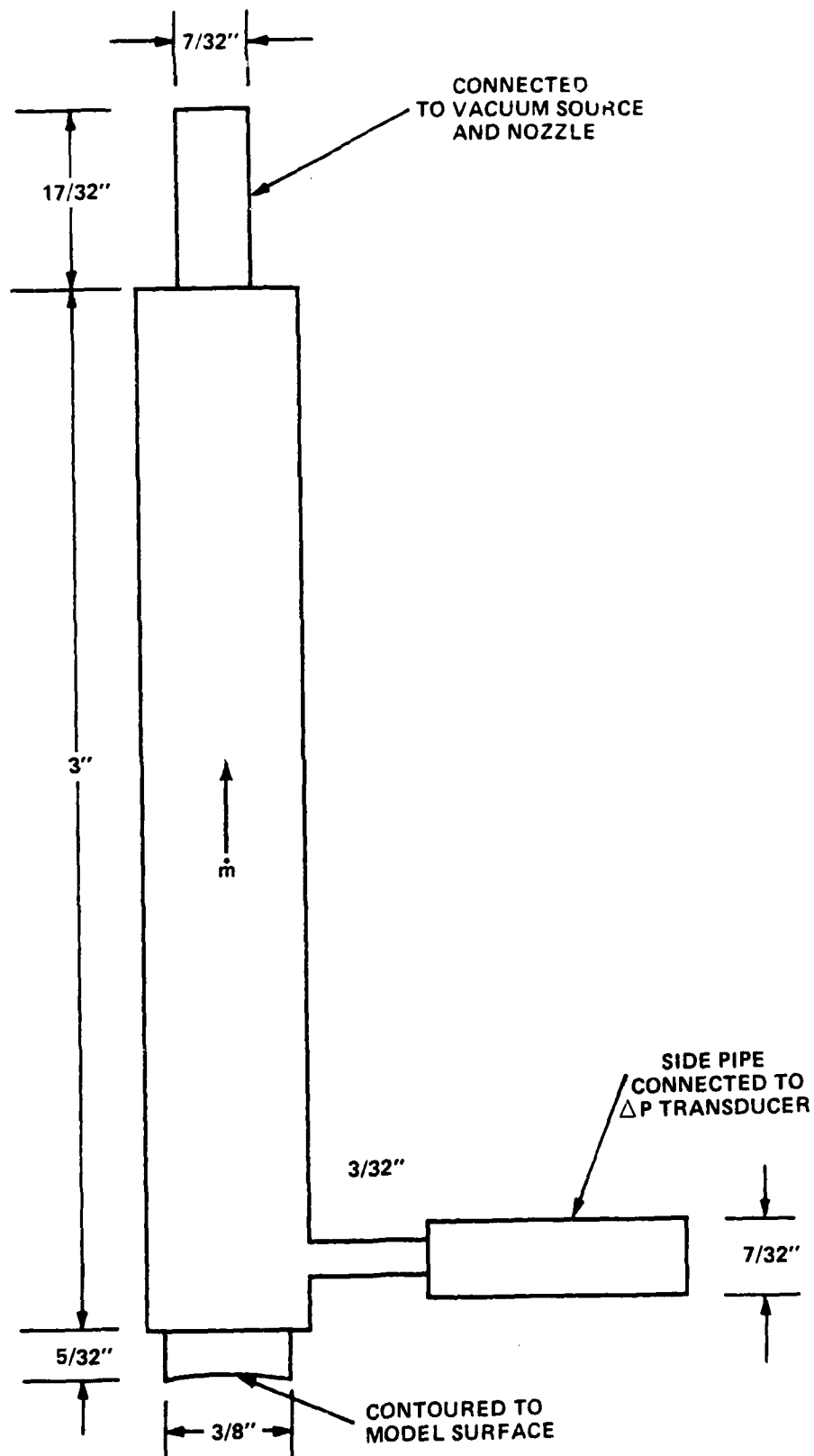


FIGURE 18. PROBE CONFIGURATION

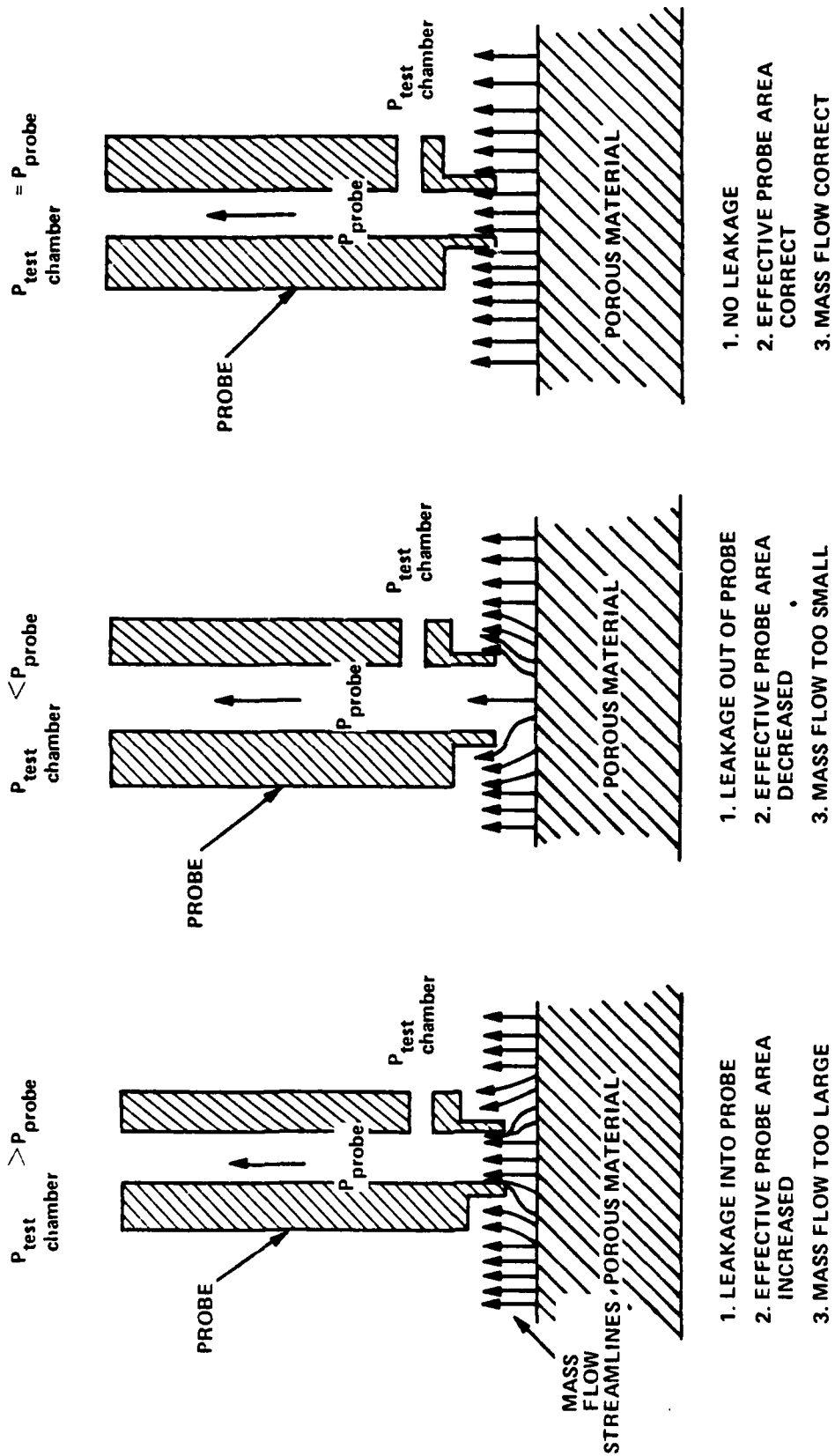


FIGURE 19. EFFECT OF PROBE PRESSURE ON MEASUREMENT TECHNIQUE

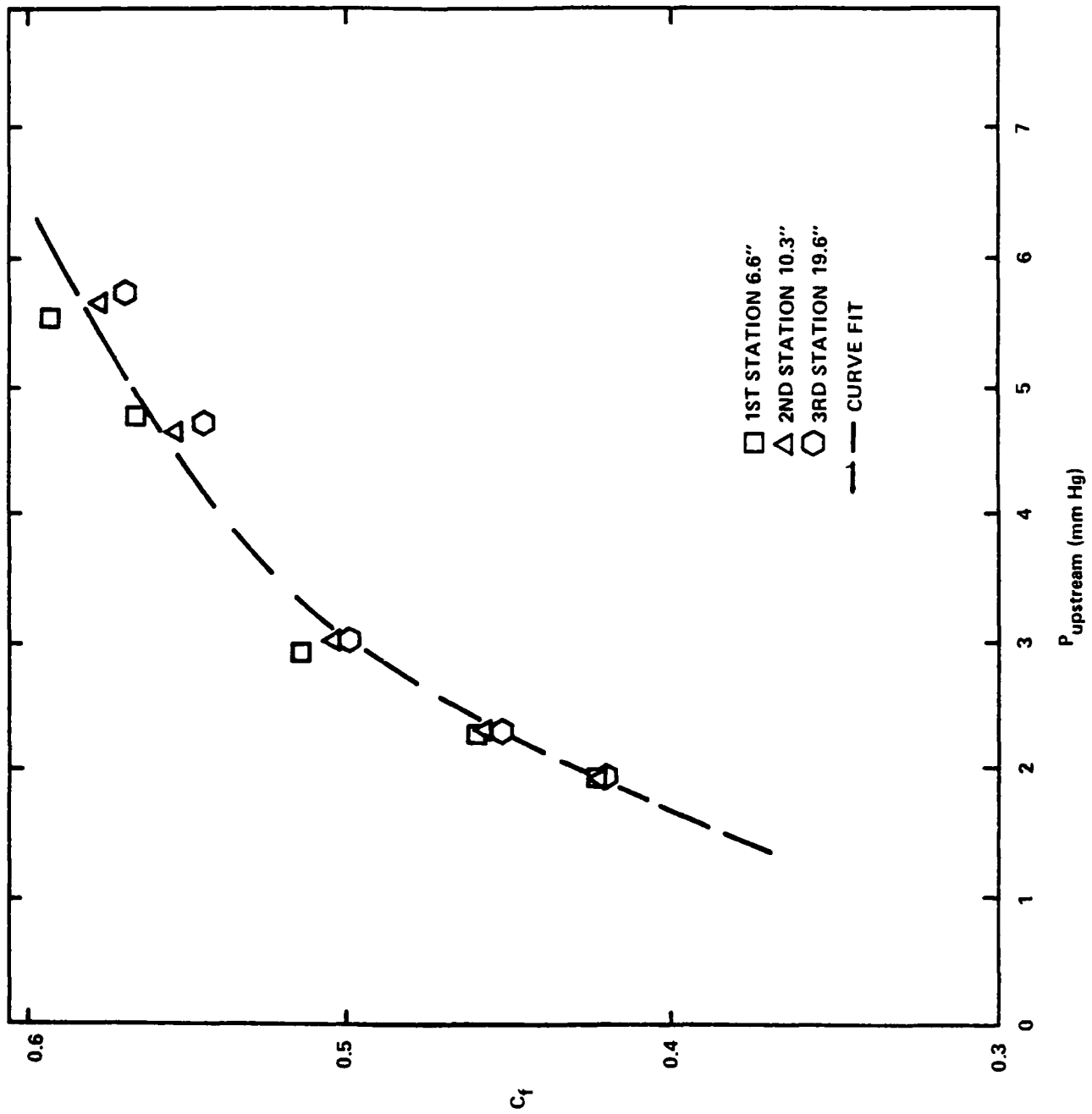
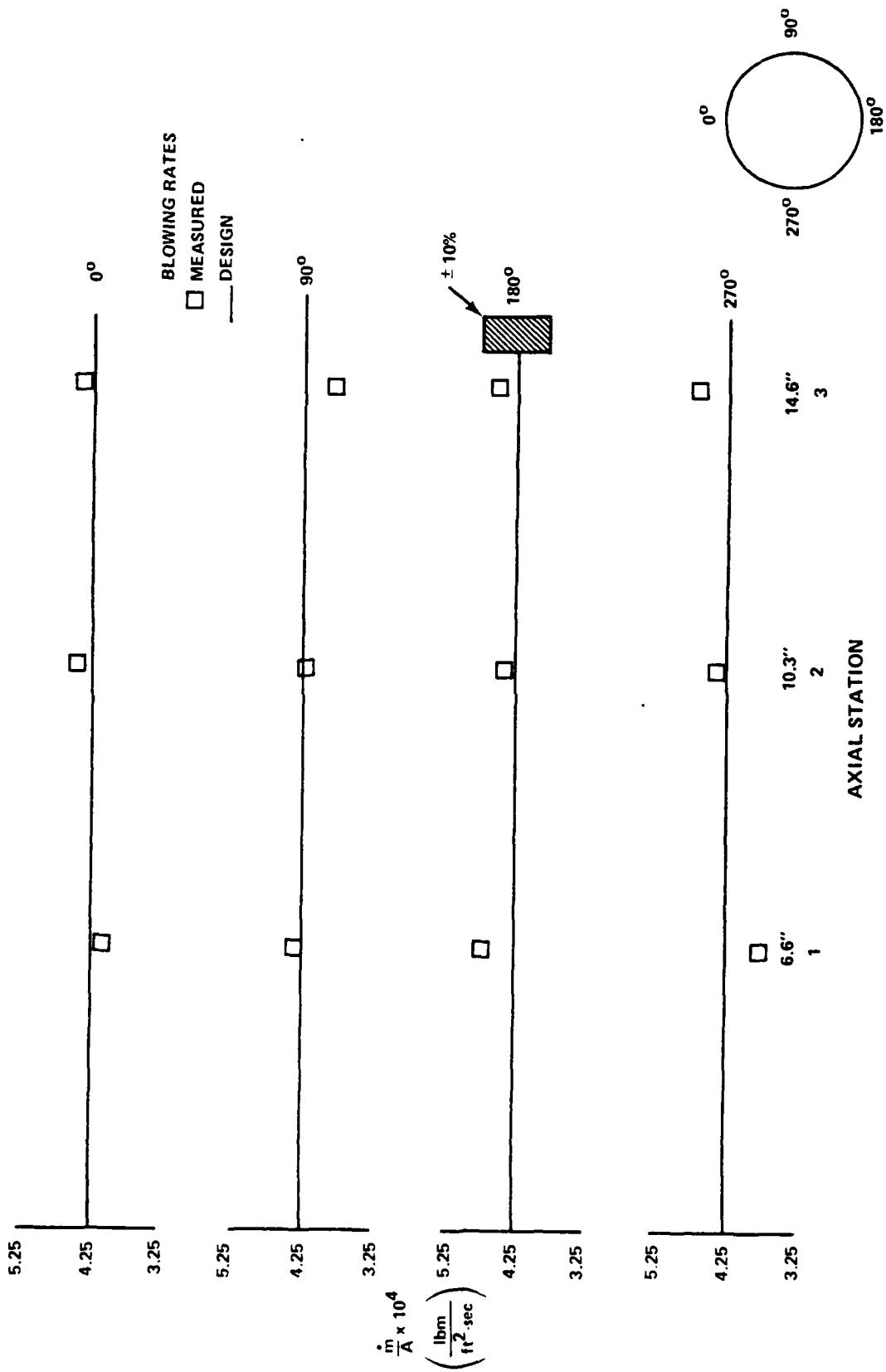


FIGURE 20. PLOT OF FLOW EFFICIENCY FACTOR



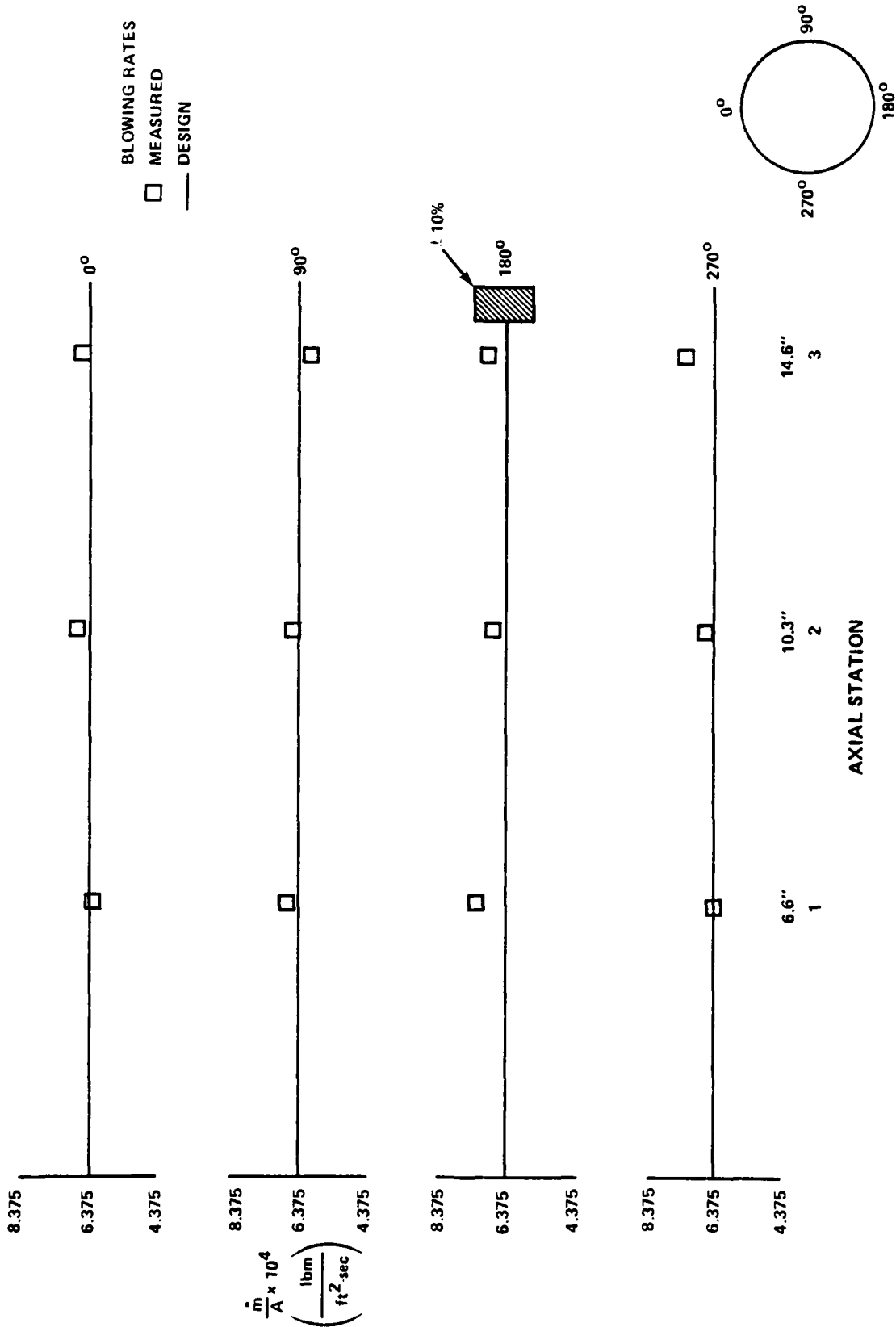


FIGURE 22. UNIFORM MODEL -- MEASURED BLOWING RATES ( $m_{TOT} = 0.7$  SCFM)

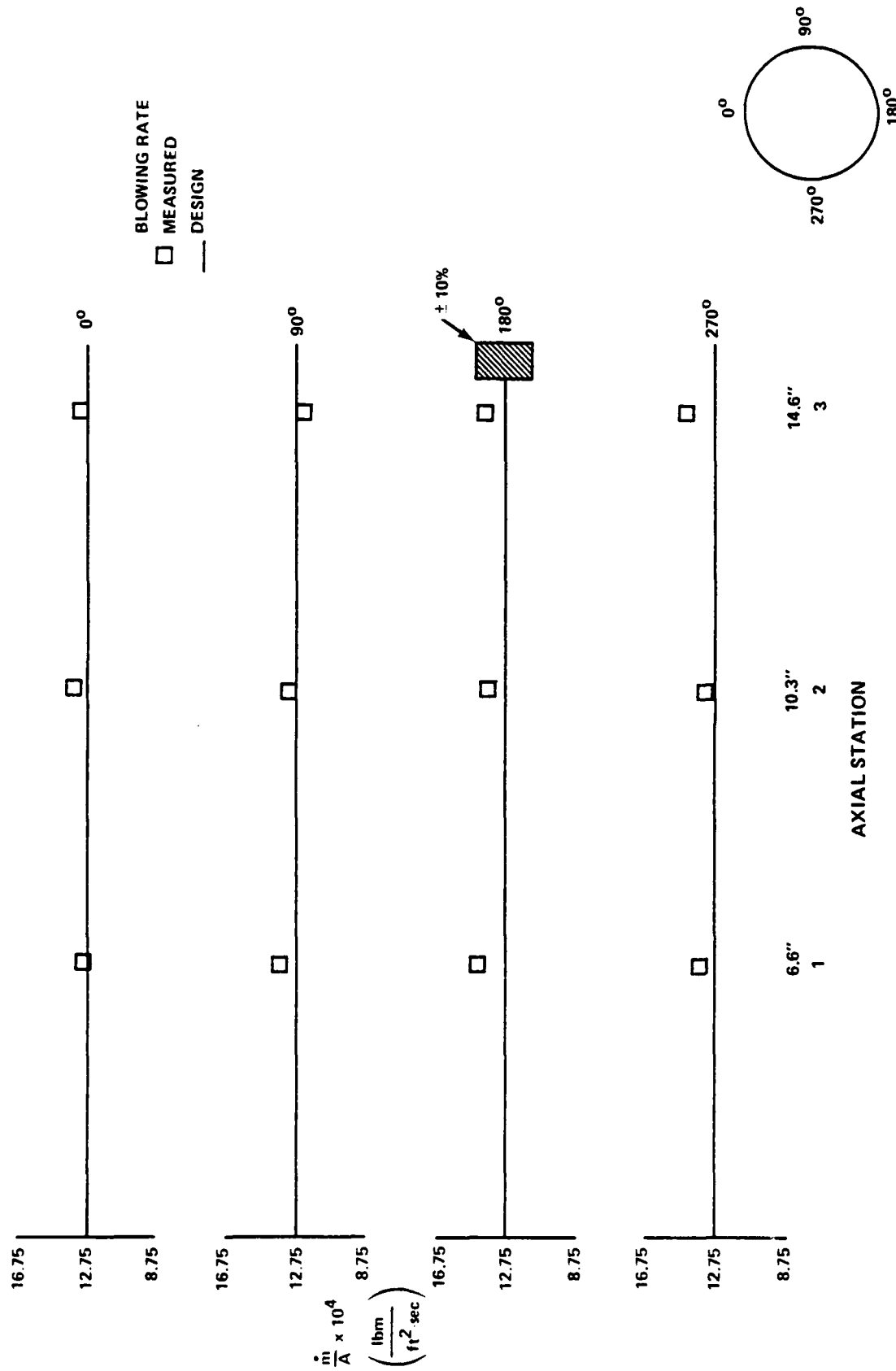


FIGURE 23. UNIFORM MODEL — MEASURED BLOWING RATES ( $m_{TOT} = 1.4$  SCFM)

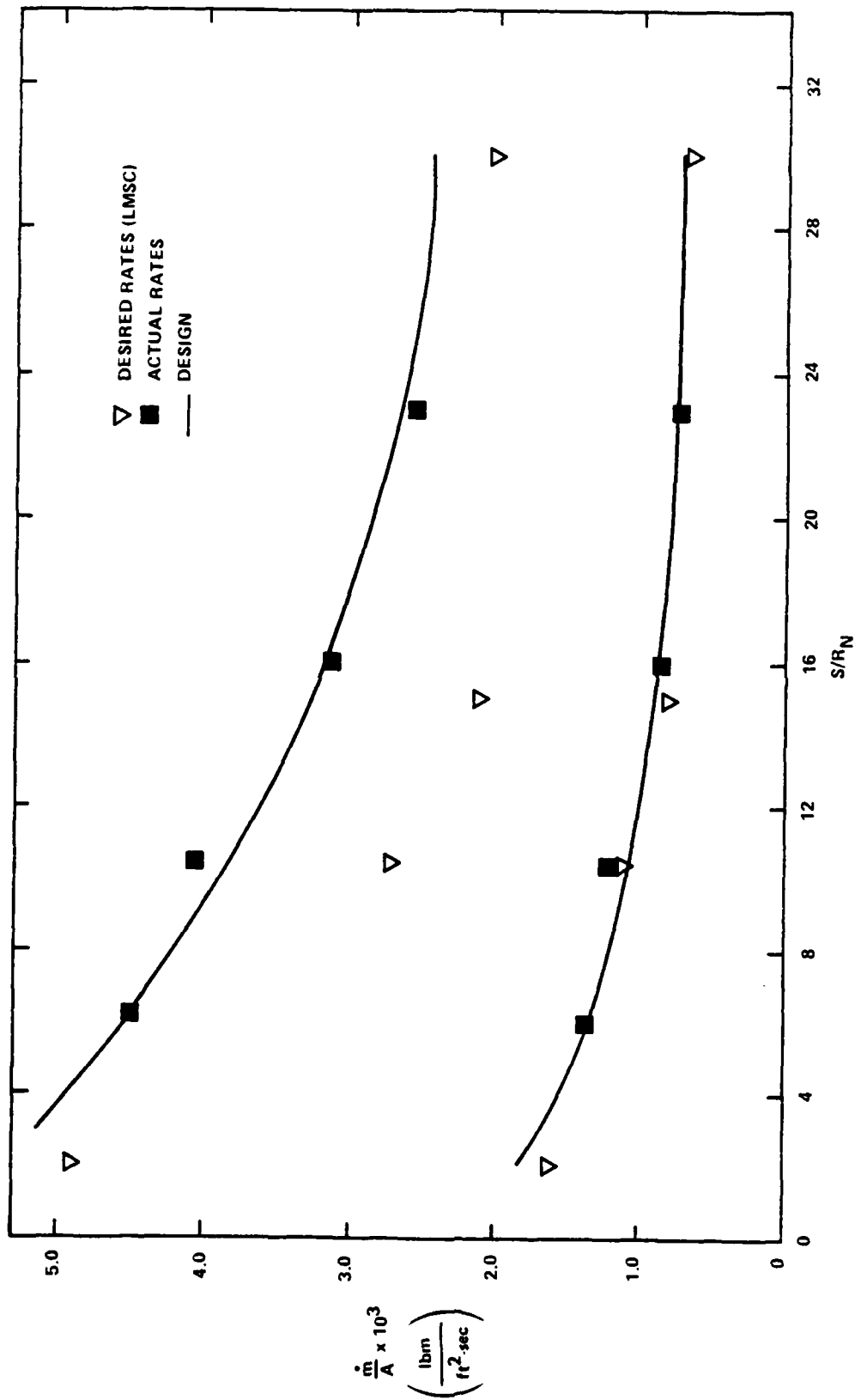


FIGURE 24A. MEASURED BLOWING DISTRIBUTION - TYPE 3

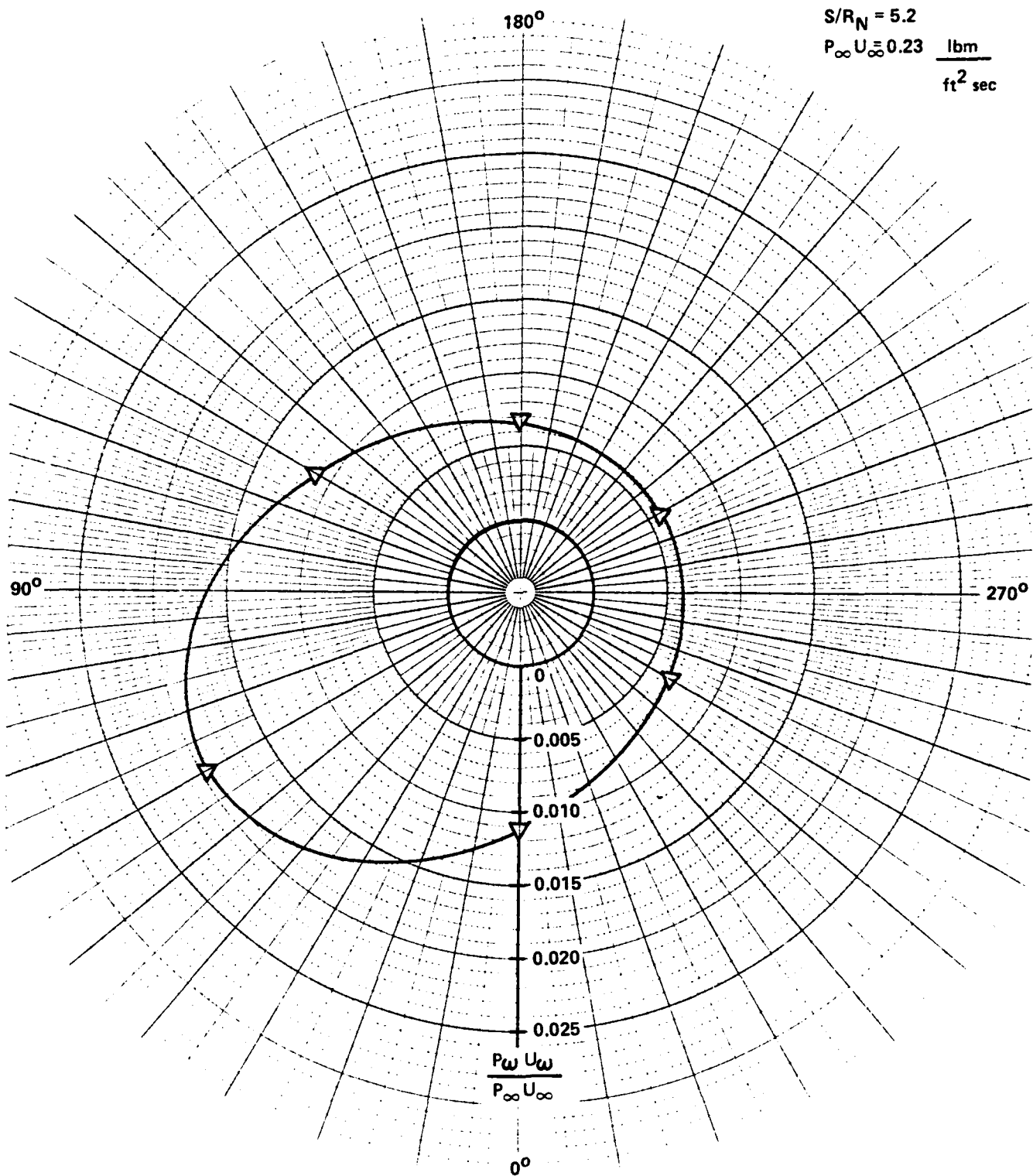


FIGURE 24B. MEASURED BLOWING DISTRIBUTION - TYPE 3



$$\frac{S}{R_N} = 10.4$$

$$P_\infty U_\infty = 0.23 \frac{\text{lbm}}{\text{ft}^2 \cdot \text{sec}}$$

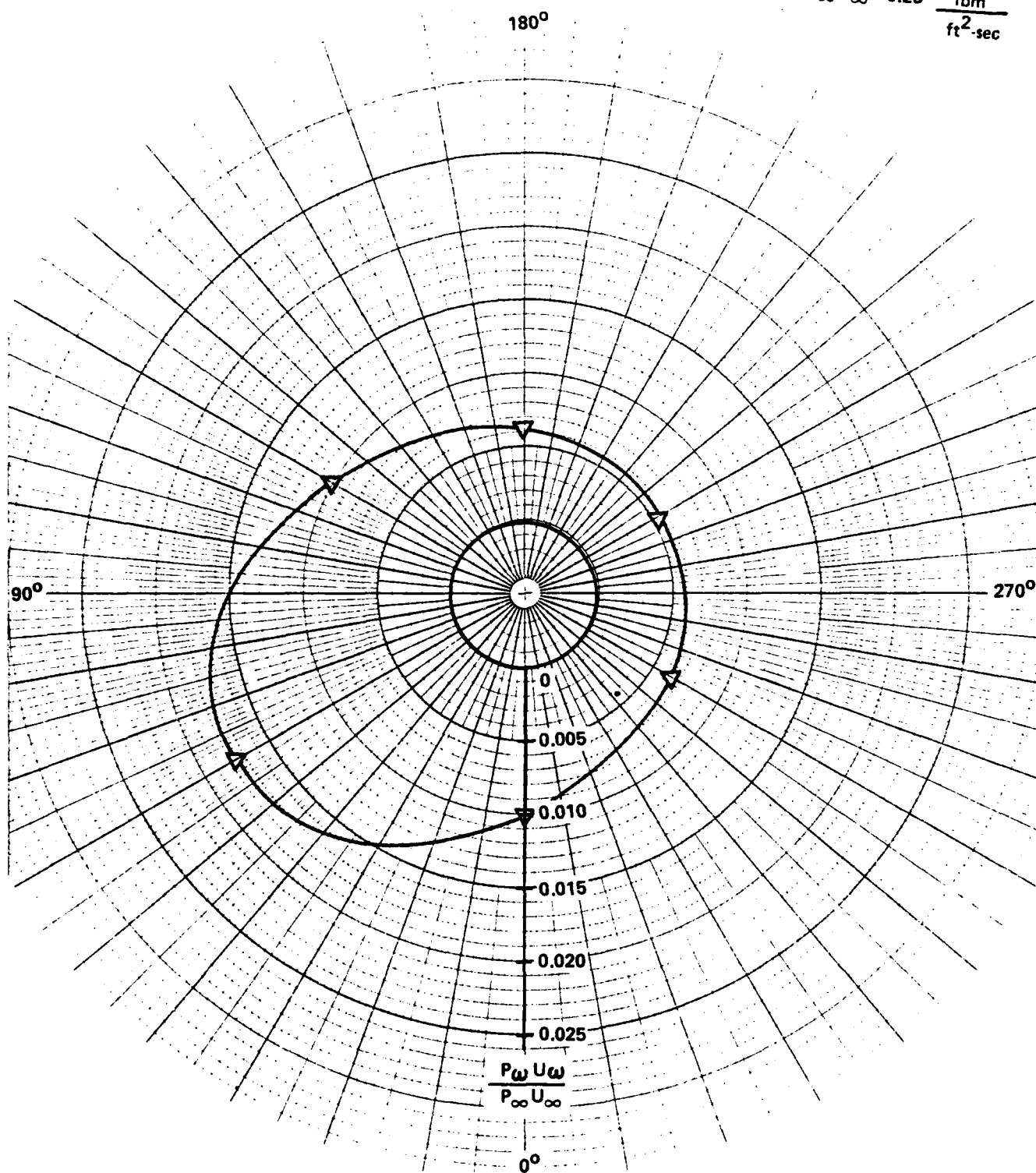


FIGURE 24C. MEASURED BLOWING DISTRIBUTION - TYPE 3

$$S/R_N = 15.1$$

$$P_\infty U_\infty = 0.23 \frac{\text{lbm}}{\text{ft}^2 \cdot \text{sec}}$$

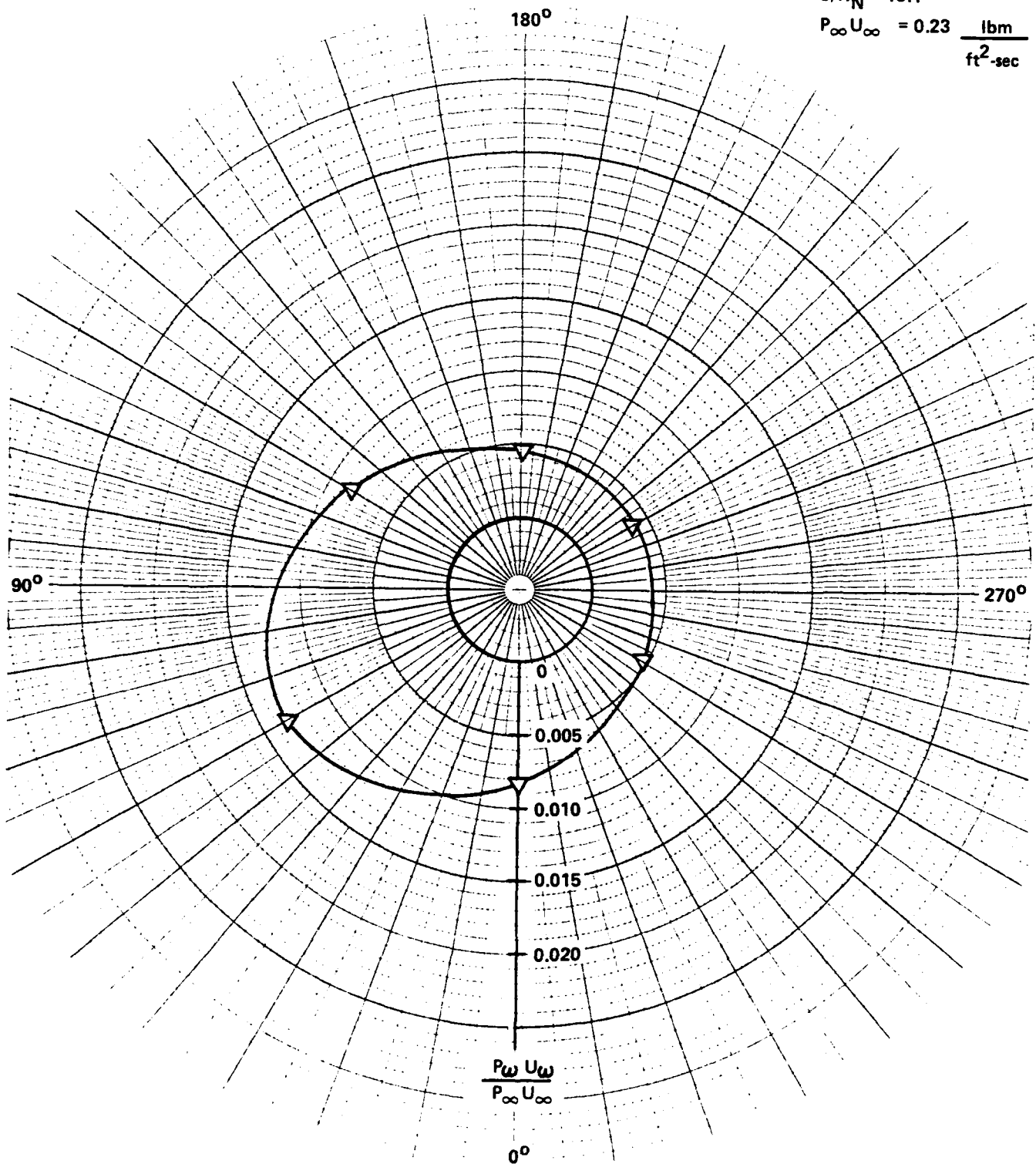


FIGURE 24D. MEASURED BLOWING DISTRIBUTION - TYPE 3

$$\frac{S}{R_N} = 23$$

$$P_\infty U_\infty = 0.23 \frac{\text{lbm}}{\text{ft}^2 \cdot \text{sec}}$$

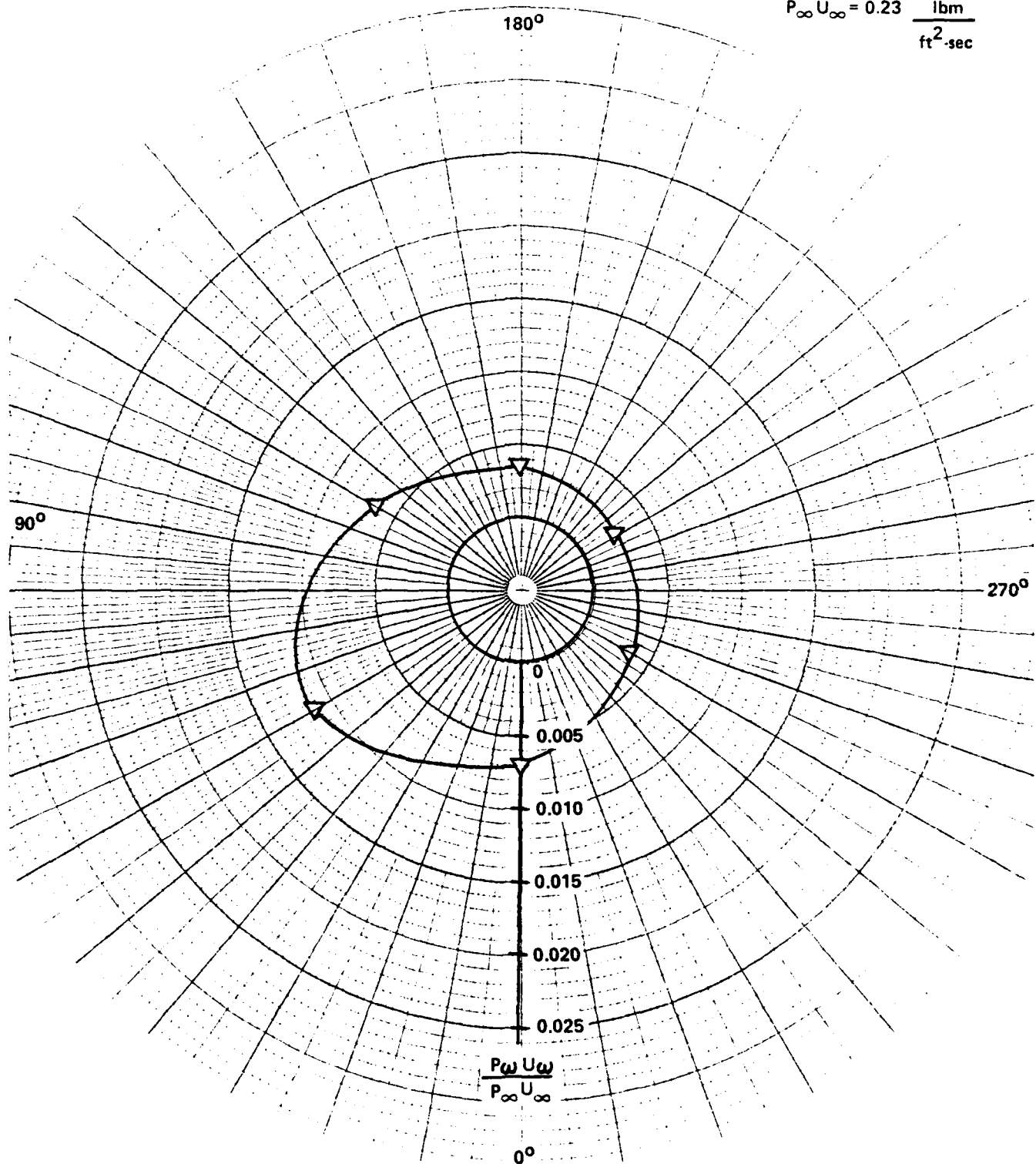


FIGURE 24E. MEASURED BLOWING DISTRIBUTION - TYPE 3

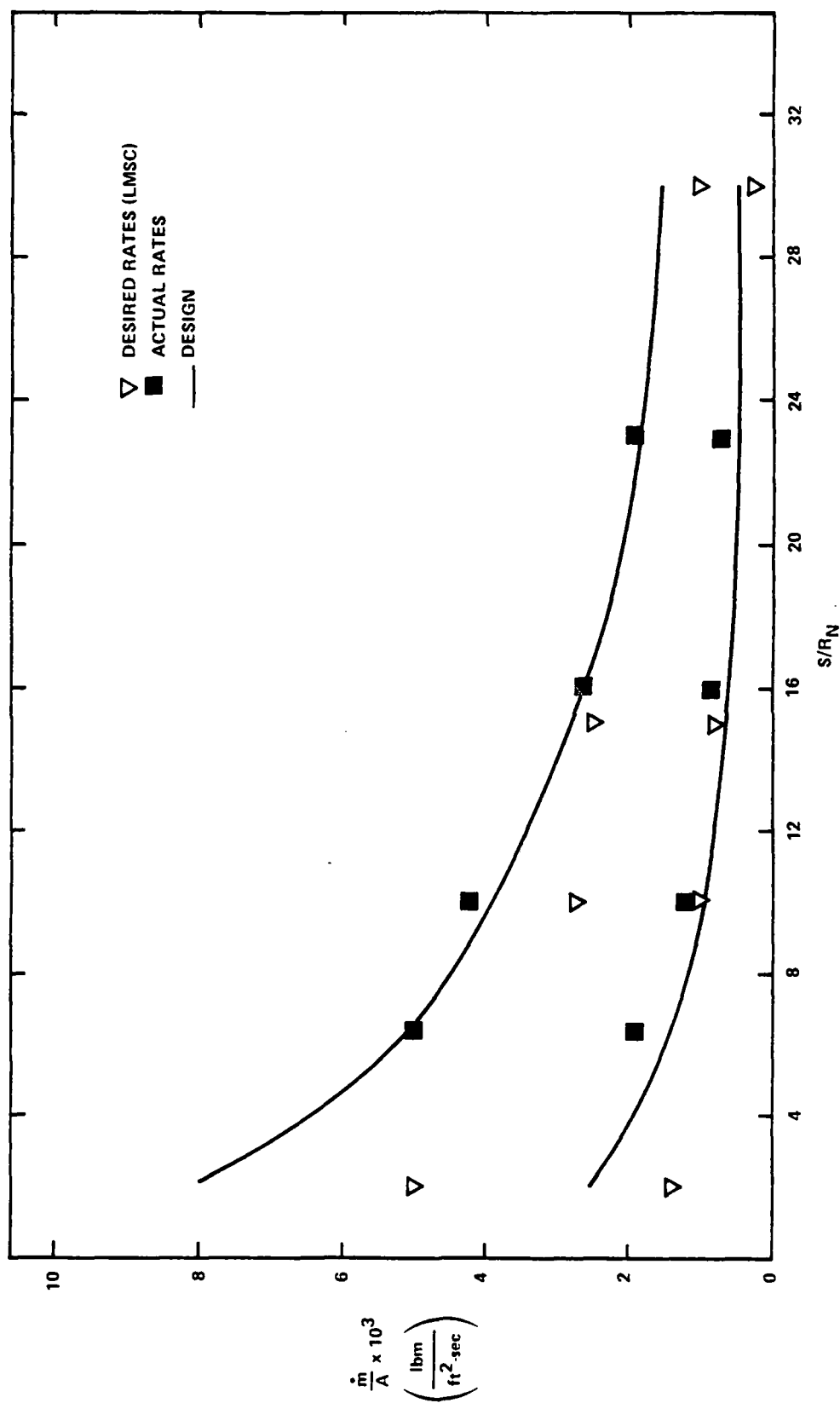


FIGURE 25A. MEASURED BLOWING DISTRIBUTION - TYPE NOMINAL

$$\frac{S}{R_N} = 5.2$$

$$P_\infty U_\infty = 0.23 \frac{\text{lbm}}{\text{ft}^2 \cdot \text{sec}}$$

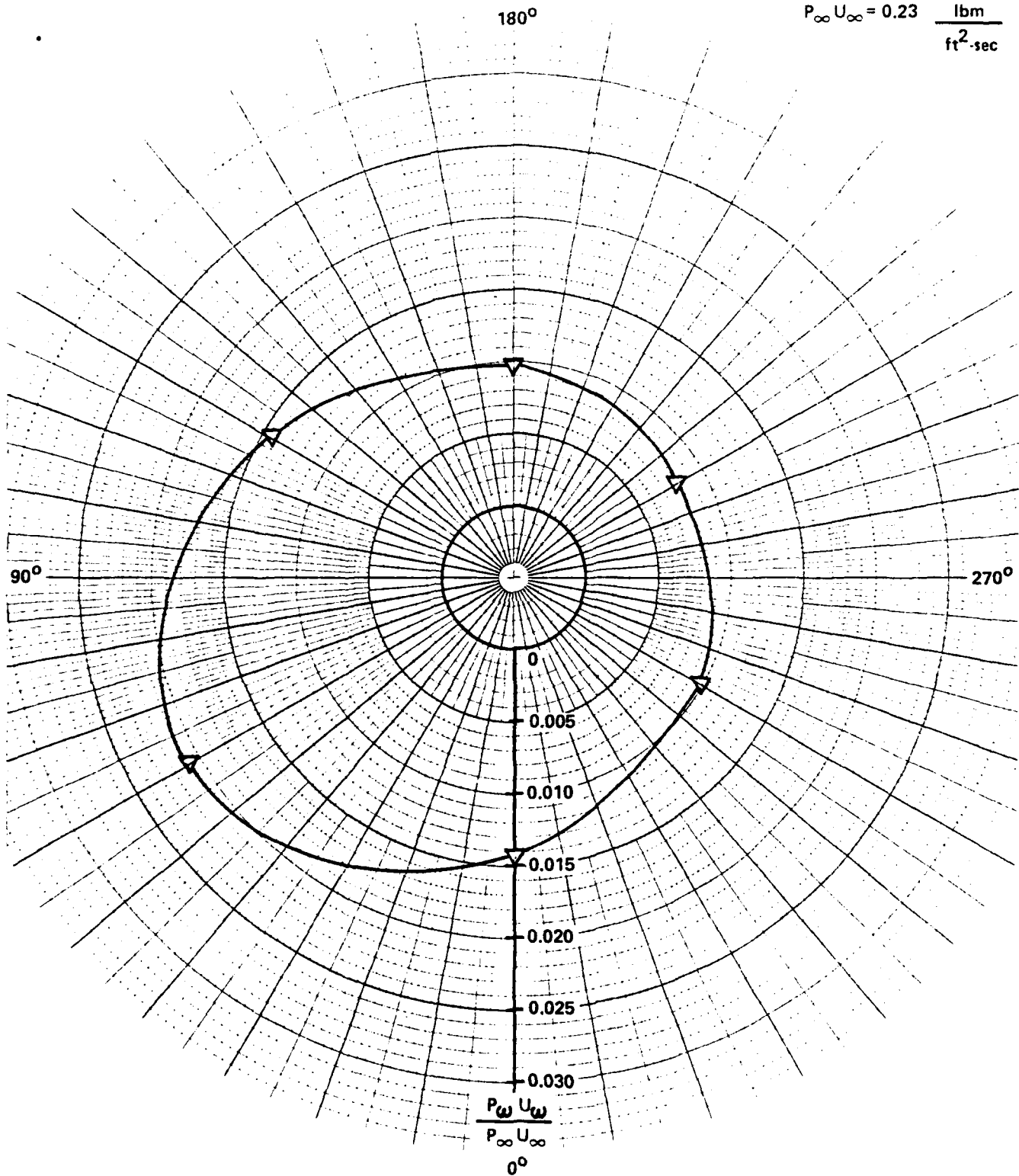


FIGURE 25B. MEASURED BLOWING DISTRIBUTION - TYPE NOMINAL

$$\frac{S}{R_N} = 10.4$$

$$P_\infty U_\infty = 0.23 \frac{\text{lbm}}{\text{ft}^2 \cdot \text{sec}}$$

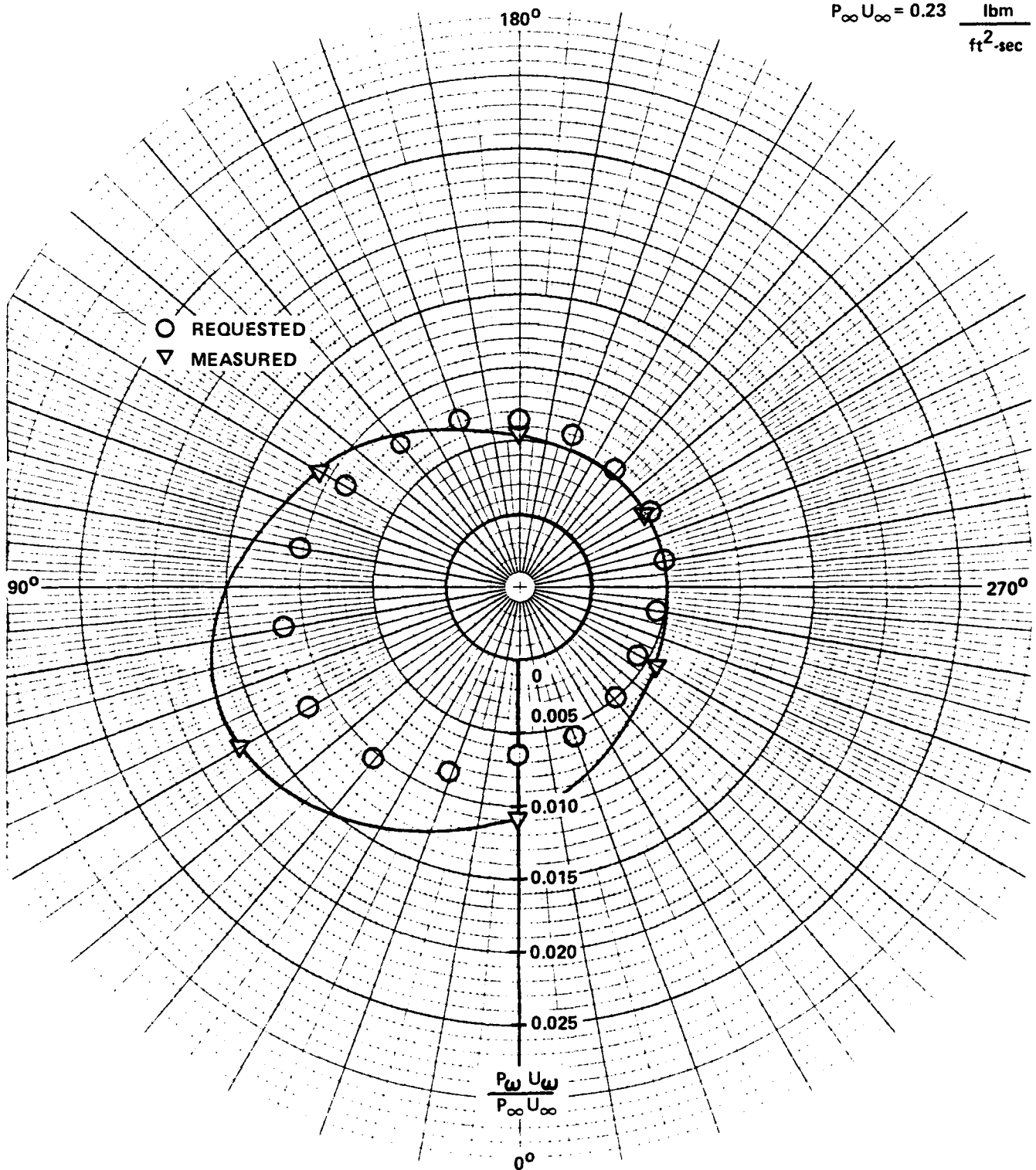


FIGURE 25C. MEASURED BLOWING RATES - TYPE NOMINAL

$$S/R_N = 15.1$$

$$P_\infty U_\infty = 0.23 \frac{\text{lbm}}{\text{ft}^2 \cdot \text{sec}}$$

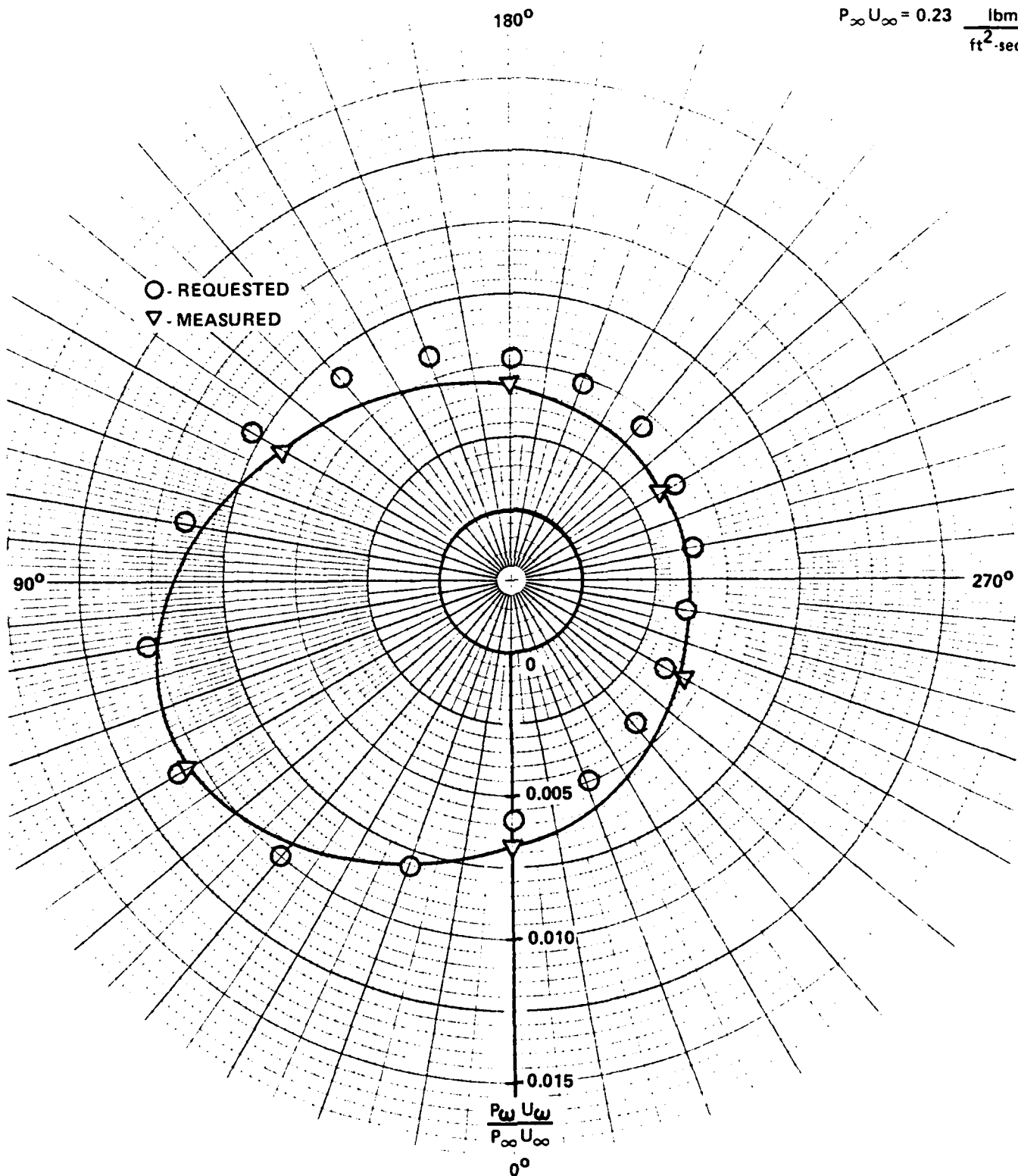


FIGURE 25D. MEASURED BLOWING DISTRIBUTION - TYPE NOMINAL

$$\frac{S}{R_N} = 23$$
$$P_\infty U_\infty = 0.23 \quad \frac{\text{lbm}}{\text{ft}^2 \cdot \text{sec}}$$

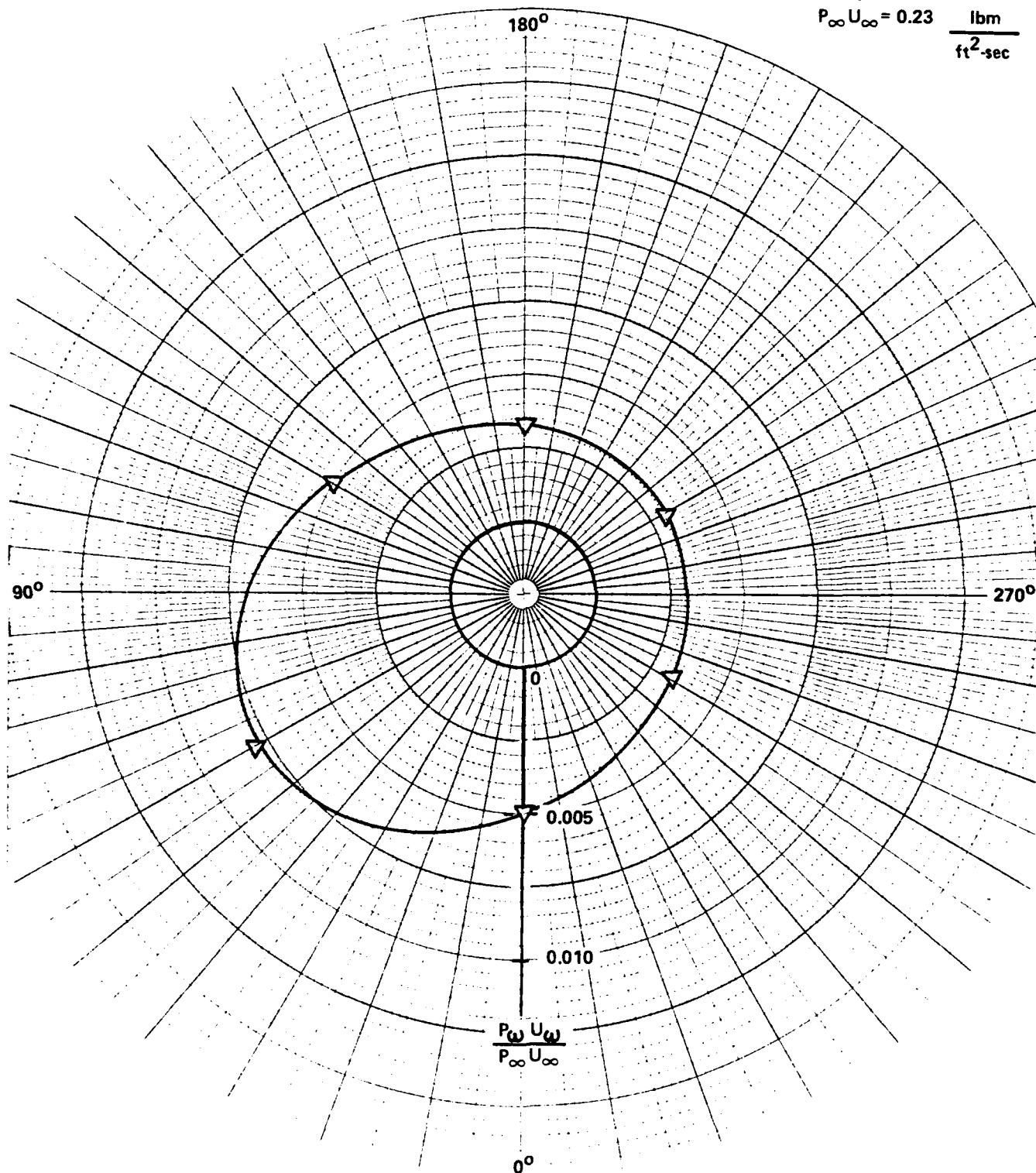


FIGURE 25E. MEASURED BLOWING DISTRIBUTION - TYPE NOMINAL



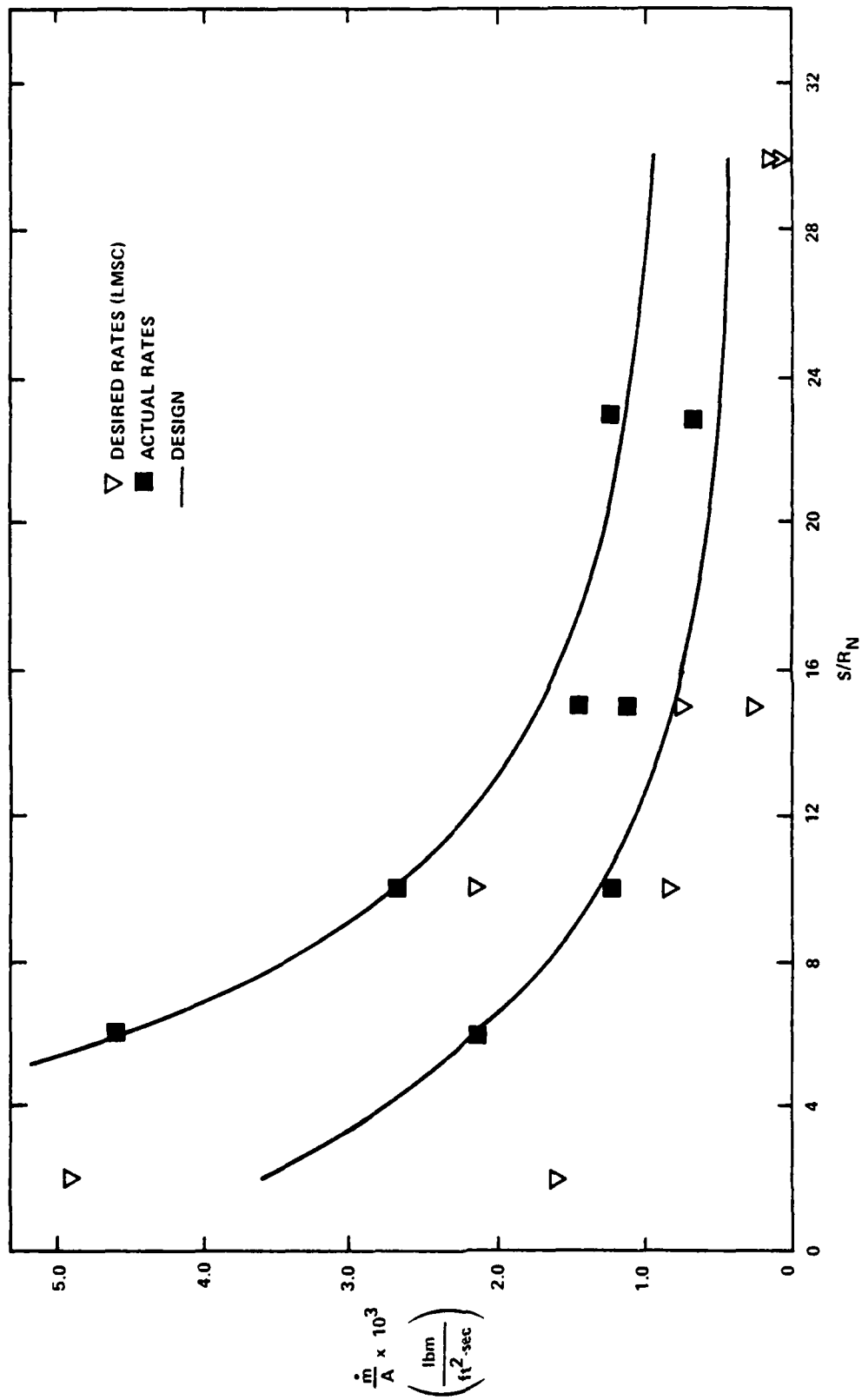


FIGURE 26A. MEASURED BLOWING DISTRIBUTION - TYPE 2

$$S/R_N = 5.2$$

$$P_\infty U_\infty = 0.23 \frac{\text{lbm}}{\text{ft}^2 \cdot \text{sec}}$$

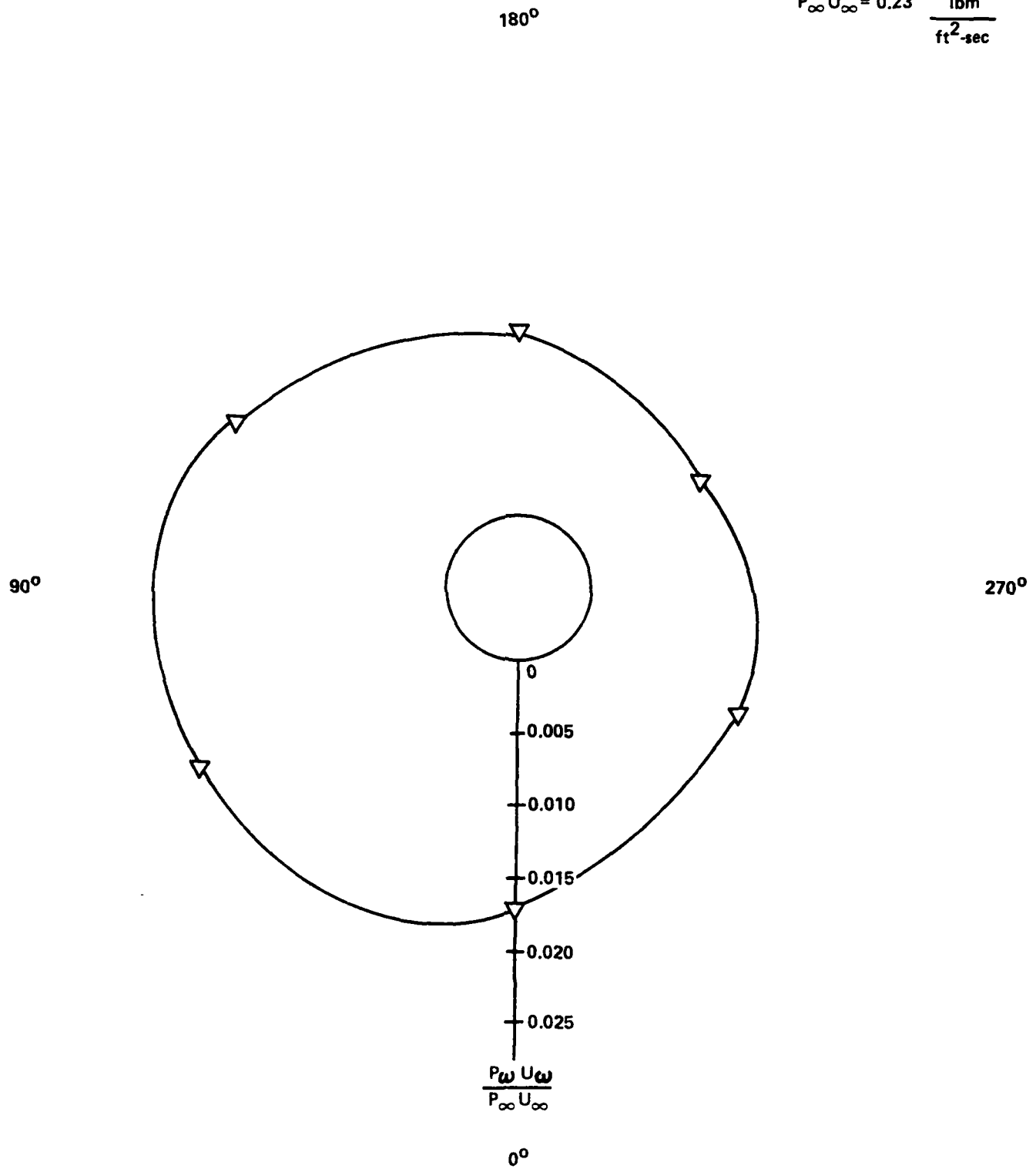


FIGURE 26B. MEASURED BLOWING DISTRIBUTION - TYPE 2

$$\frac{S}{R_N} = 10.4$$

$$P_\infty U_\infty = 0.23 \frac{\text{lbm}}{\text{ft}^2 \cdot \text{sec}}$$

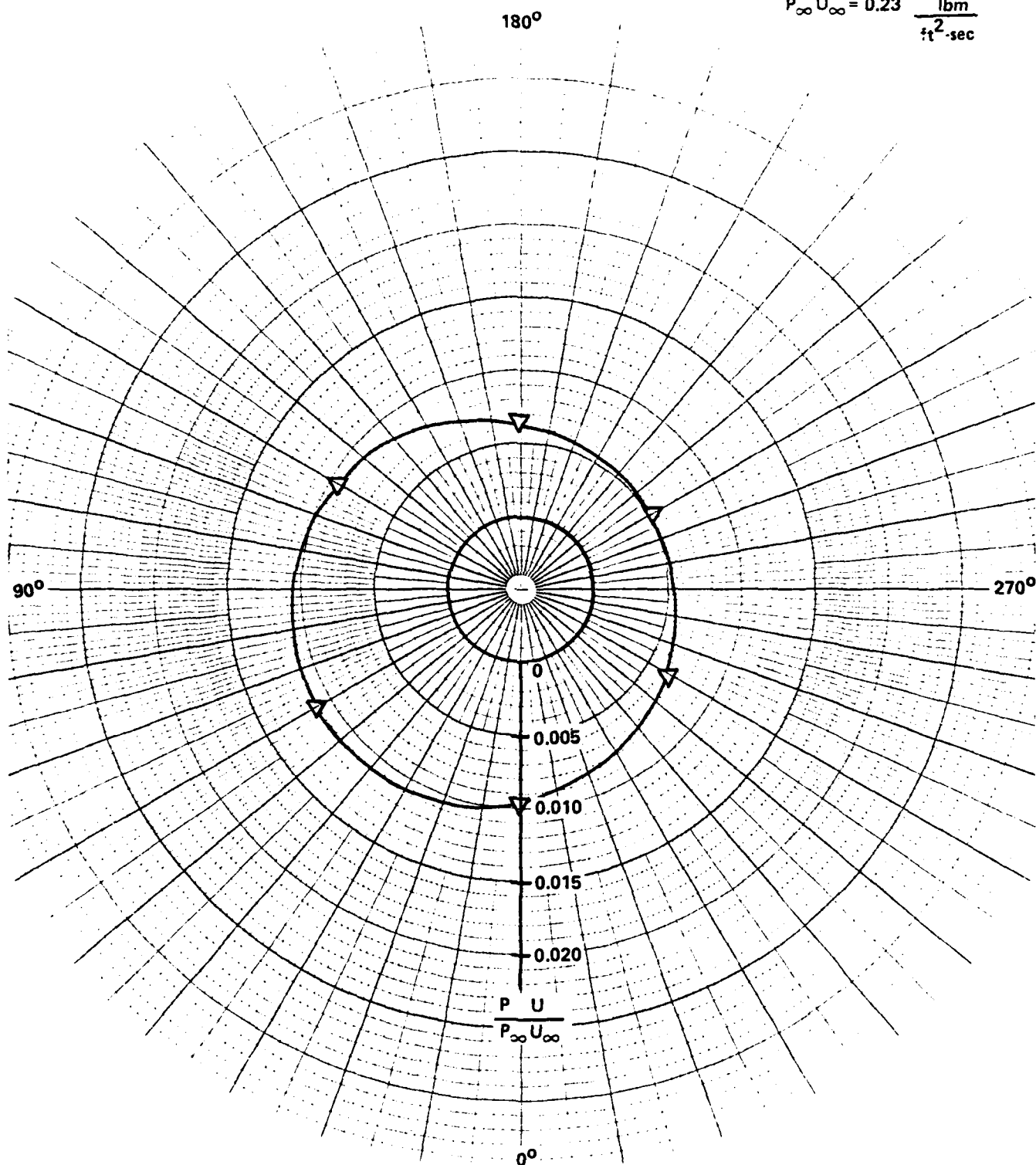


FIGURE 26C. MEASURED BLOWING DISTRIBUTION - TYPE 2

$$\frac{S}{R_N} = 15.1$$

$$P_\infty U_\infty = 0.23 \frac{\text{lbm}}{\text{ft}^2 \cdot \text{sec}}$$

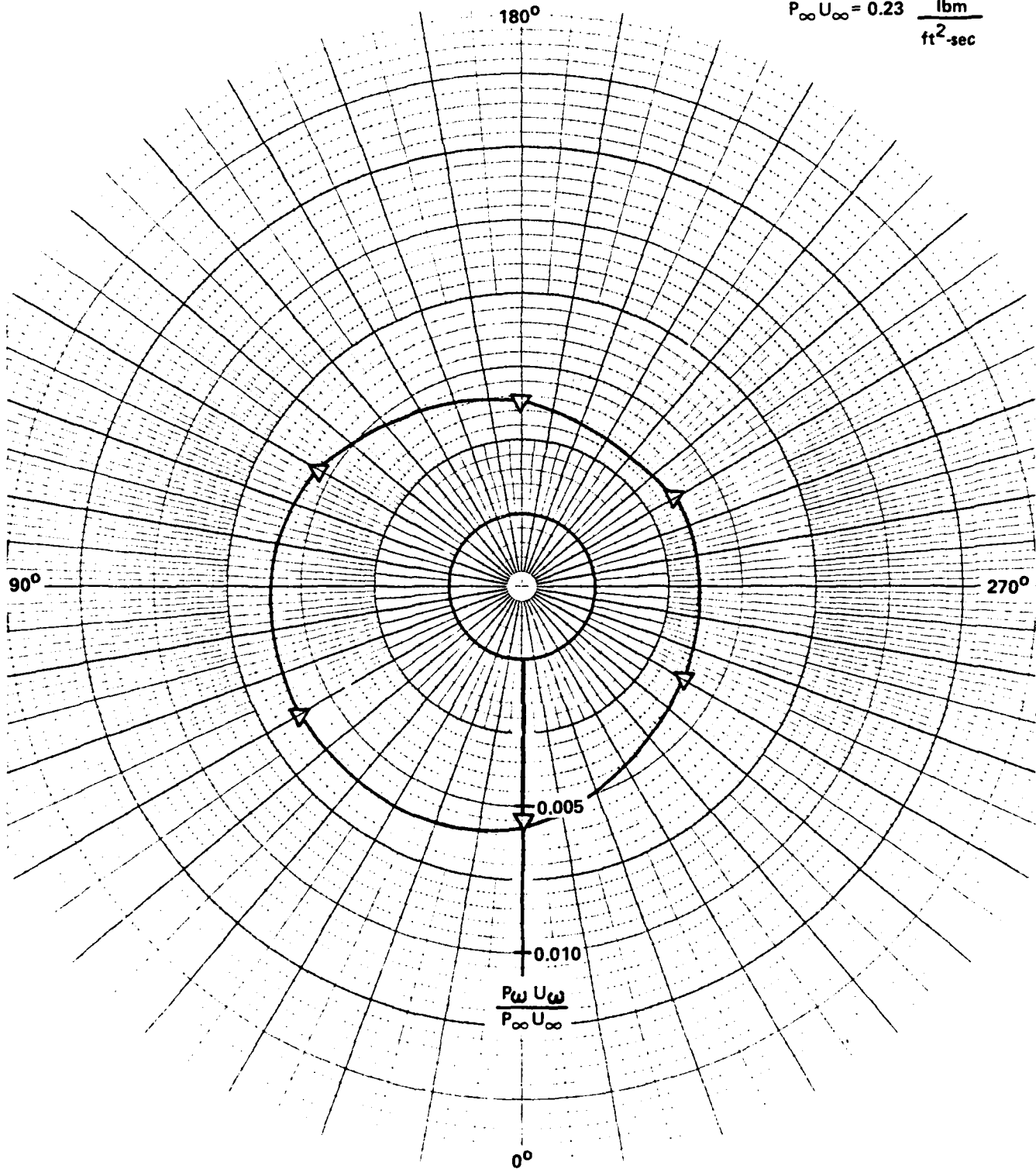


FIGURE 26D. MEASURED BLOWING DISTRIBUTION - TYPE 2

$$\frac{S}{R_N} = 23$$

$$P_\infty U_\infty = 0.23 \frac{\text{lbm}}{\text{ft}^2 \cdot \text{sec}}$$

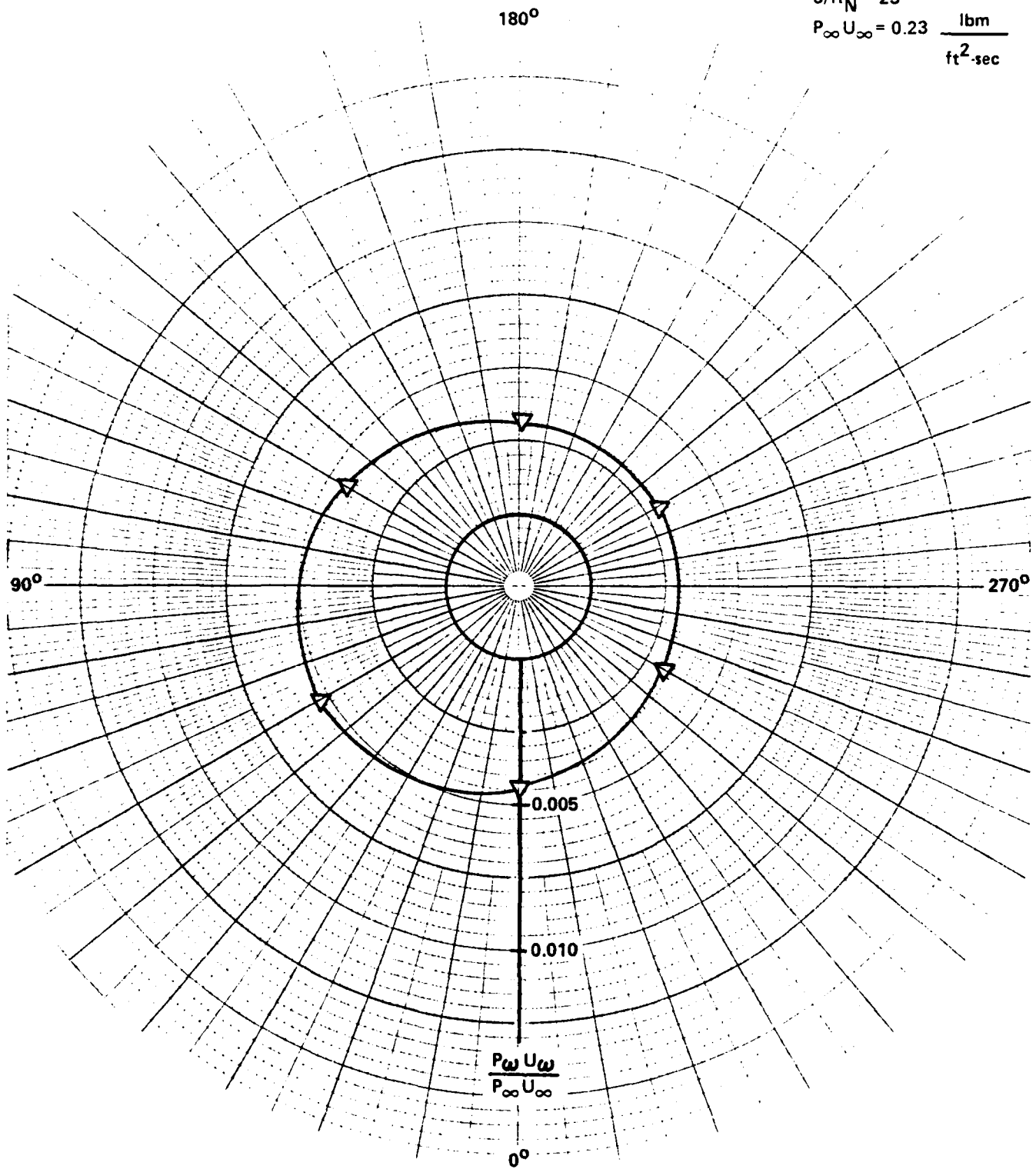


FIGURE 26E. MEASURED BLOWING DISTRIBUTION - TYPE 2

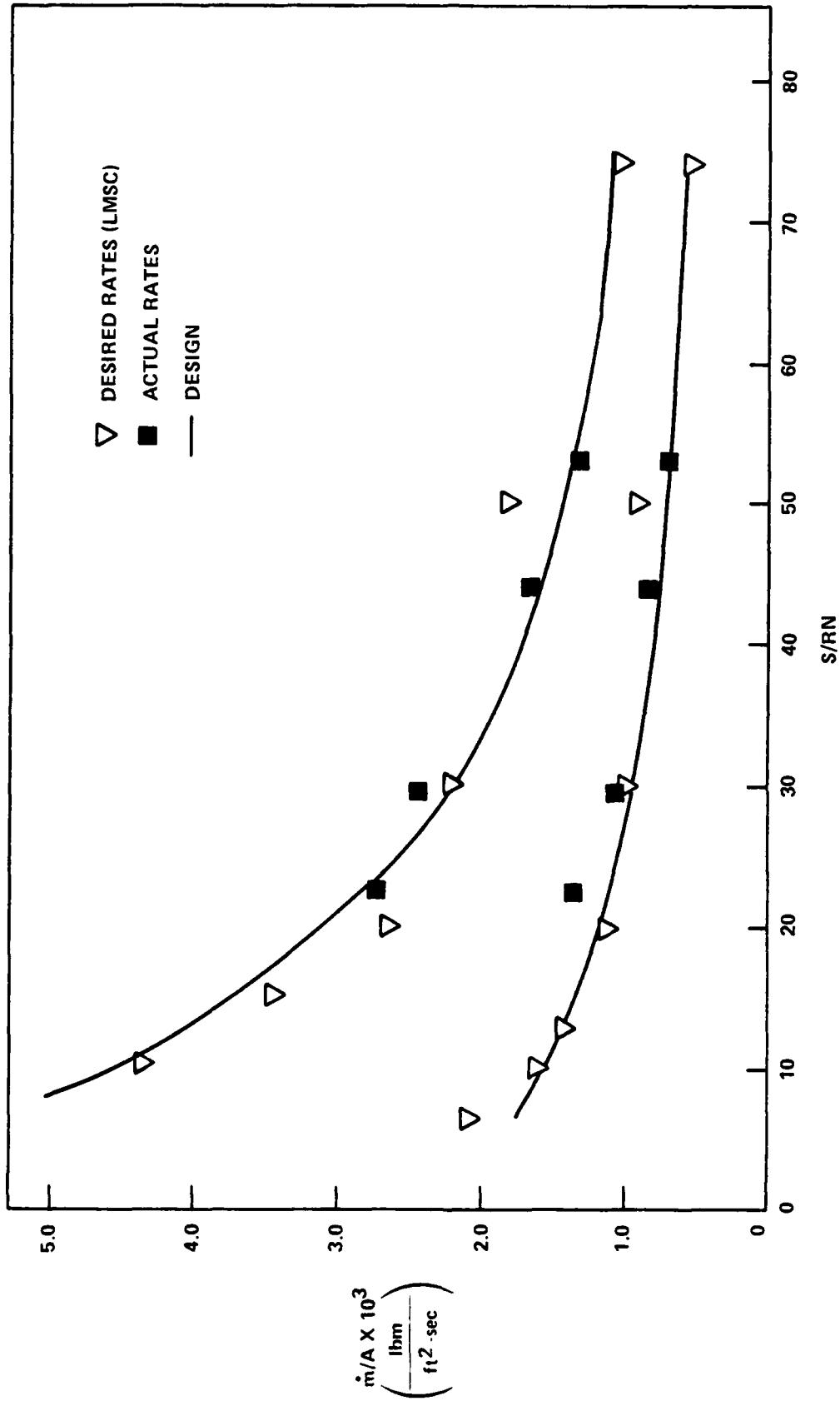


FIGURE 27A. MEASURED BLOWING DISTRIBUTION - TYPE 4

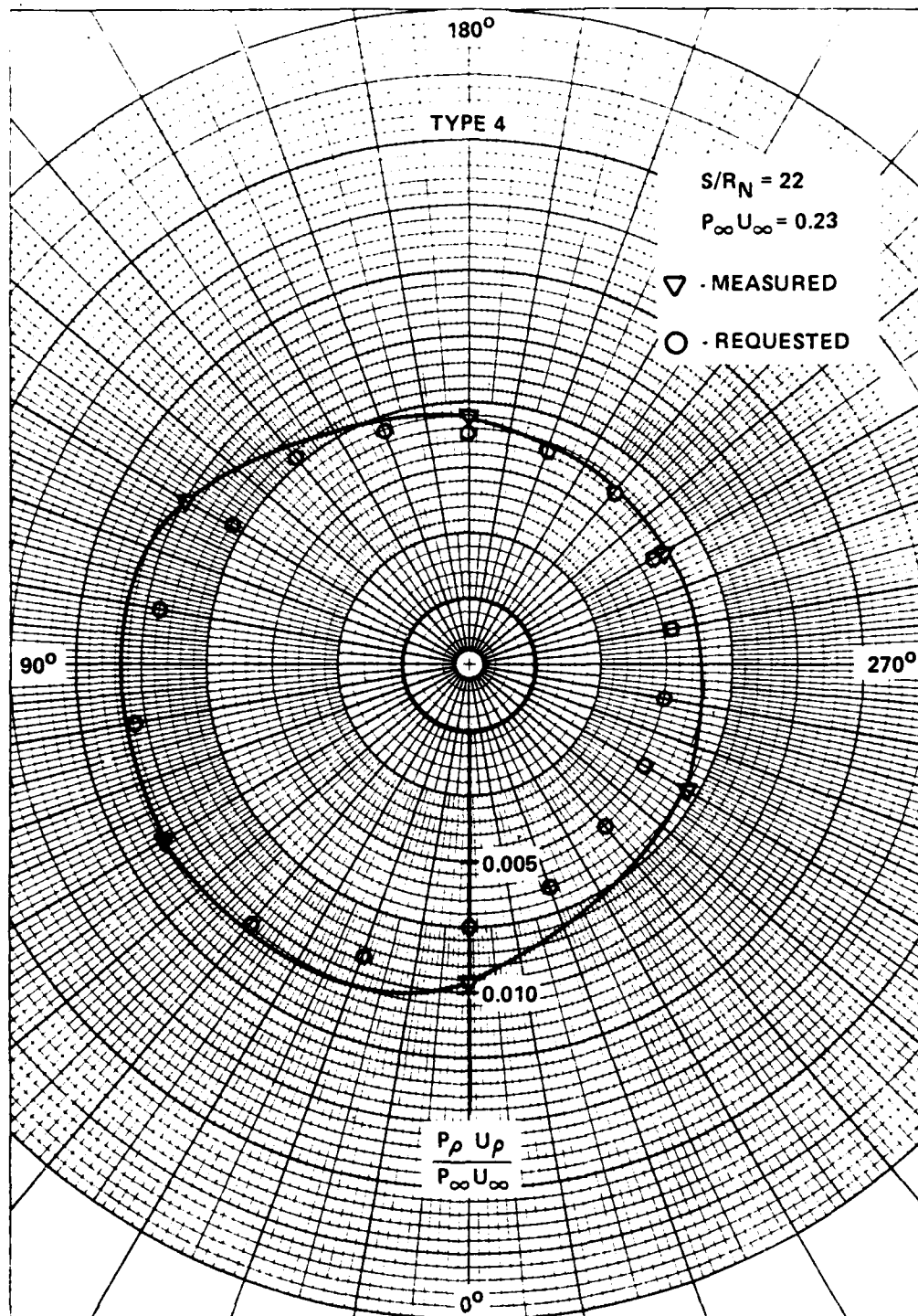


FIGURE 27B. MEASURED BLOWING DISTRIBUTION - TYPE 4

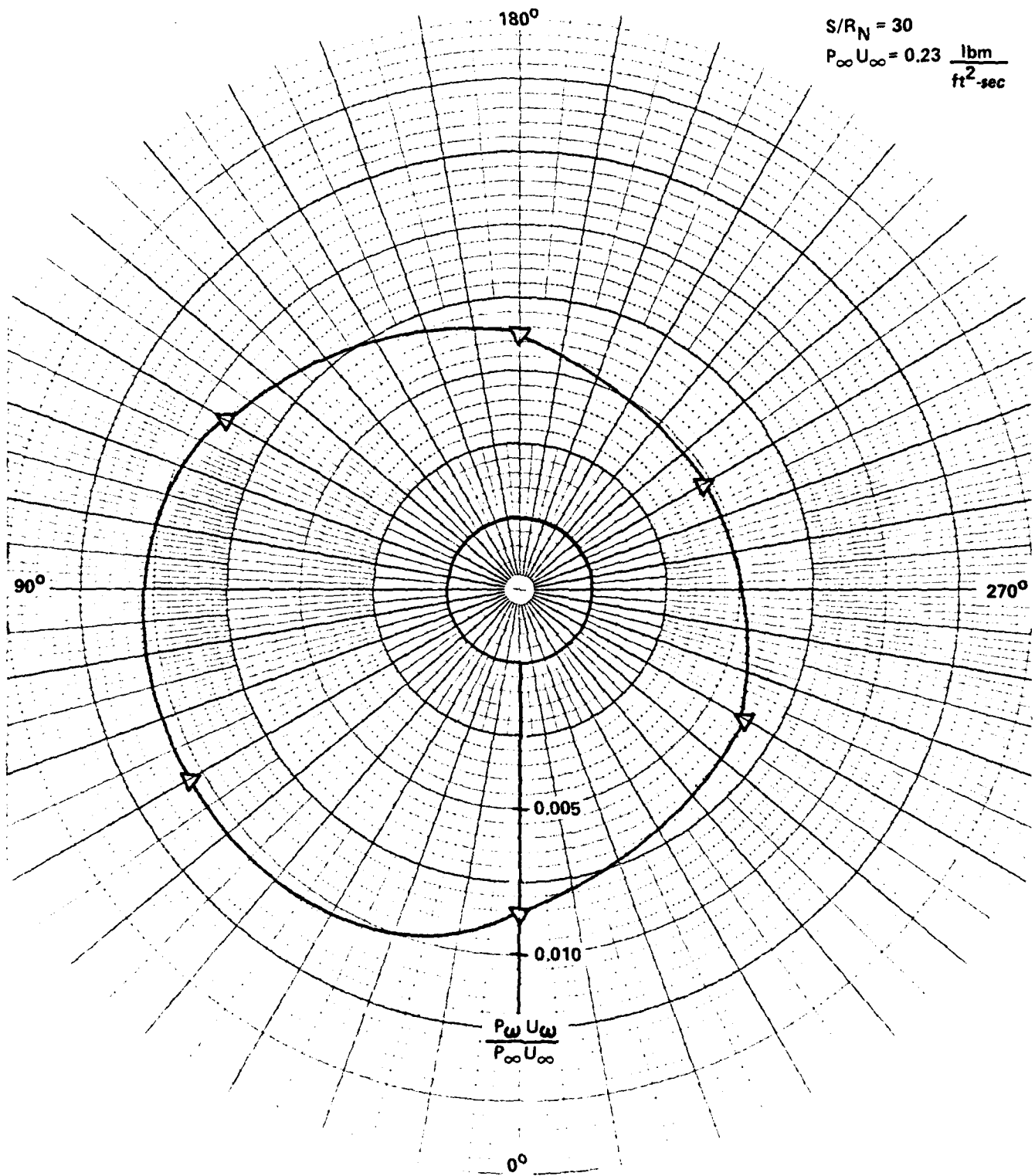


FIGURE 27C. MEASURED BLOWING DISTRIBUTION - TYPE 4



$$S/R_N = 44$$

$$P_\infty U_\infty = 0.23 \frac{\text{lbm}}{\text{ft}^2 \cdot \text{sec}}$$

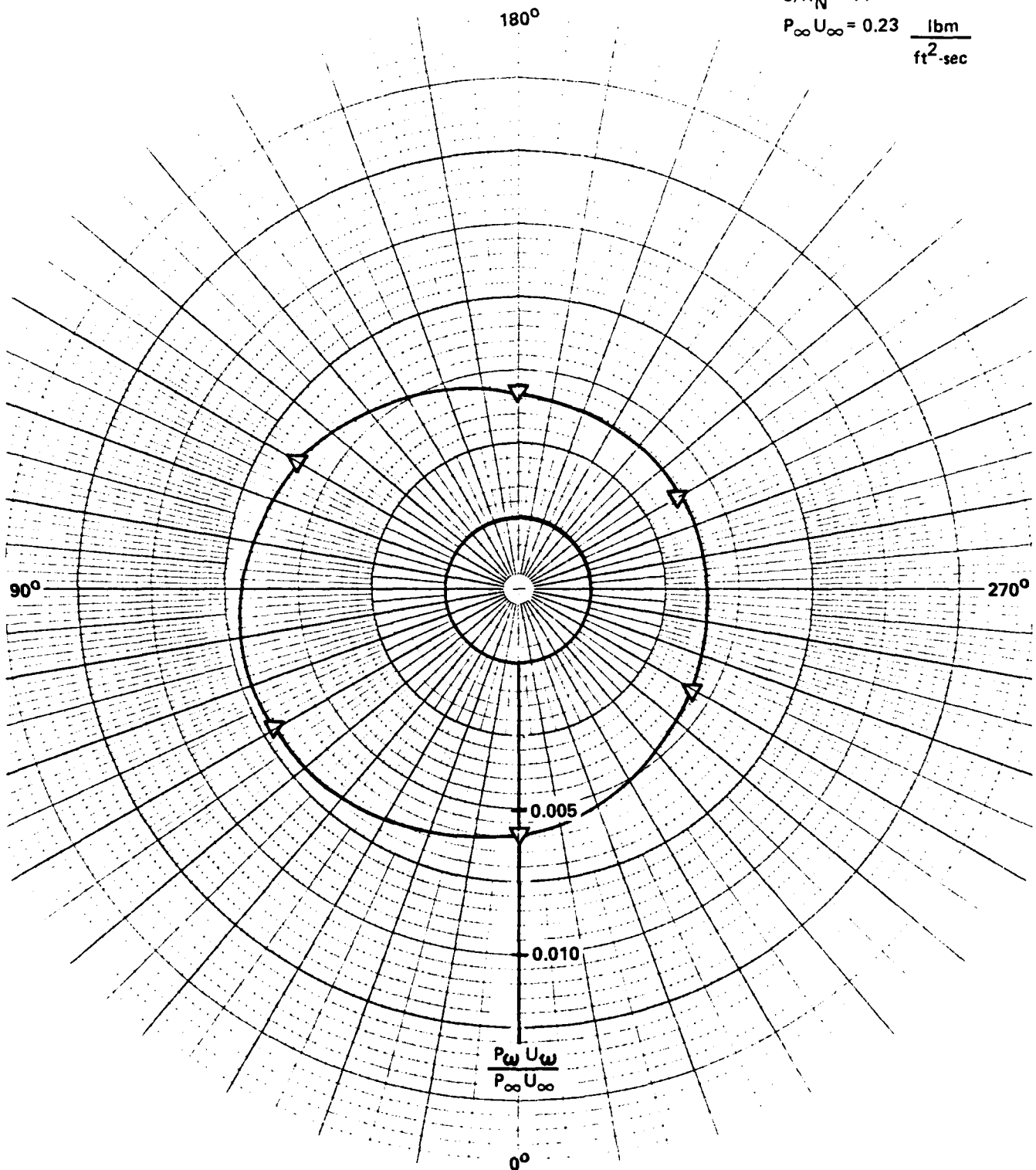


FIGURE 27D. MEASURED BLOWING DISTRIBUTION - TYPE 4

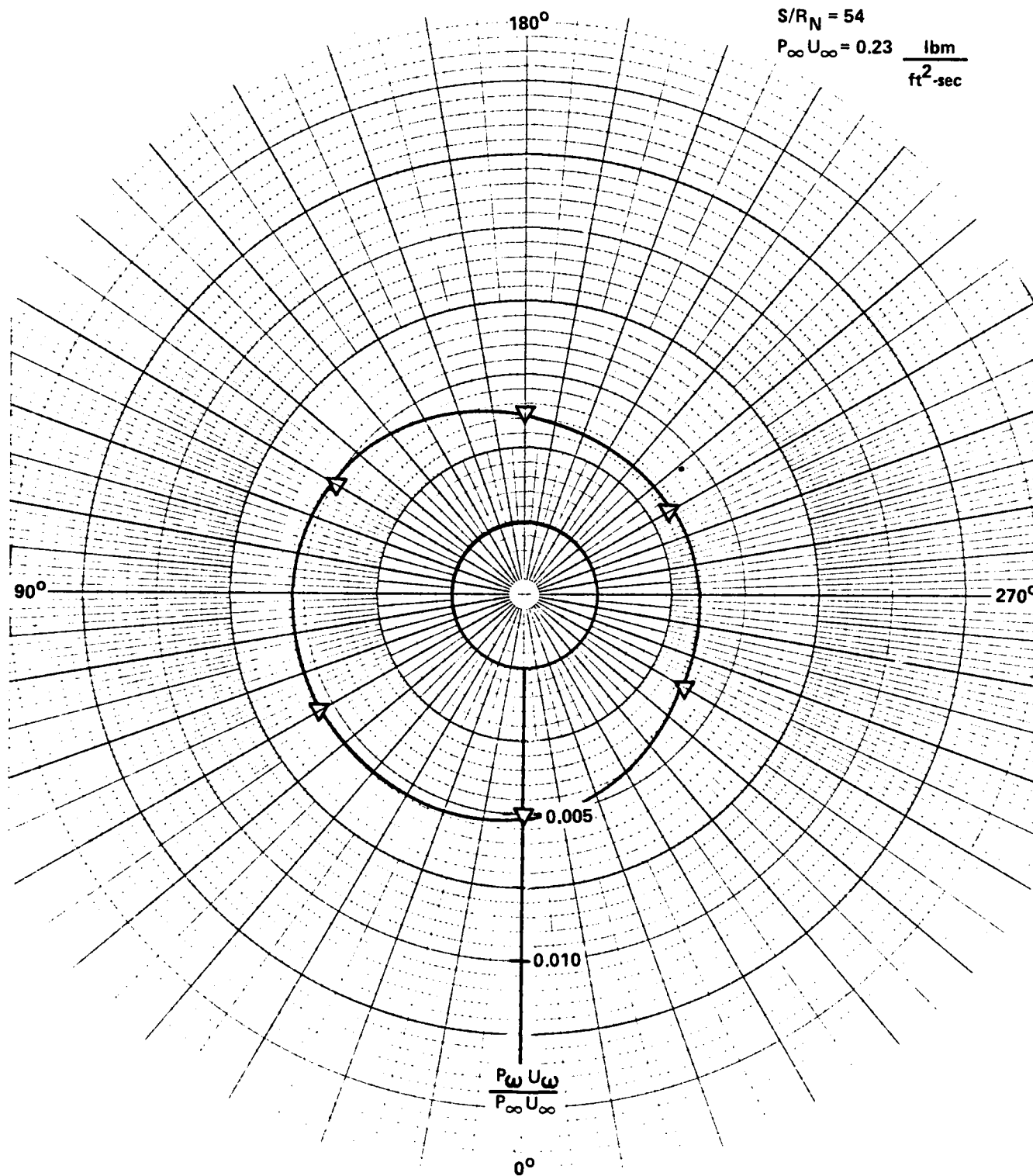


FIGURE 27E. MEASURED BLOWING DISTRIBUTION - TYPE 4

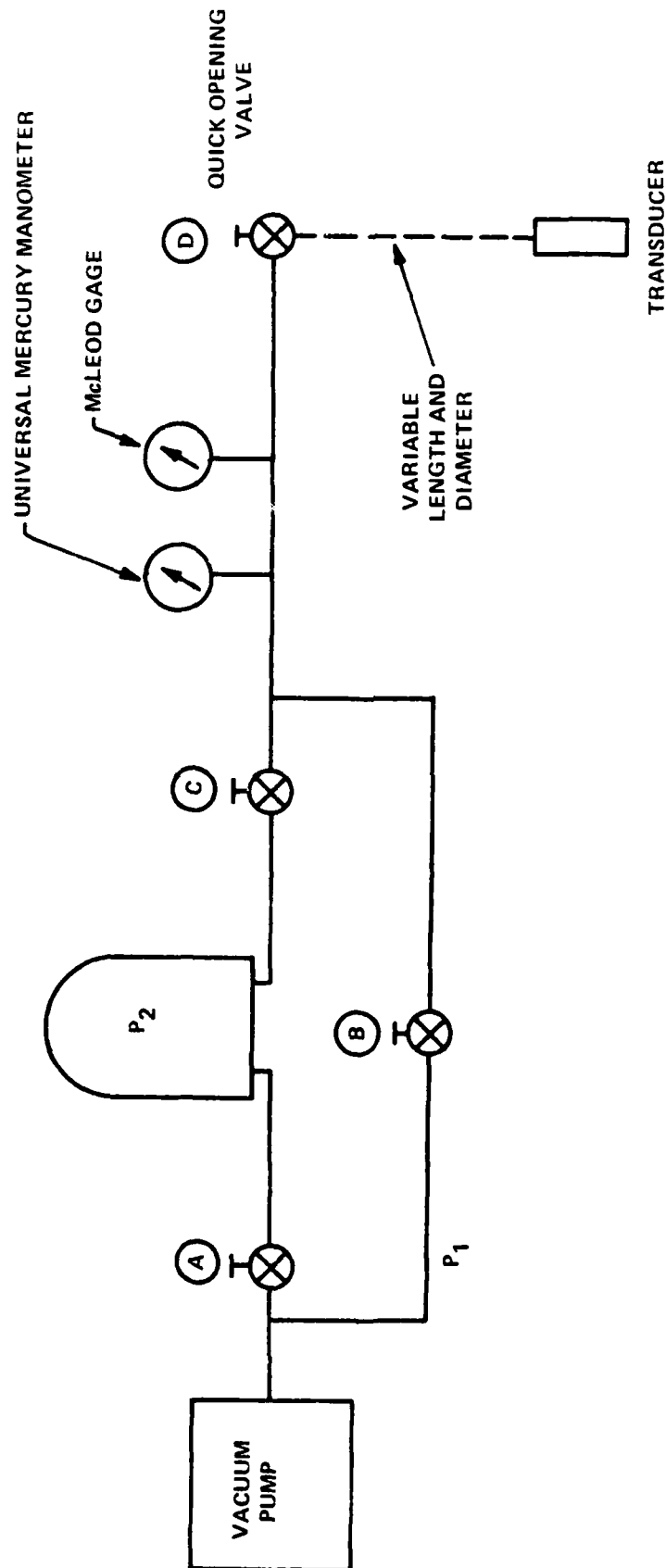


FIGURE 28. CALIBRATION SETUP

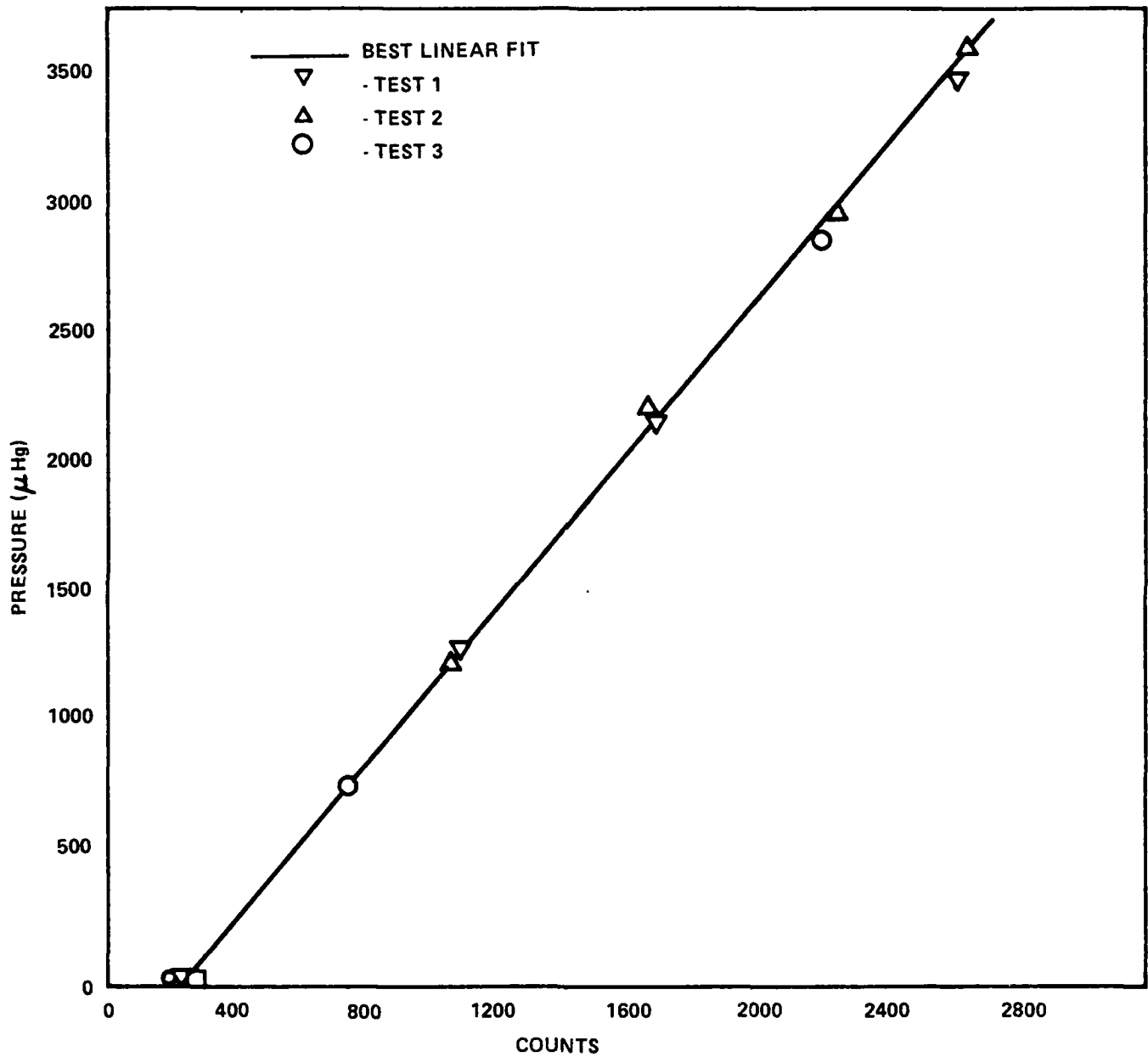


FIGURE 29. CALIBRATION OF TYPICAL TRANSDUCER

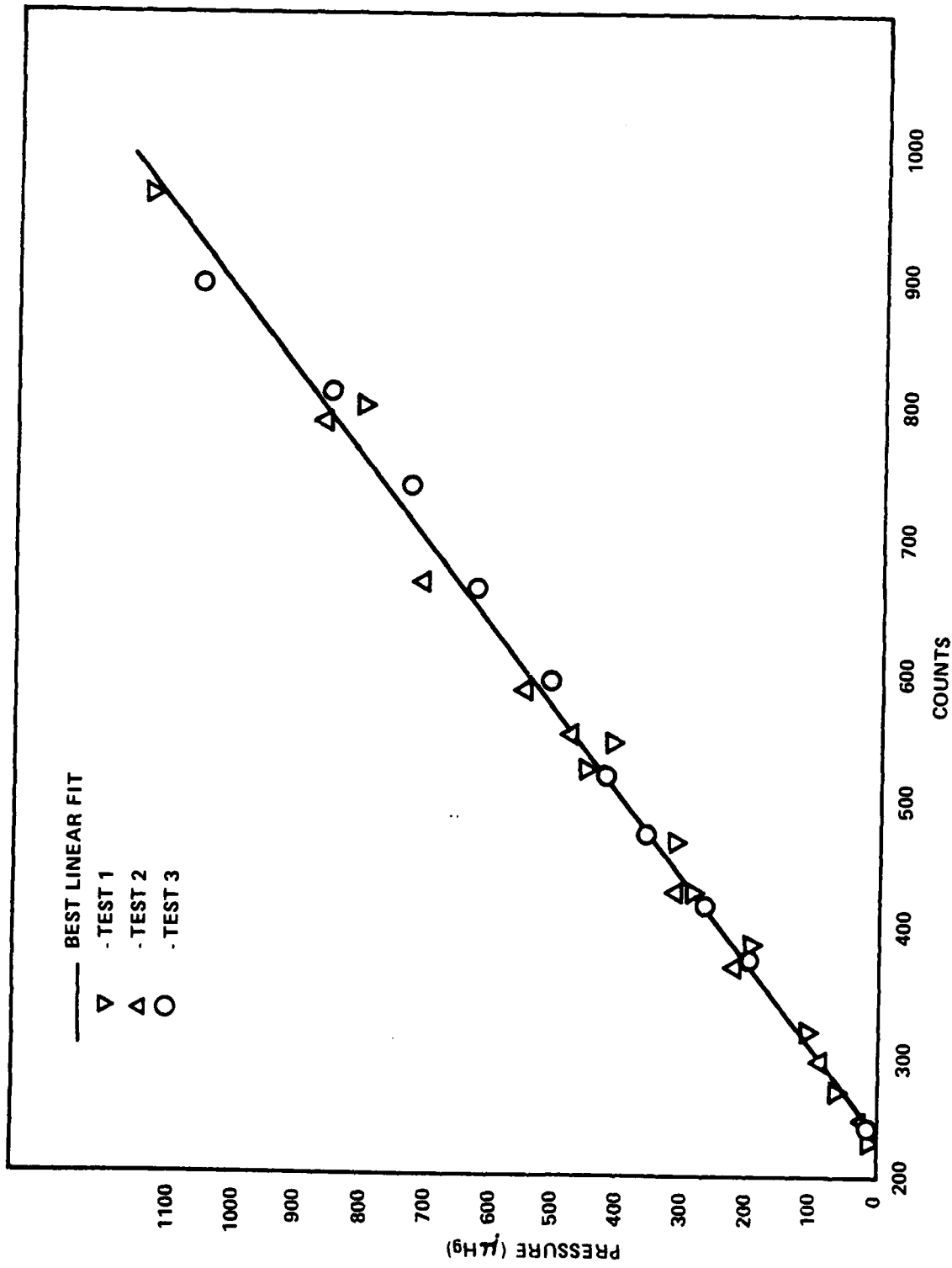


FIGURE 30. REPEATABILITY OF CALIBRATION

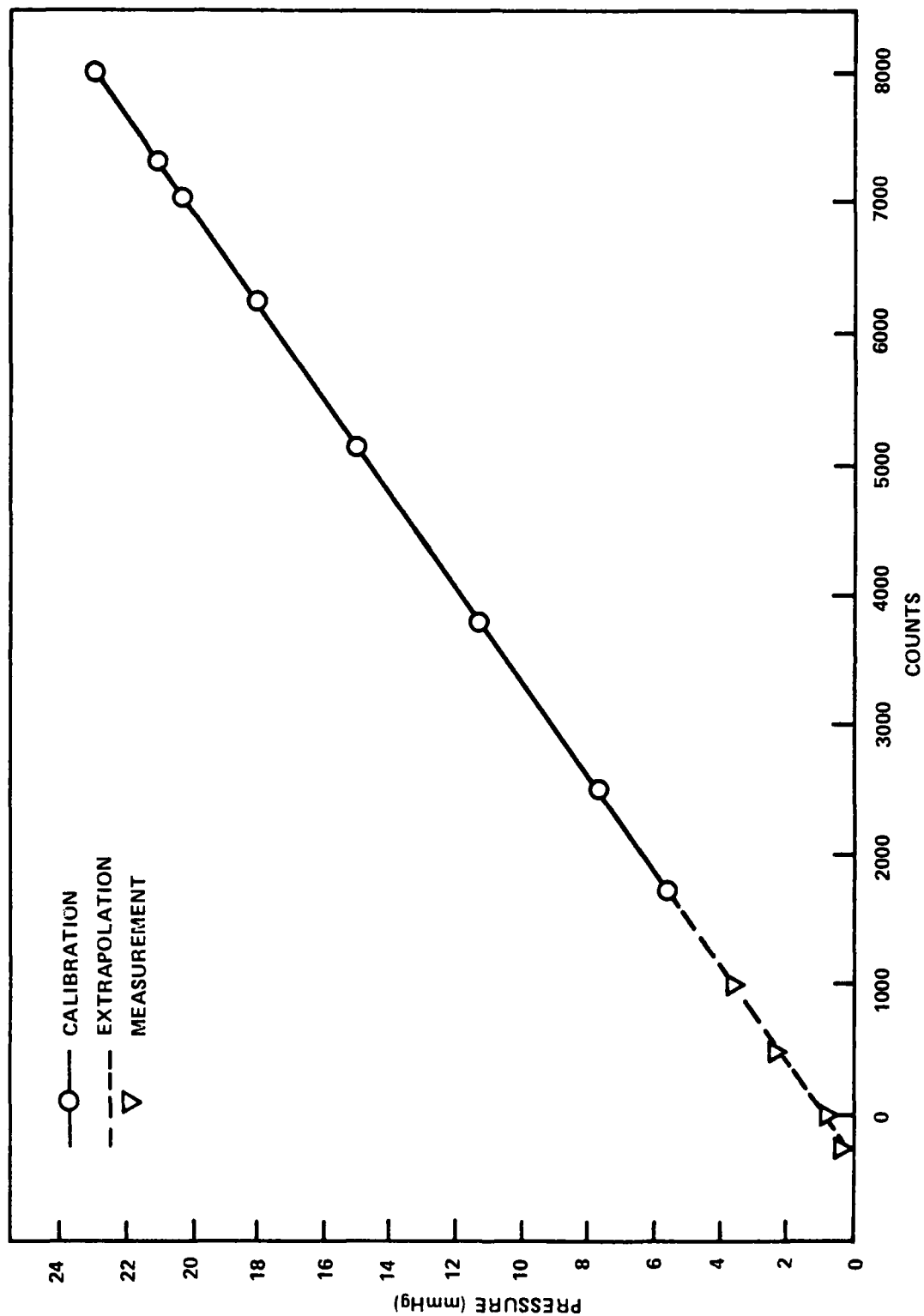


FIGURE 31. EXTRAPOLATED CALIBRATION CURVE

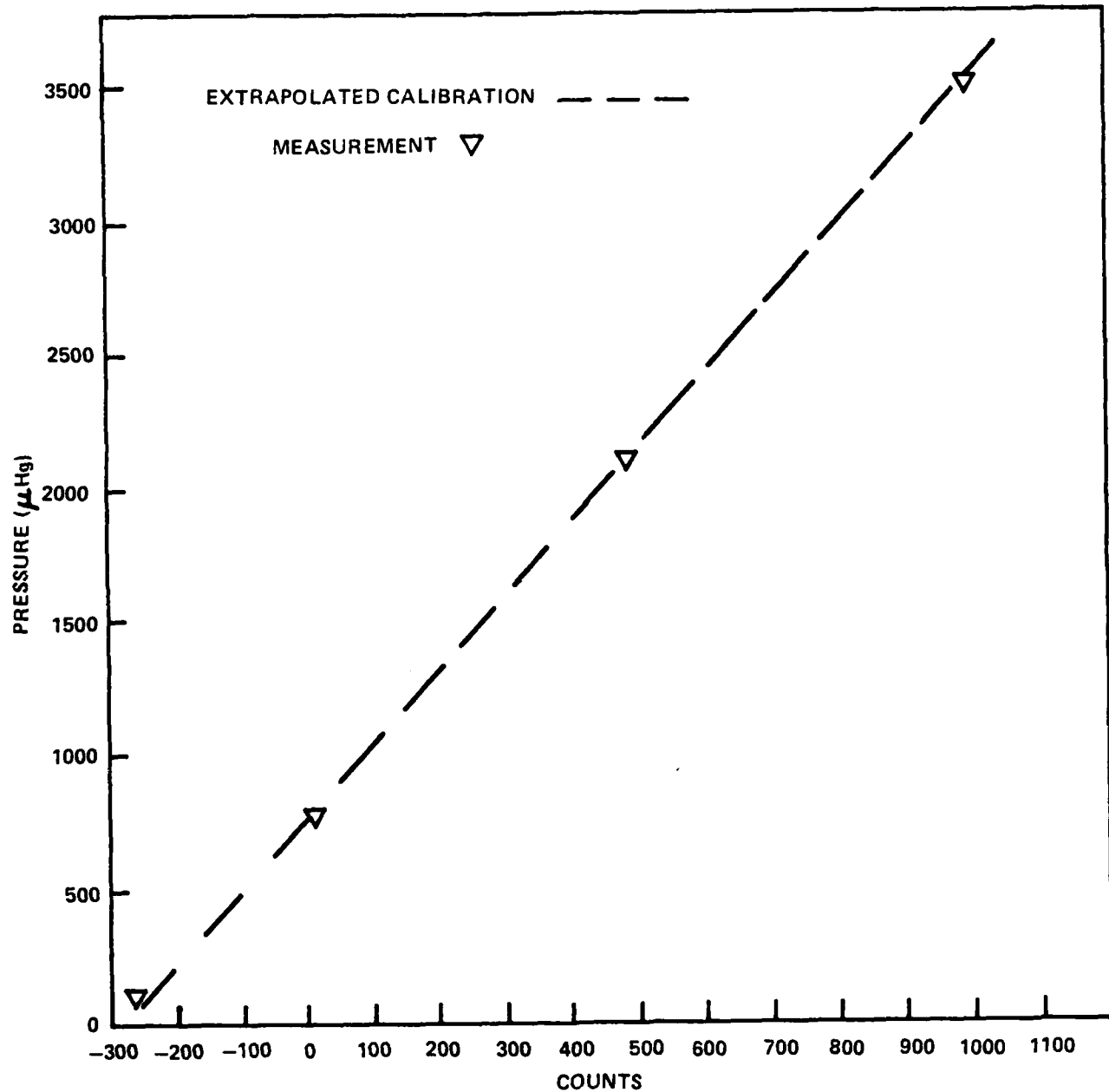


FIGURE 32. COMPARISON OF EXTRAPOLATED TO ACTUAL CALIBRATION

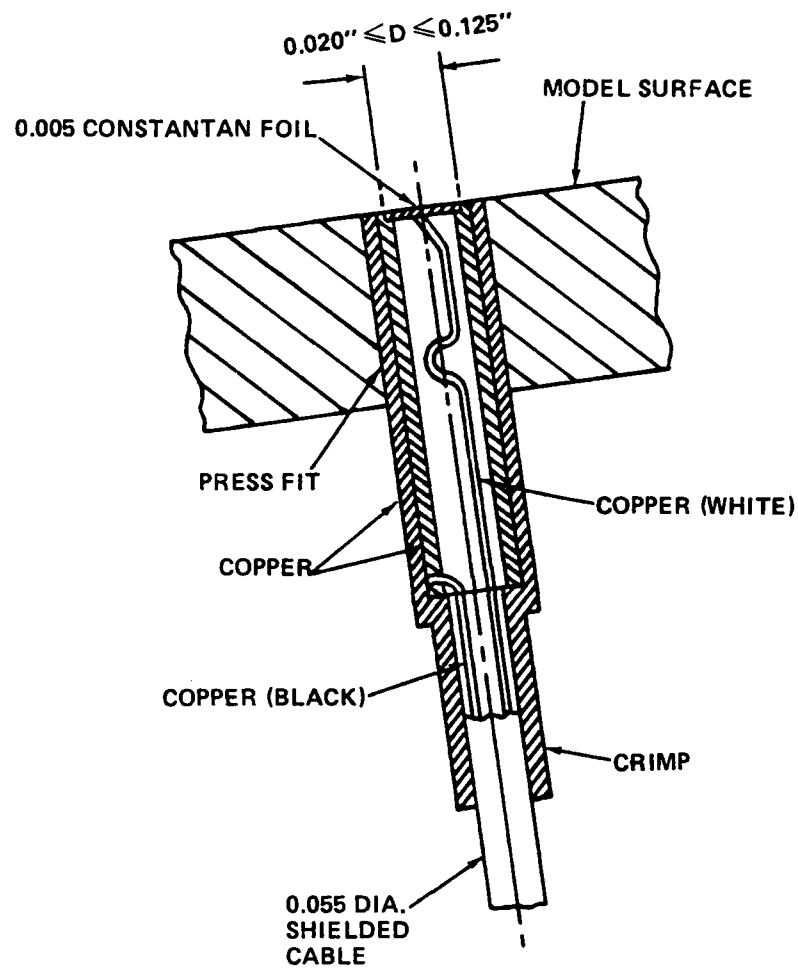


FIGURE 33. SCHEMATIC OF GARDON GAGE INSTALLATION



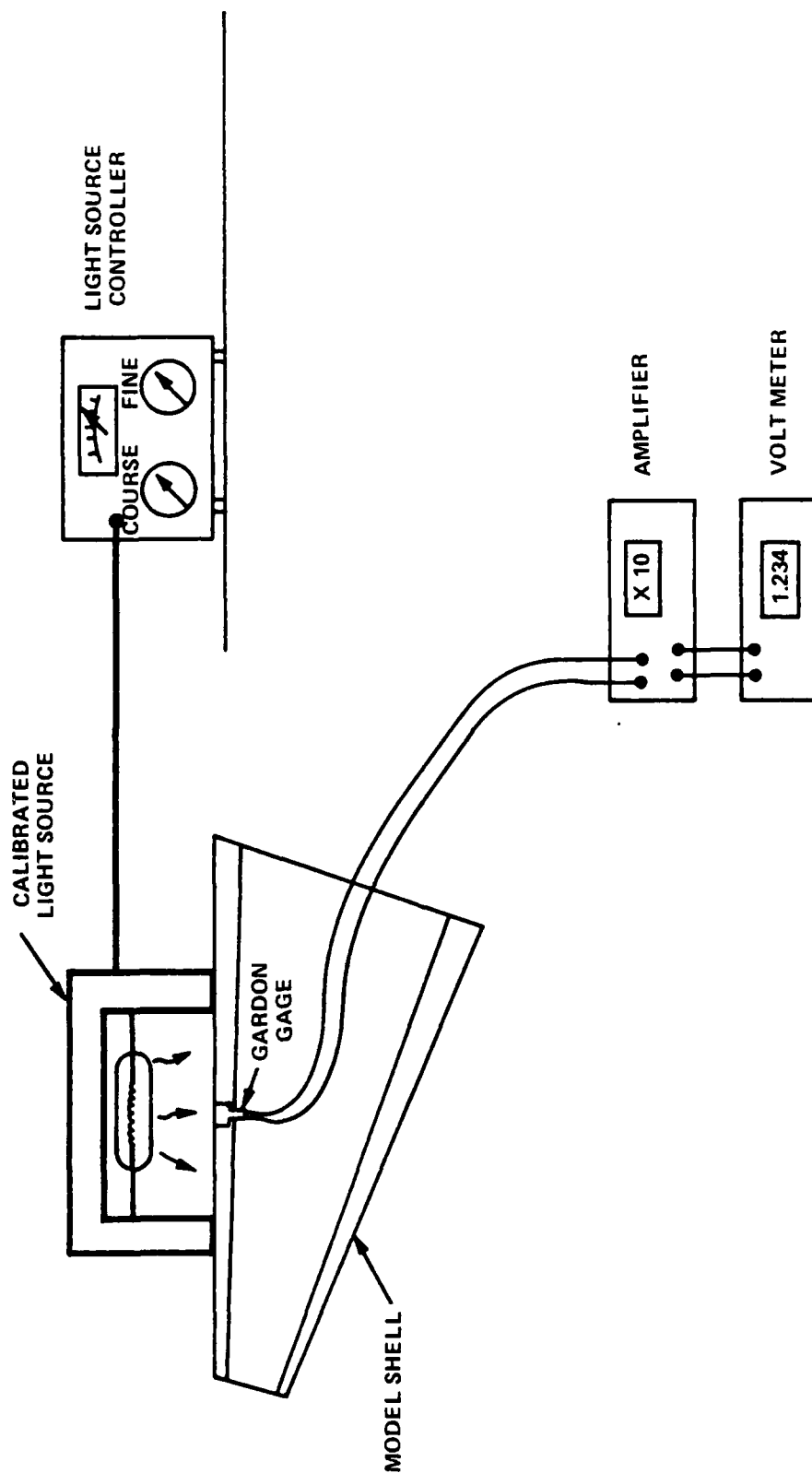


FIGURE 34. SCHEMATIC OF GARDON GAGE CALIBRATION SETUP



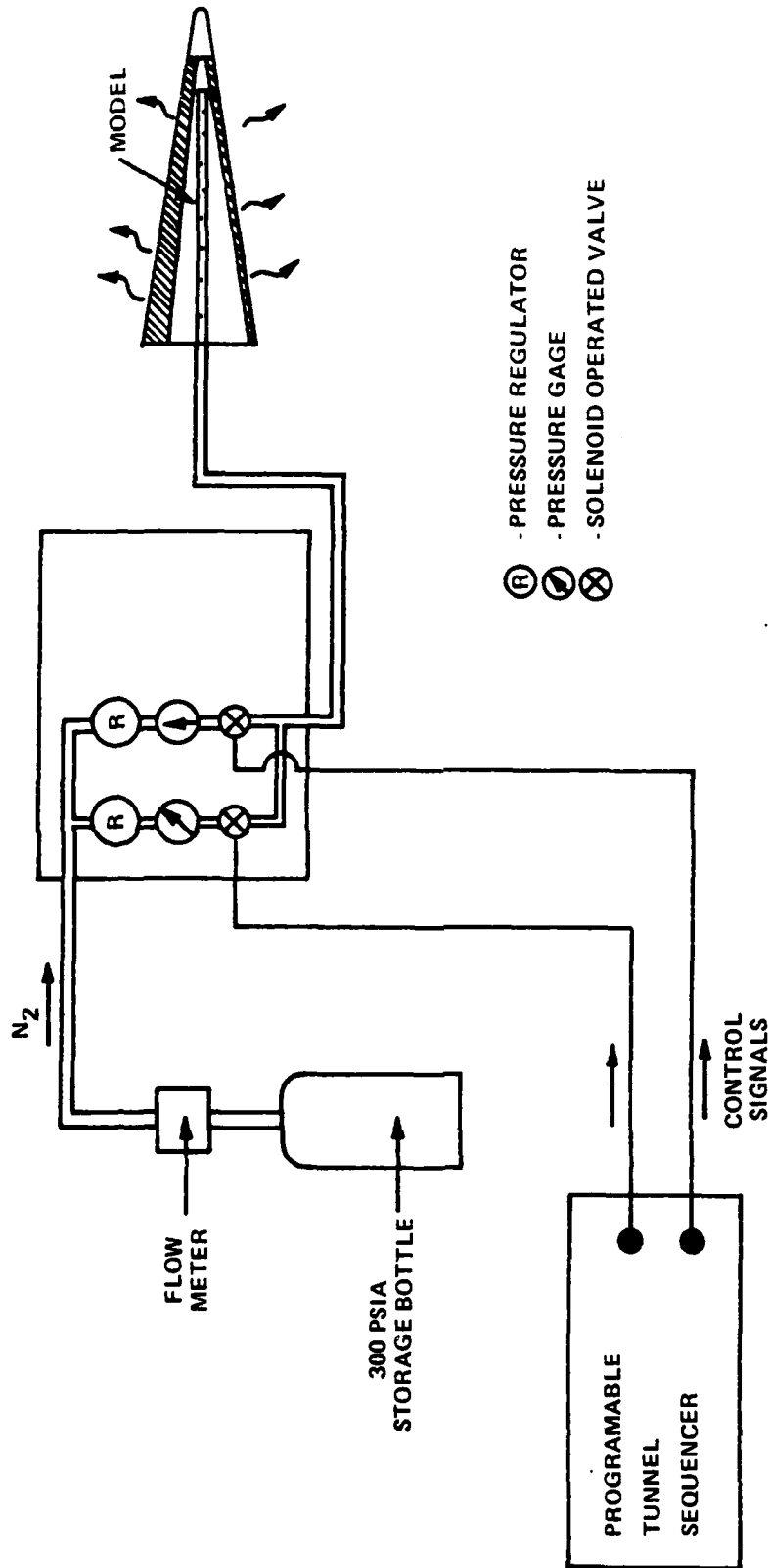


FIGURE 36. NITROGEN SUPPLY SYSTEM

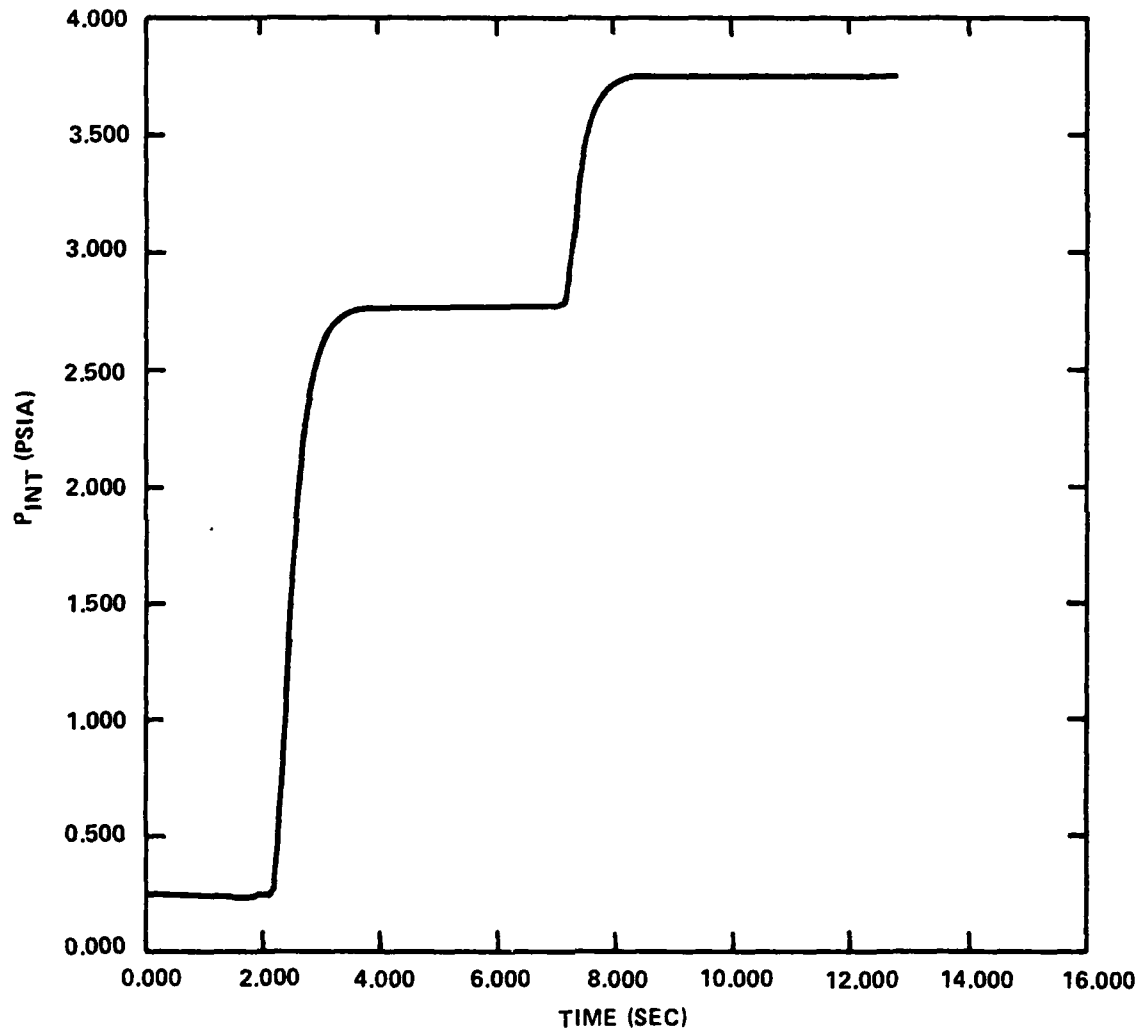


FIGURE 37. TIMING FOR CHANGING MASS FLOW RATES

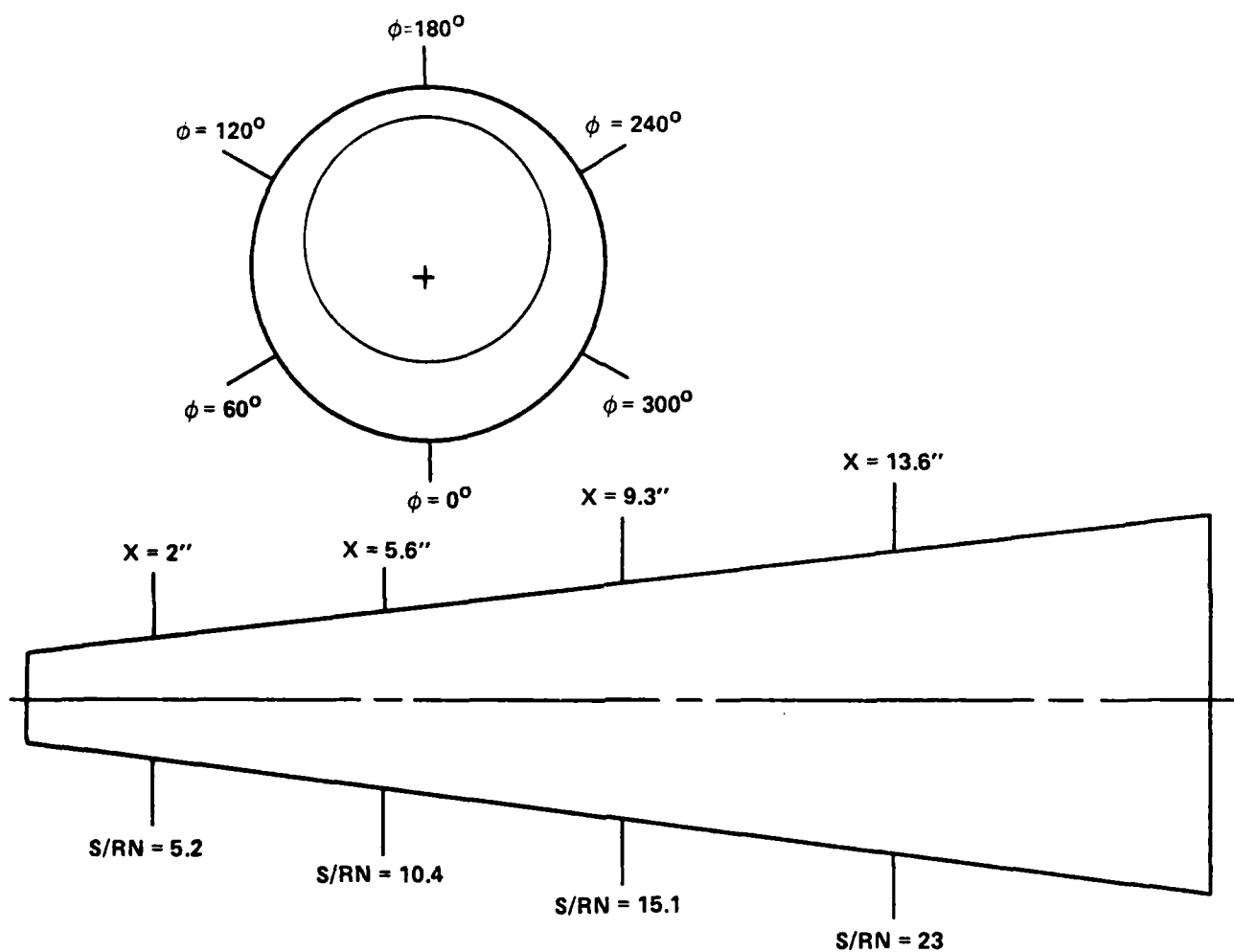


FIGURE 38. INSTRUMENTATION LOCATIONS

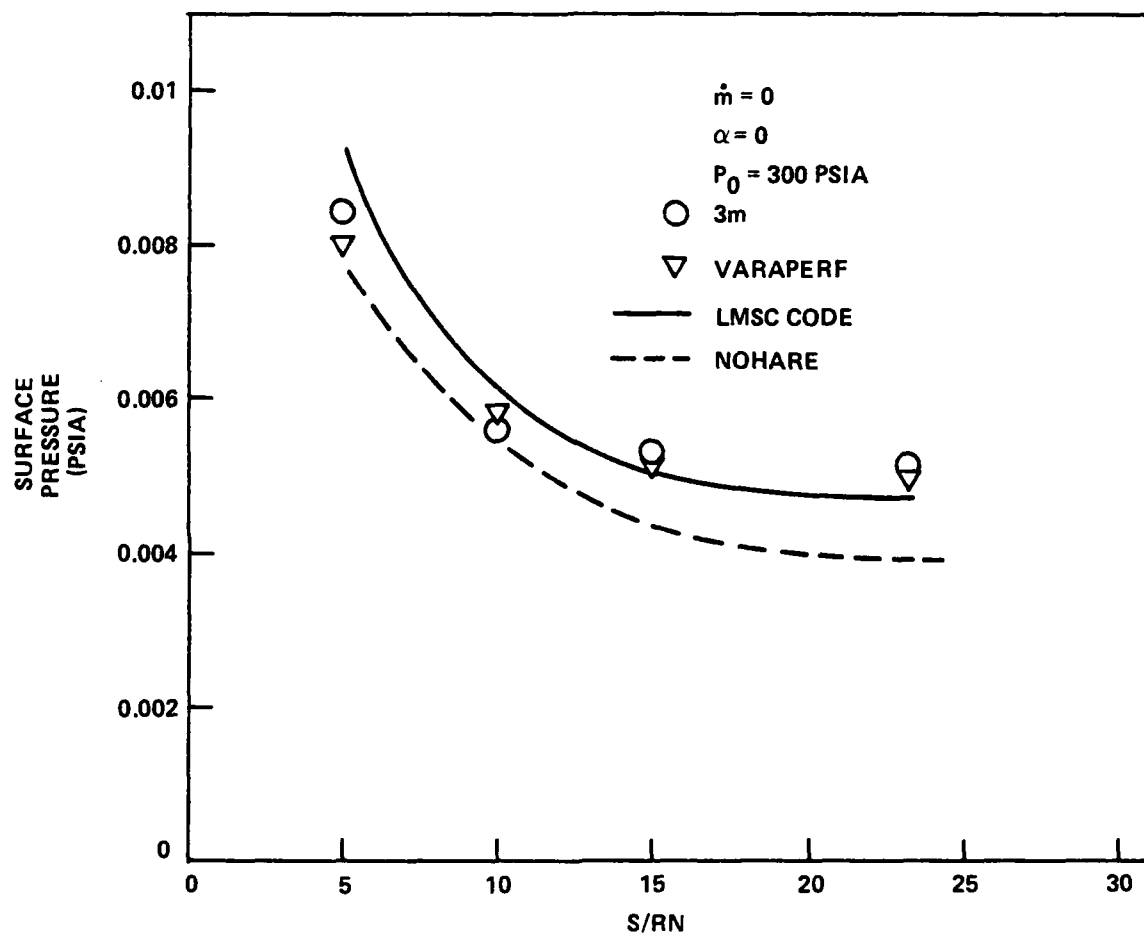


FIGURE 39. PRESSURE vs S/RN

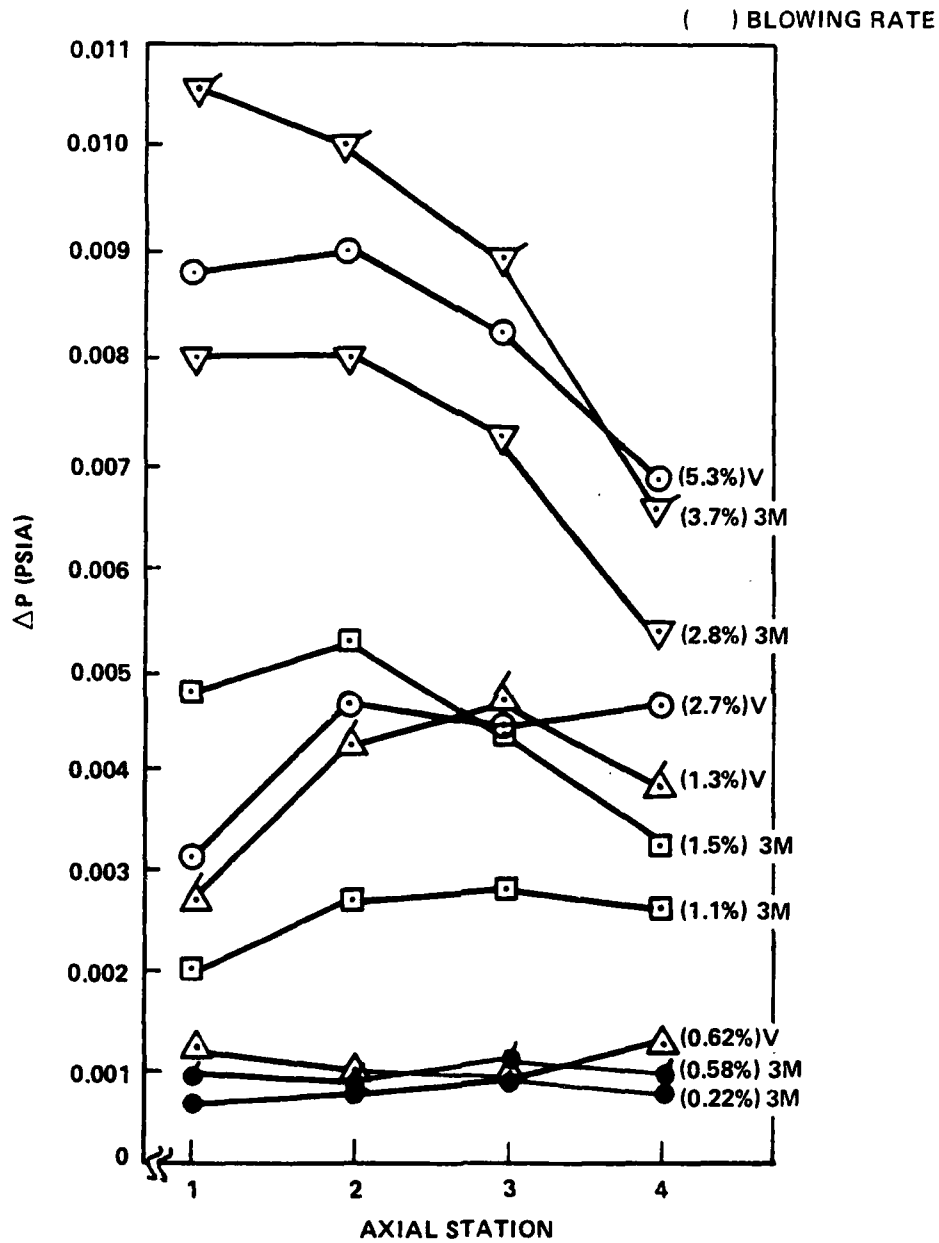
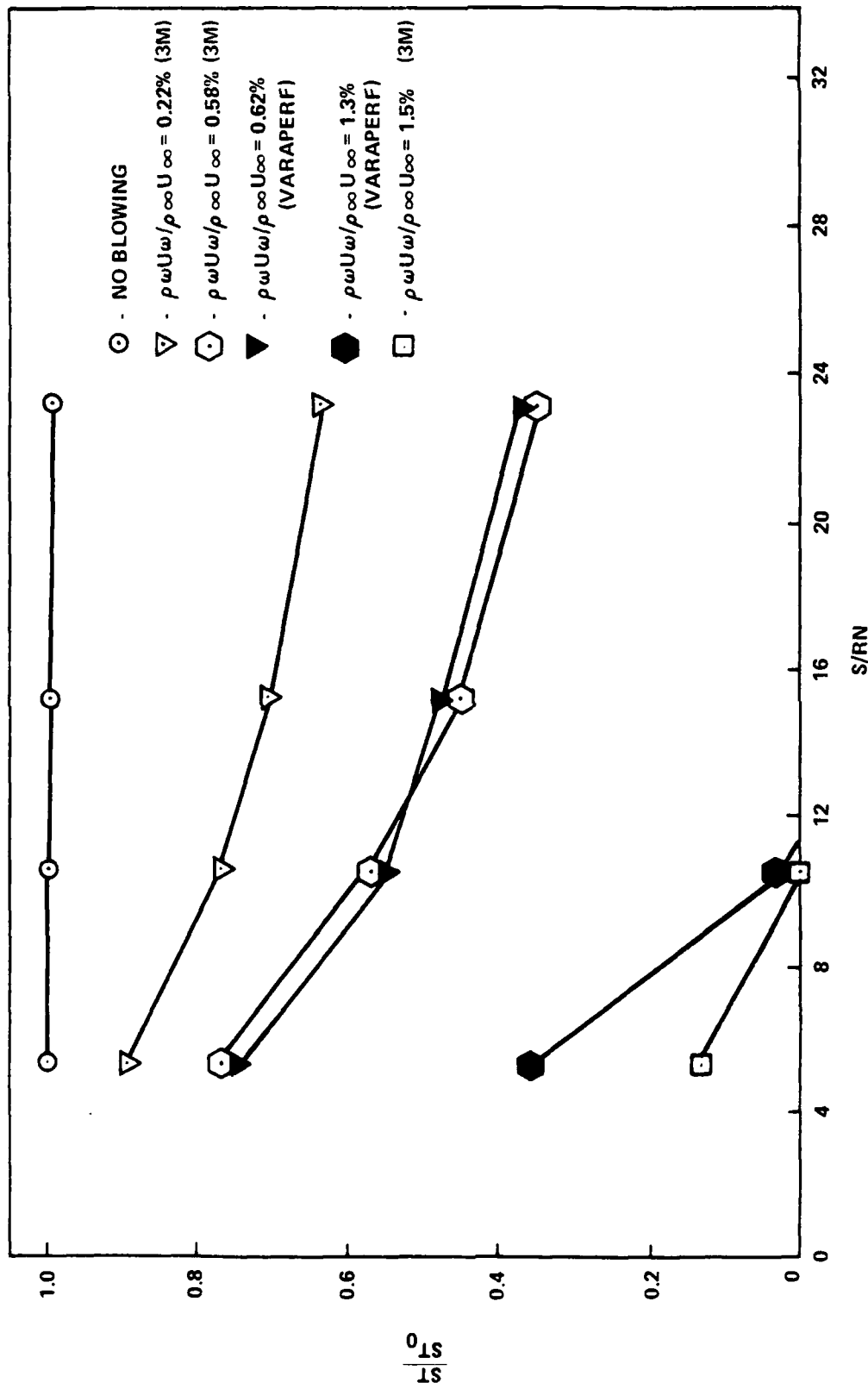


FIGURE 40. INDUCED PRESSURE vs AXIAL STATION

FIGURE 41.  $ST/ST_0$  vs  $S/RN$  - UNIFORM DISTRIBUTION



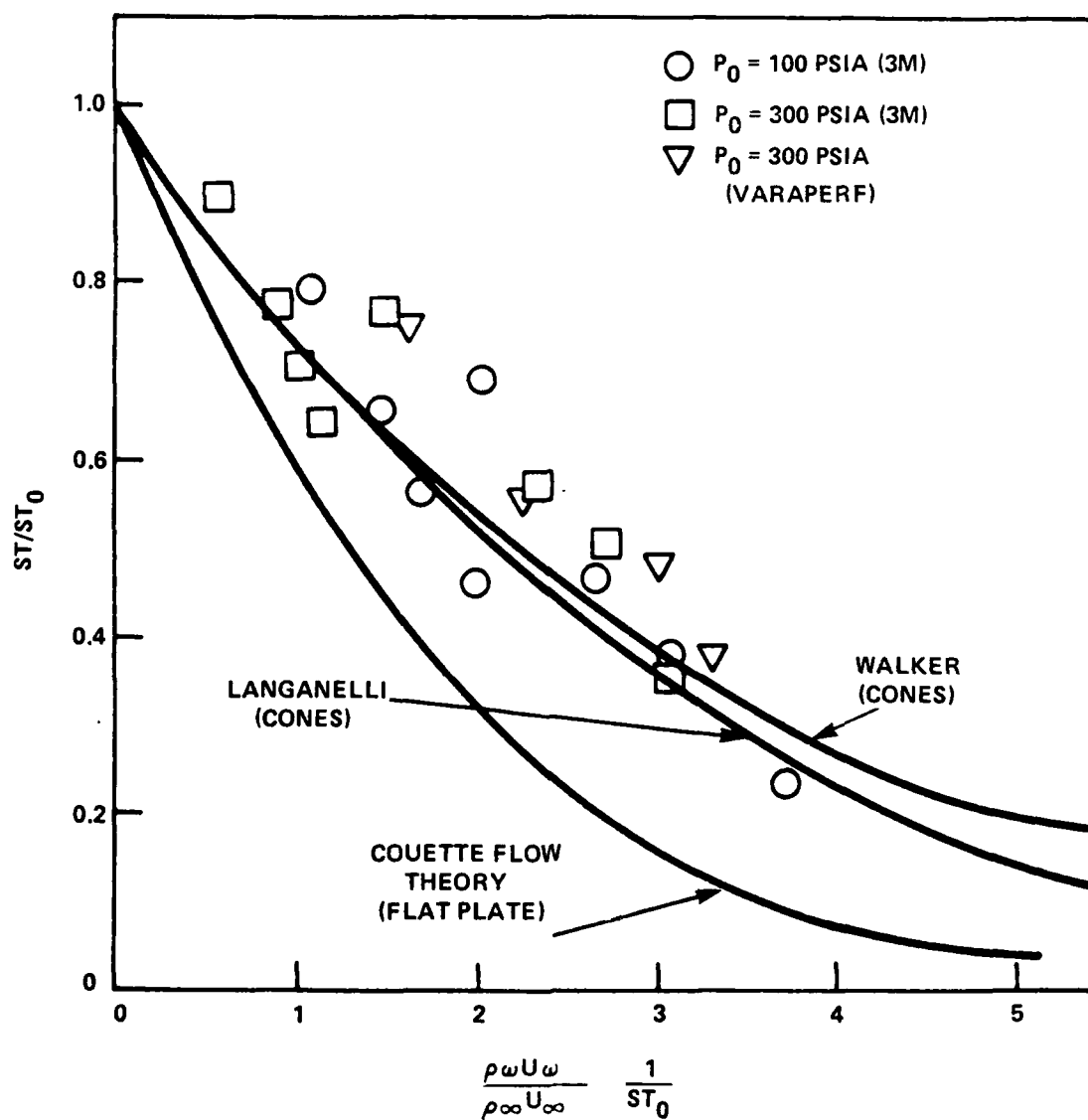


FIGURE 42. COMPARISON OF EXPERIMENT TO THEORY (SYMMETRIC BLOWING)

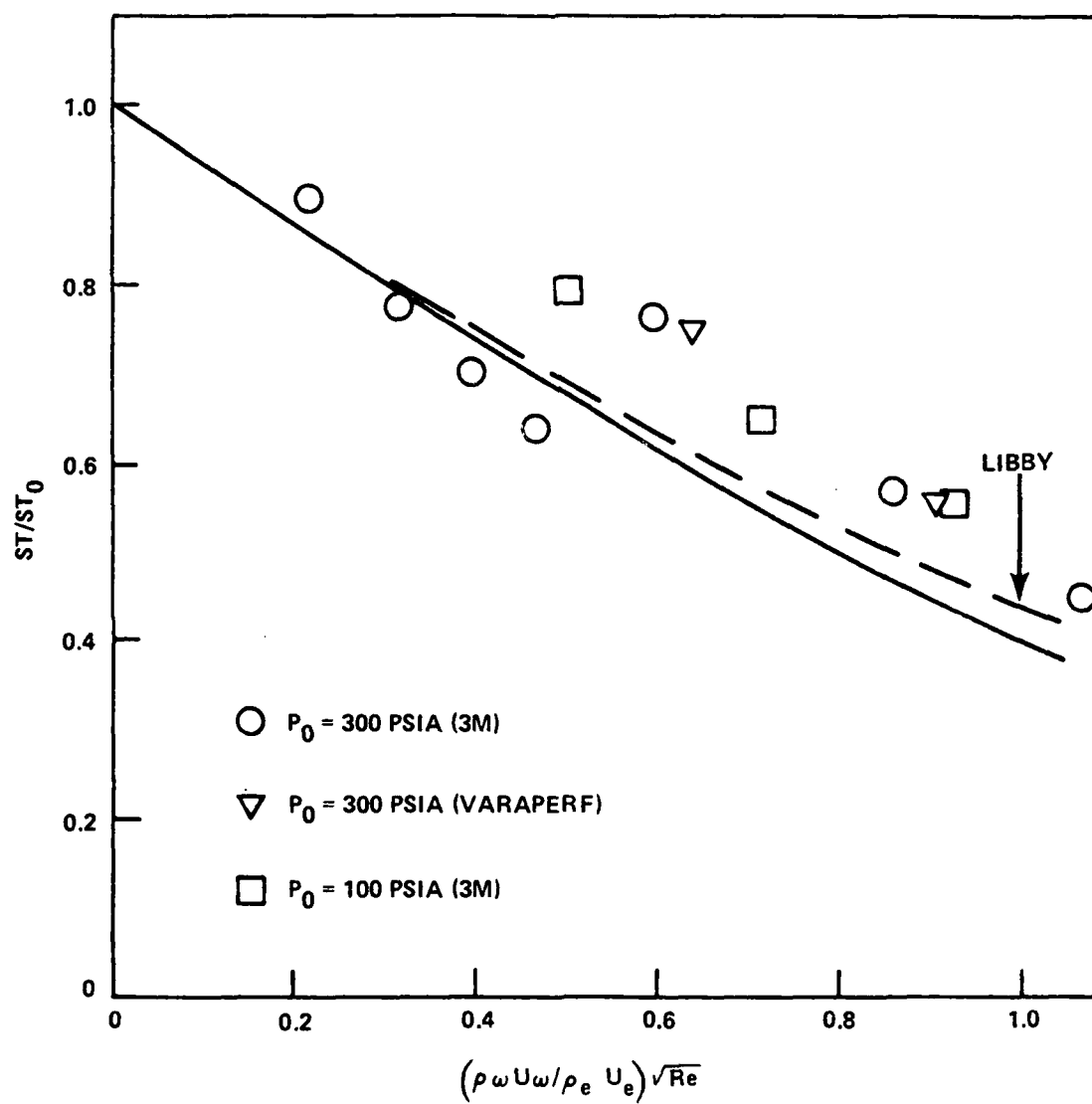
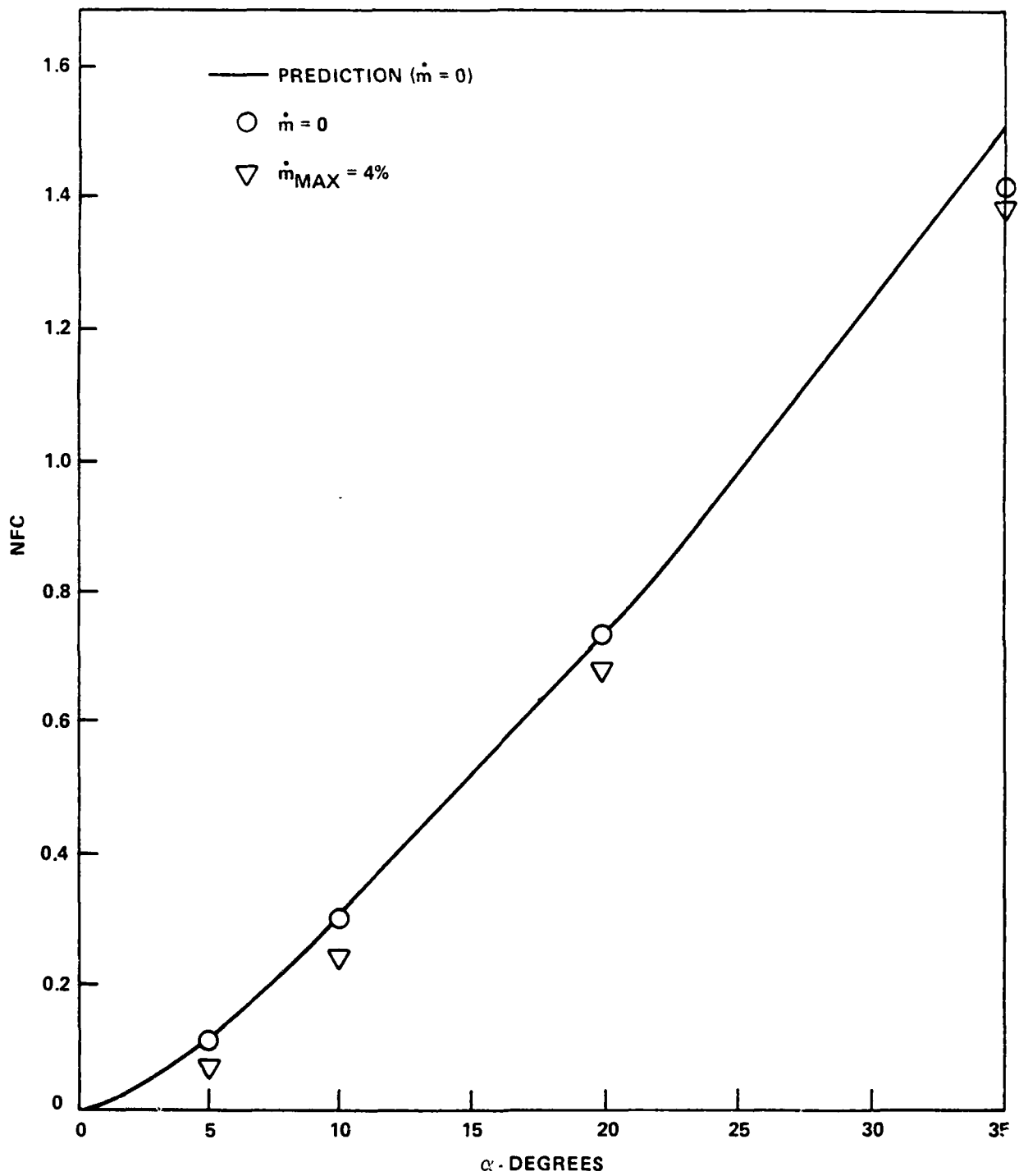
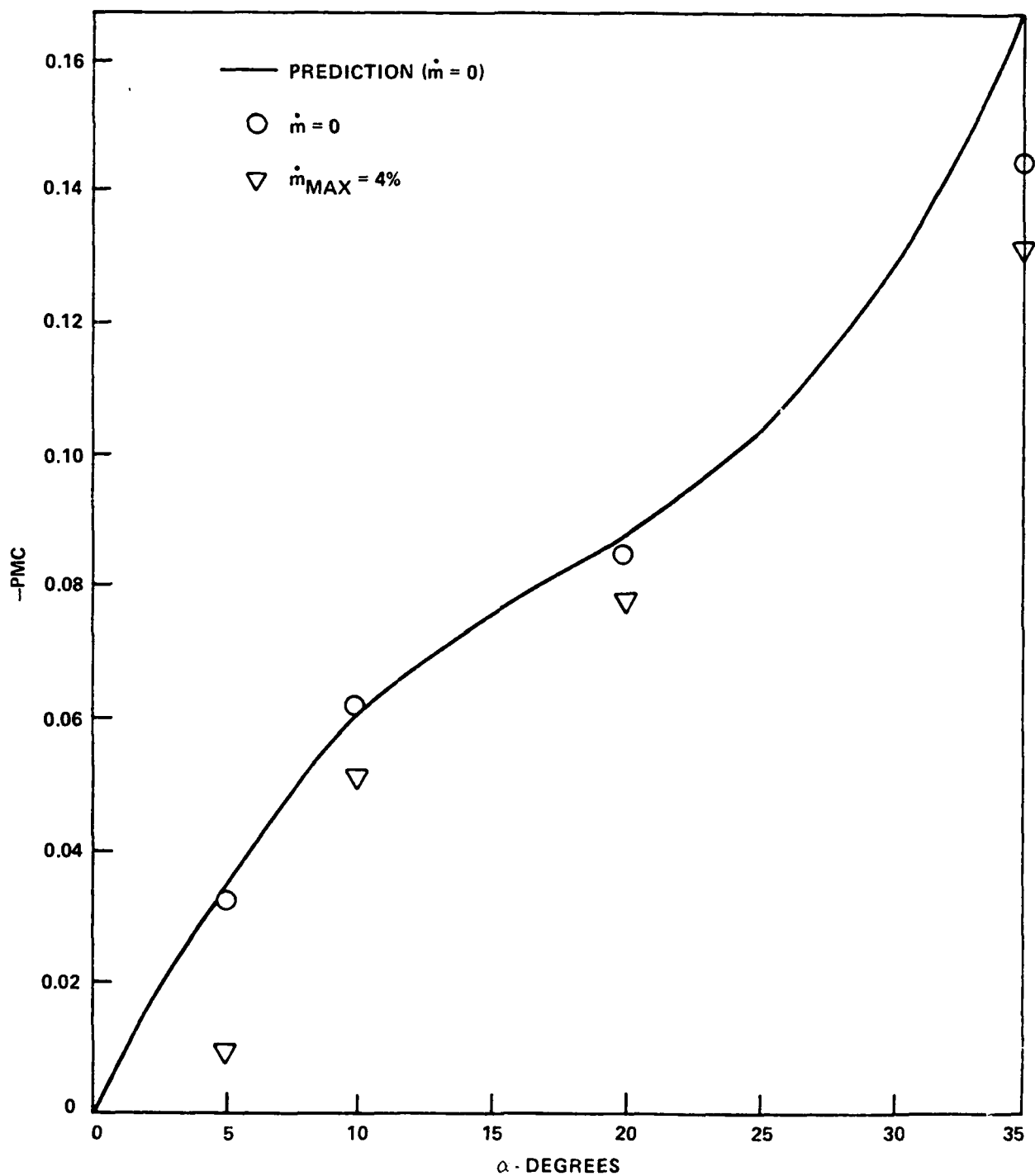
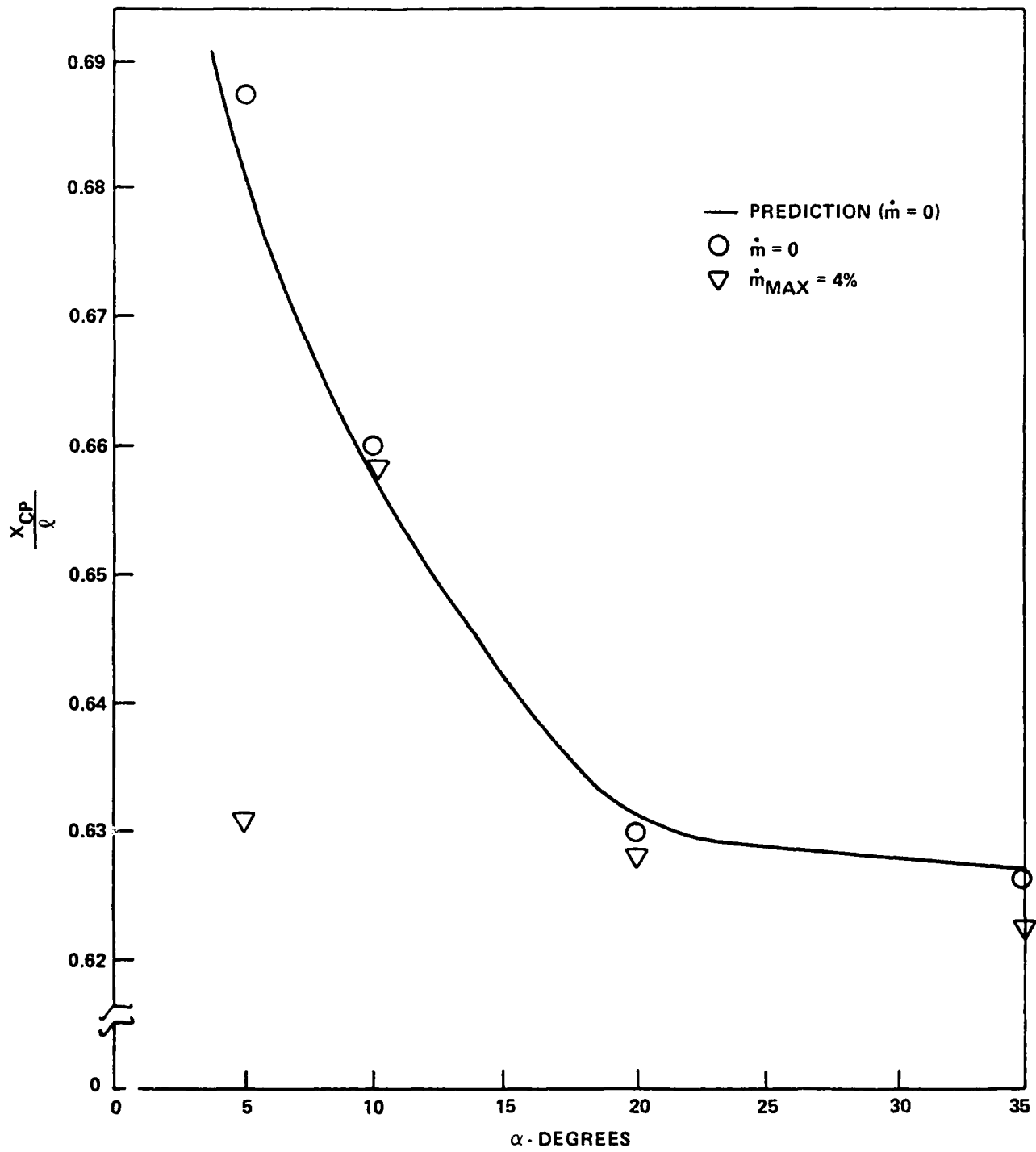
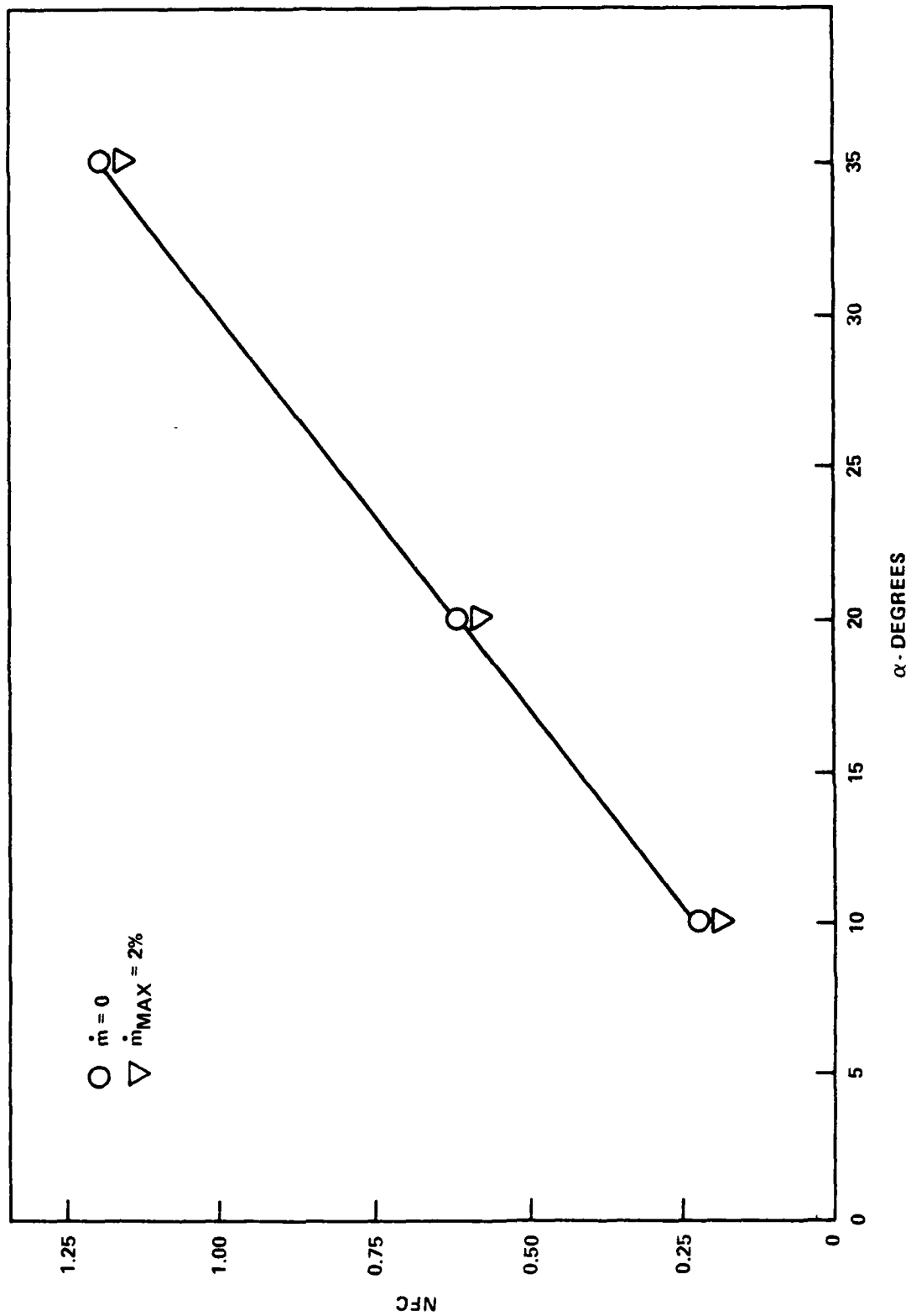


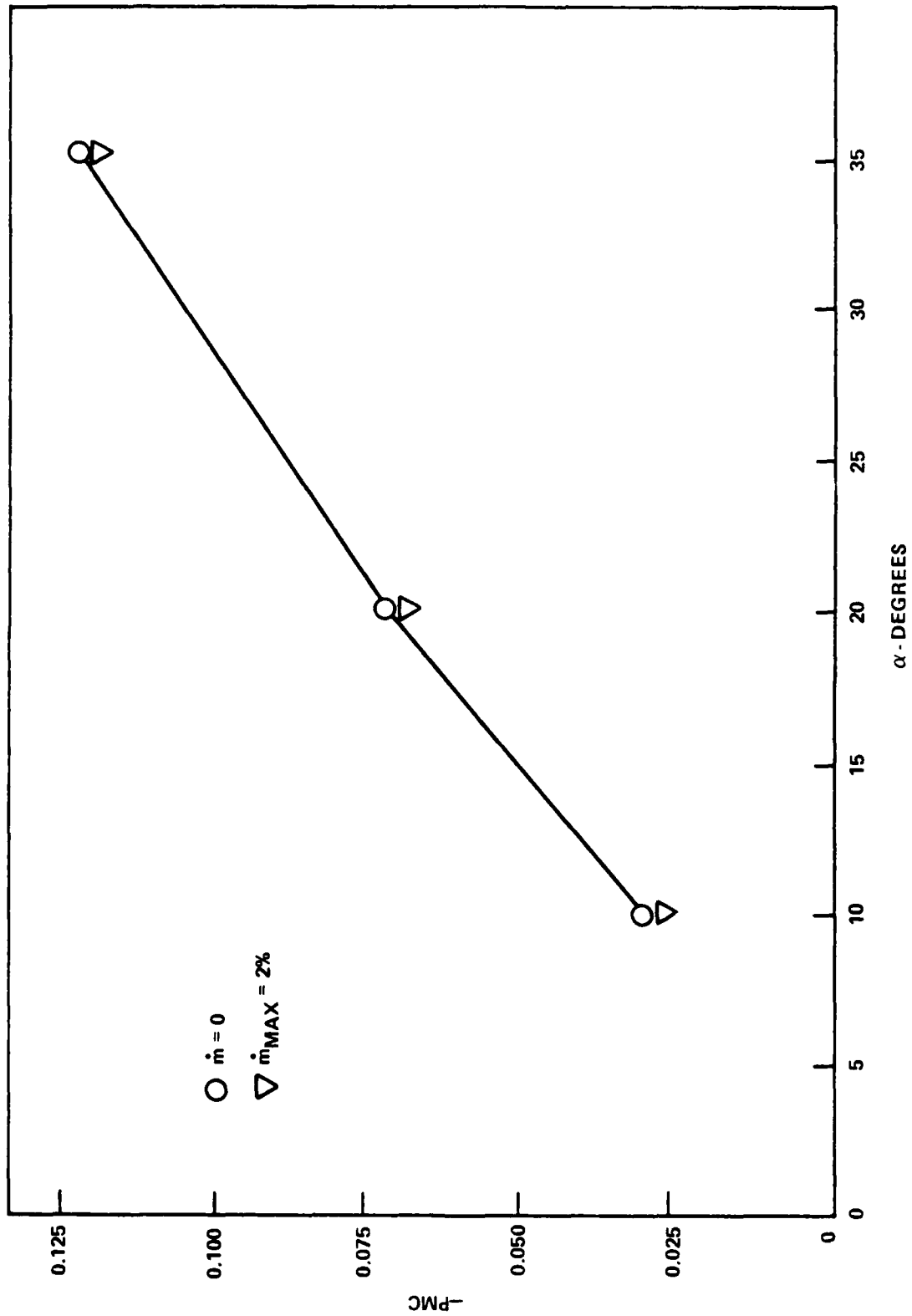
FIGURE 43. COMPARISON OF EXPERIMENT TO THEORY (SYMMETRIC BLOWING)

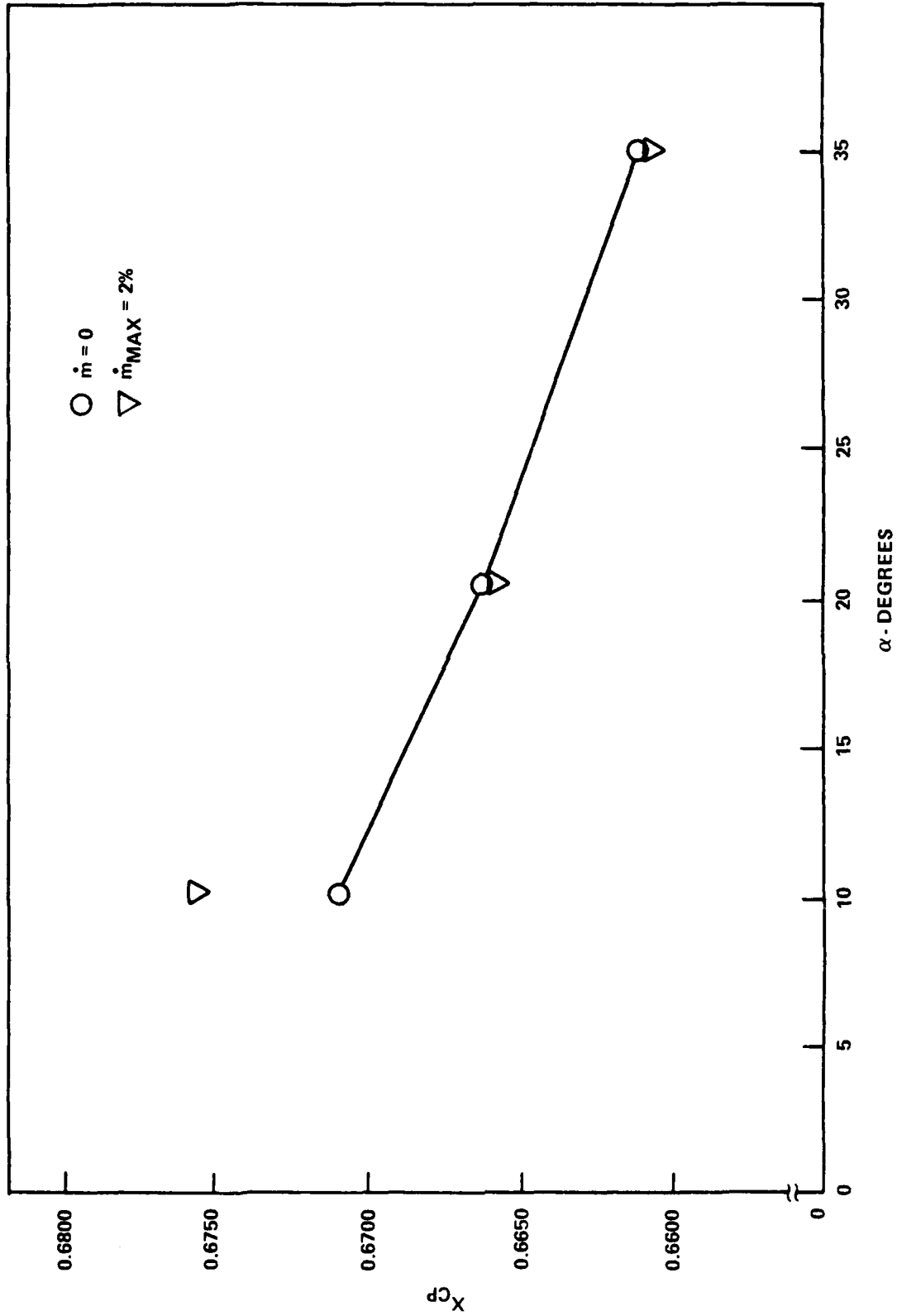
FIGURE 44. NFC vs  $\alpha$  - 7° CONE

FIGURE 45. PMC vs  $\alpha$  - 7° CONE

FIGURE 46.  $X_{CP}/l$  vs  $\alpha - 7^\circ$  CONE

FIGURE 47. NFC vs  $\alpha$  - 9° CONE

FIGURE 48. PMC vs  $\alpha$  - 90° CONE

FIGURE 49.  $X_{Cp}/\ell - 9^\circ$  CONE



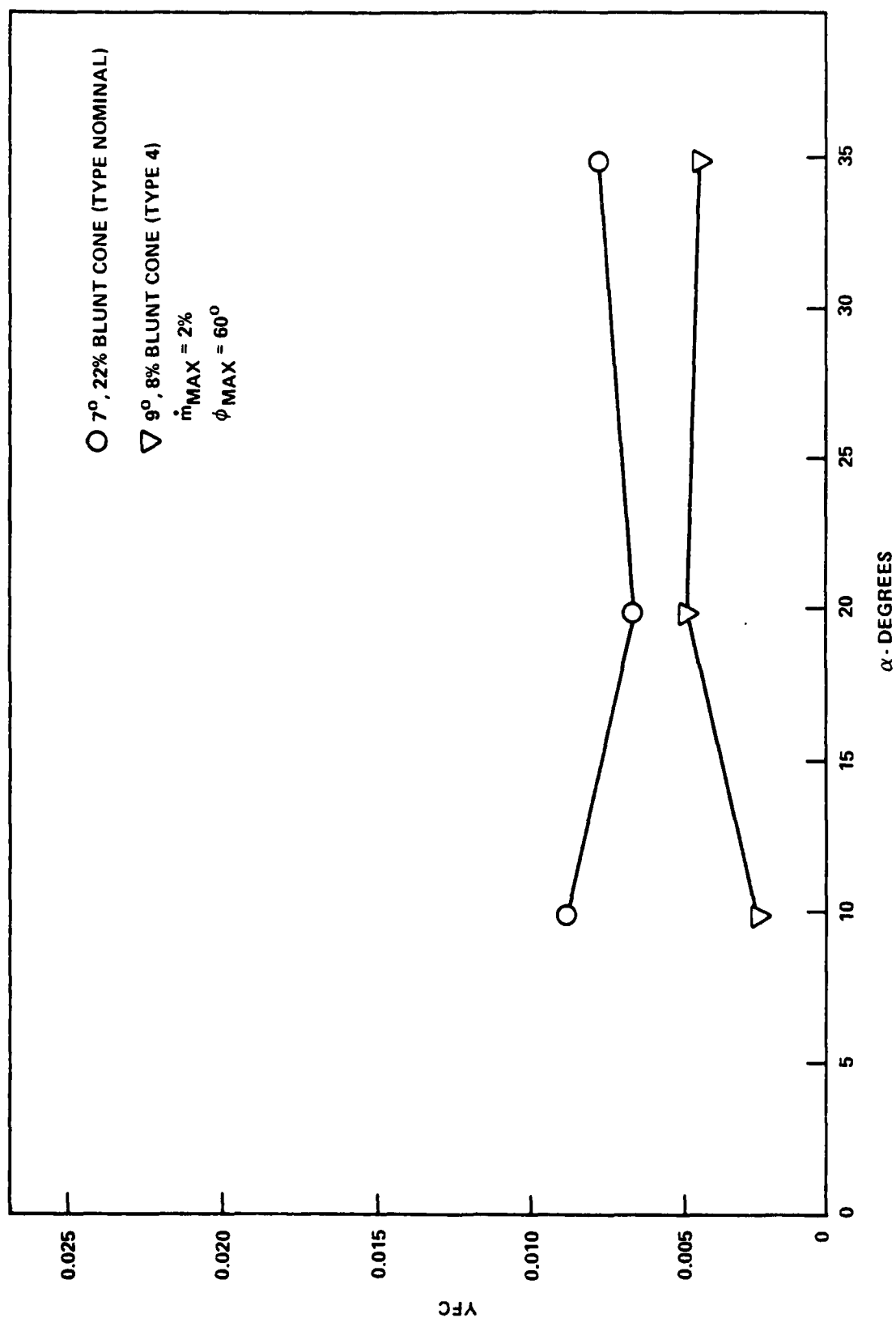


FIGURE 50. SIDE FORCE COMPARISON

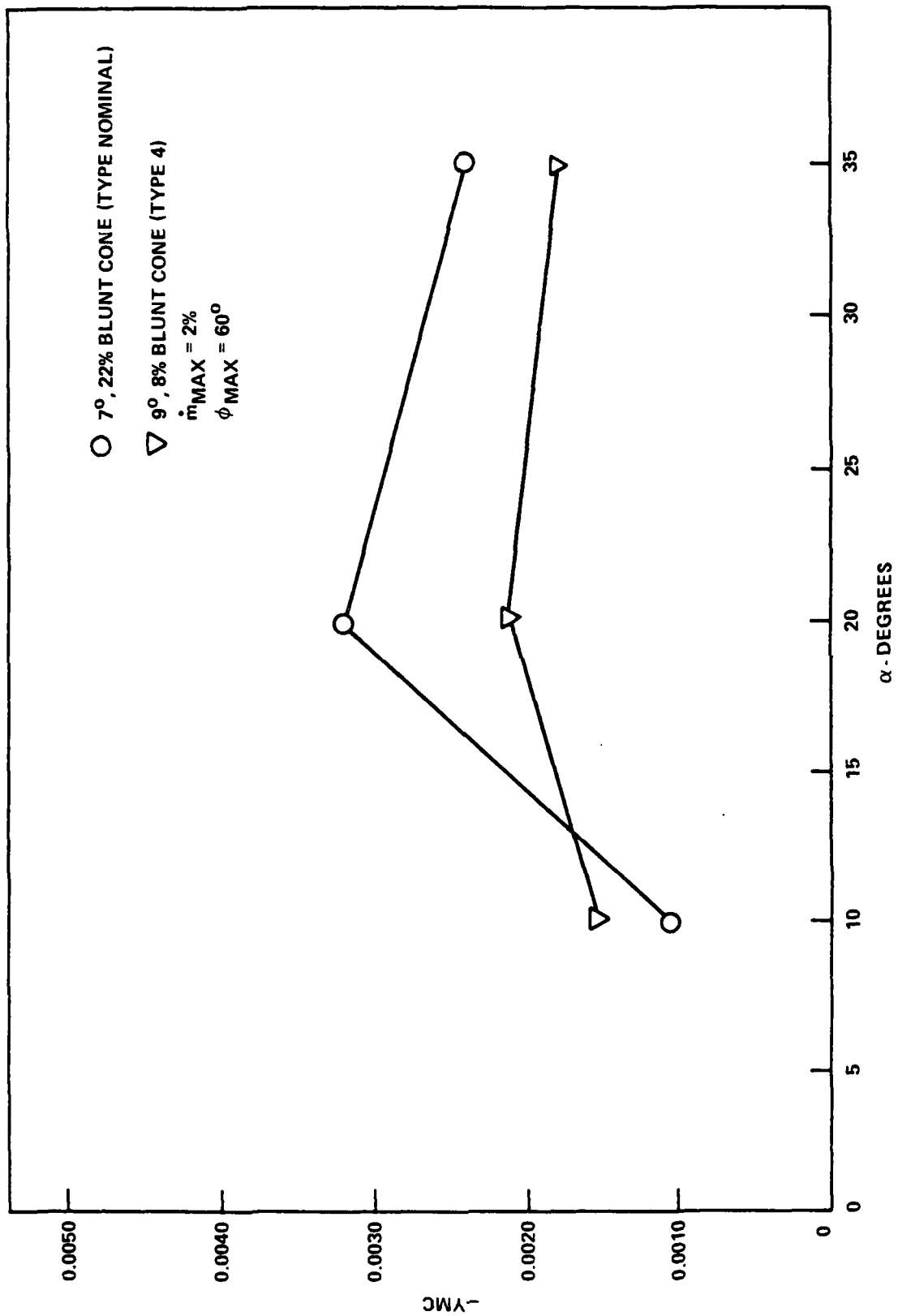


FIGURE 51. SIDE MOMENT COMPARISON

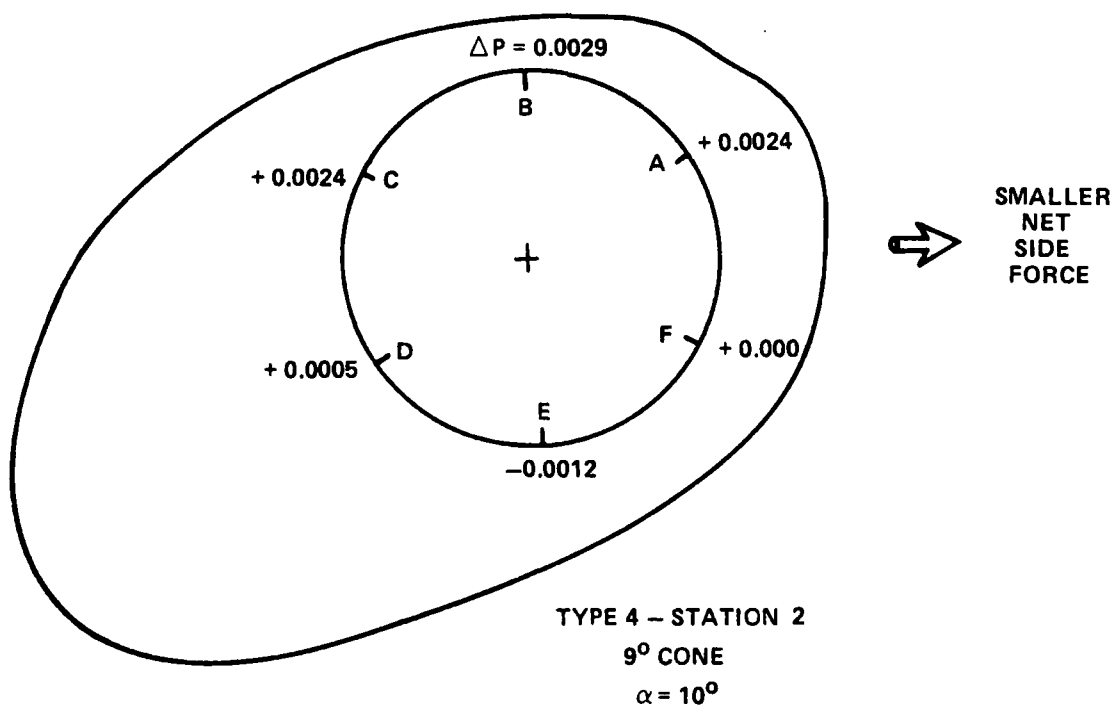
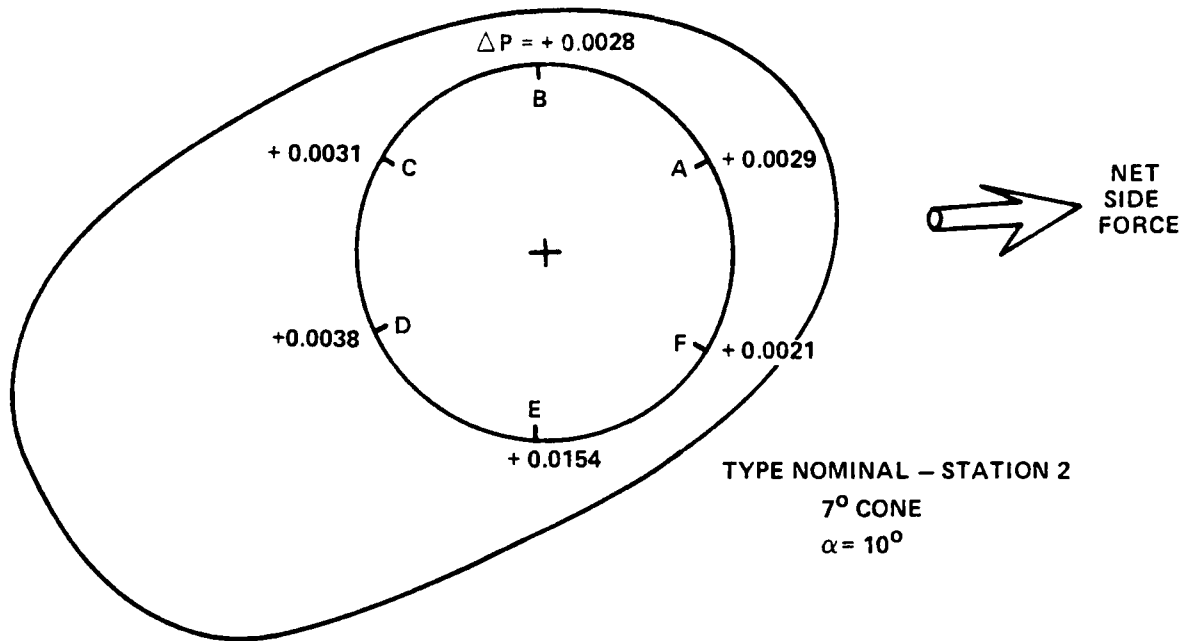
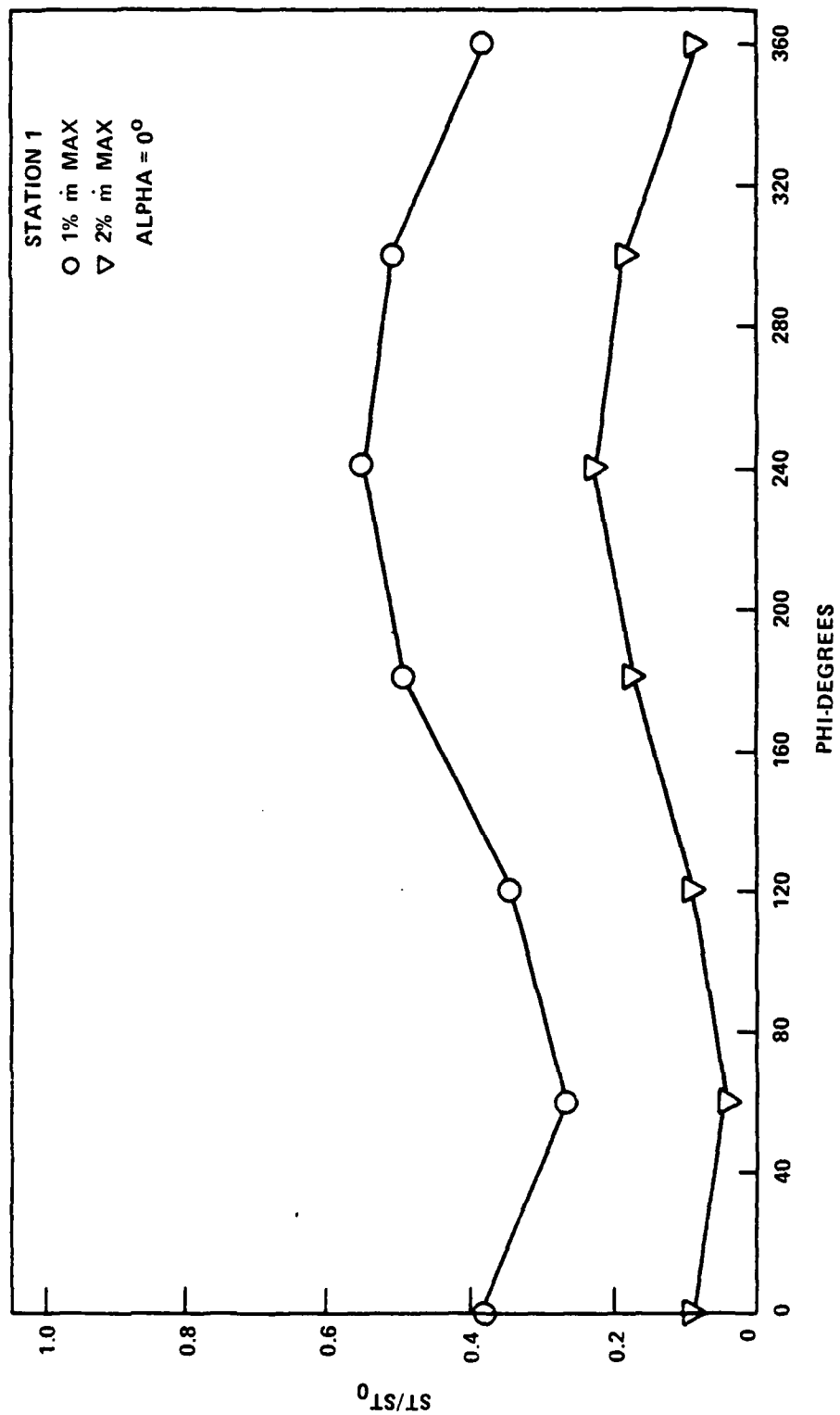


FIGURE 52. INDUCED PRESSURE VARIATION

FIGURE 53. ST/ST<sub>0</sub> vs PHI - TYPE 4

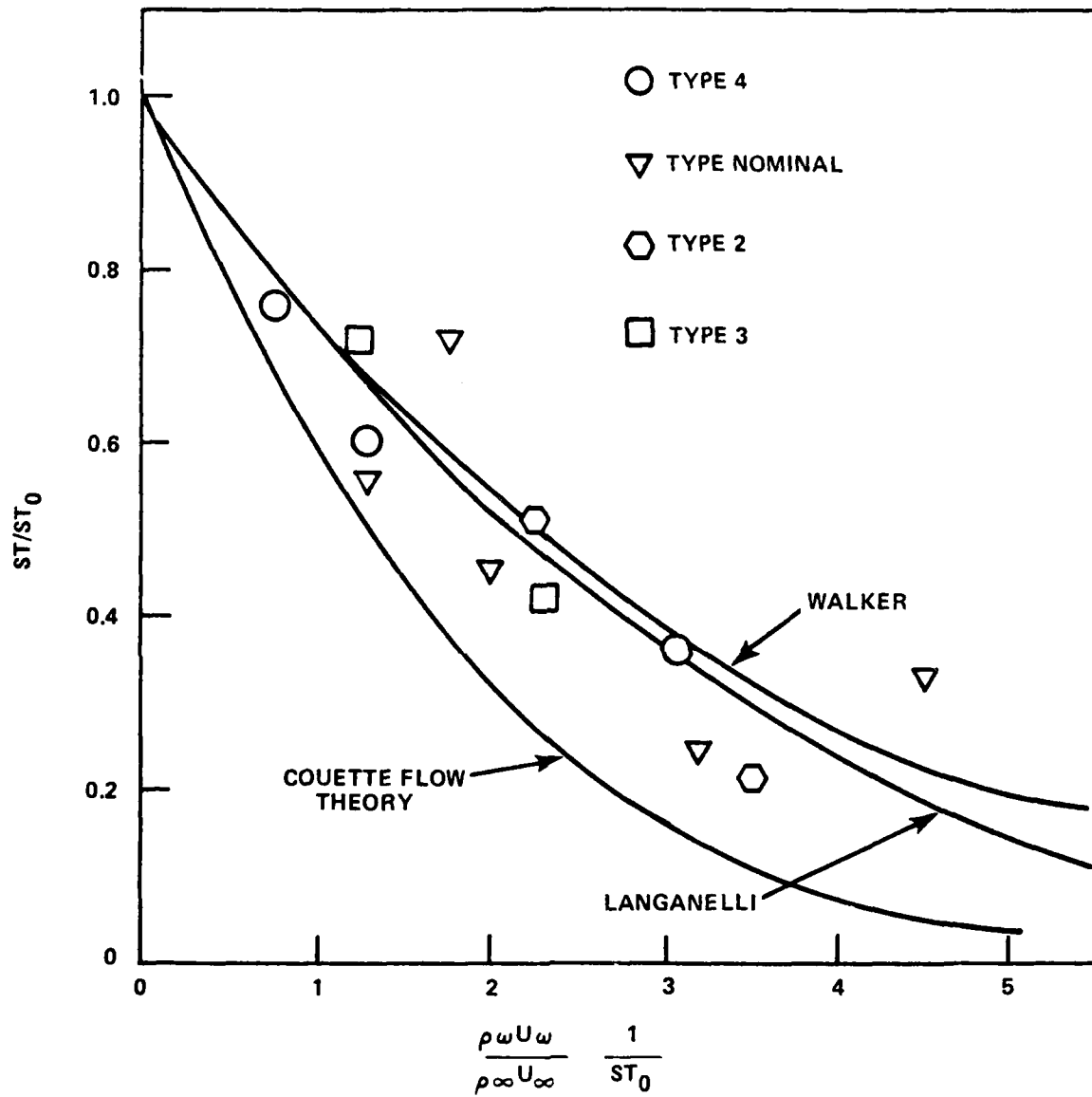


FIGURE 54. COMPARISON OF EXPERIMENT TO THEORY (ASYMMETRIC BLOWING)

TABLE 1. TEST MATRIX  
HIGH ALT., HIGH -  $\alpha$  AERO. TEST  
T-9 RUN MATRIX

RUN	MODEL/SHELL	Po(Psi)	$\alpha$	(MAX)	TEST TYPE
1	MK-4, 3M, uniform	100	0°	N/A	P & H.T.
2	"	300			
3	"				
4	"				
5	MK-4, VARAPERF, UNIFORM				
6	"				
7	MK-4, 3M, Type III		10°	+60°	F & M
8	"		20°	"	"
9	"		5°	"	"
10	MK-4, 3M, Type Nominal		10°	+60°	F & M
11	"		20°	"	"
12	"		10°	-60°	"
13	"		35°	+60°	"
14	MK-4, 3M, Type II		10°	+60°	"
15	"		20°	"	"
16	"		35°	"	"
17	MK-12A, 3M		10°	+60°	F & M
18	"		10°	-60°	"
19	"		20°	+60°	"
20	"		35°	+60°	"
21	MK-4, 3M, Type nominal		5°	+60°	P & H.T.
22	"		10°		"
23	"		20°		"
24	MK-4, 3M, Type III		0°		P & H.T.
25	"		5°		"
26	"		10°		"
27	"		20°		"
28	MK-4, 3M, Type II		10°		P & H.T.
29	"		20°		"
30	"		35°		"
31	MK-12A, 3M		0°		P & H.T.
32	"		10°		"
33	"		20°		"
34	"		35°		"

TABLE 2. ACTUAL OUTGASSING RATES

## Uniform Distribution:

Run #	Rate 1	Rate 2
1	0.466%	0.830%
2	0.220%	0.580%
3	1.07%	1.58%
4	2.78%	3.68%
5	0.62%	1.30%
6	2.69%	5.30%

## 1. Rates Defined As:

$$\frac{P_w}{P_\infty} \frac{U_w}{U_\infty}$$

## Assymetric Distributions:

Run #'s	Rate 1	Rate 2
10-13 21-23	2.13%	3.6%
7-9 24-27	1.99%	4.10%
14-16 28-30	1.89%	4.10%
17-20 31-34	1.25%	2.1%

## 2. Rates Defined As:

$$\frac{(P_w U_w)}{P_\infty U_\infty} \max$$

## REFERENCES

1. Zahm, A. F., "Superaerodynamics," Journal of the Franklin Institute, Vol. 217, 1934, pp. 153-166.
2. Tsien, H. S., "Superaerodynamics, Mechanics of Rarefied Gases," Journal of the Aeronautical Sciences, Vol. 13, 1946, pp. 653-664.
3. Adams, M. C., and Probst, R. F., "On the Validity of Continuum Theory for Satellite and Hypersonic Flight Problems at High Altitudes," Jet Propulsion, Feb 1958, pp. 86-89.
4. Tan, H. S., "Nose Drag in Free-Molecular Flow and Its Minimization," Journal of the Aerospace Sciences, Jun 1959, pp. 360-365.
5. Ericsson, L. E., "Effect of Nose Bluntness on the Hypersonic Unsteady Aerodynamics of an Ablating Reentry Body," J. Spacecraft and Rockets, Vol. 4, No. 6, Jun 1967, pp. 811-813.
6. Waterfall, A. P., "Effect of Ablation on the Dynamics of Spinning Reentry Vehicles," J. Spacecraft and Rockets, Vol. 6, No. 9, Sep 1969, pp. 1038-1044.
7. Ragsdale, W. C., and Horanoff, E. V., "Investigation of a Side Force Due to Ablation," J. Spacecraft and Rockets, Vol. 16, No. 9, Sep 1978, pp. 1010-1011.
8. Dannenberg, R. E., Weiberg, J. A., and Gambucci, B. J., Perforated Sheets as the Porous Material for a Suction-Flap Application, NACA TN 4038, May 1957.
9. Laganelli, A. L., Foganoli, R. P., and Martillucci, A., The Effects of Mass Transfer and Angle of Attack on Hypersonic Turbulent Boundary Layer Characteristics, AFFDL-TR-75-35, Apr 1975.
10. Walker, G. K., Turbulent Boundary Layers with Mass Addition, G.E. Document No. TFM-8151-021, Nov 1963.
11. Libby, P. A., "The Homogeneous Boundary Layer at an Axisymmetric Stagnation Point with Large Rates of Injection," J. Aeronautical Sciences, Jan 1962.



## NOMENCLATURE

$A$	Model base area ( $\text{in}^2$ )
$D_B$	Model base diameter (in)
$l$	Model length (in)
$\dot{m}$	Mass flow rate ( $^1\text{bm}/\text{sec}$ )
$\dot{m}/A$	Mass flow rate per unit area ( $^1\text{bm}/\text{ft}^2\text{-sec}$ )
$p$	Pressure ( $^1\text{bf}/\text{in}^2$ )
$R_B$	Model base radius (in)
$R_N$	Model nose radius (in)
$Re$	Reynolds number
$S$	Surface length (in)
$St$	Stanton number
$t$	Shell wall thickness (in)
$u$	Velocity ( $\text{ft}/\text{sec}$ )
$x$	Axial length (in)
$\alpha$	Angle of attack (deg)
$\rho$	Density ( $^1\text{bm}/\text{ft}^3$ )
$\phi$	Circumferential position (deg)

Subscripts

$e$	Boundary layer edge values
$\text{max}$	Value at location of maximum blowing
$o$	Non-blowing values
$w$	Wall values
$\infty$	Free-stream values

# APPENDIX A

## TABULAR LISTING OF TEST DATA

This appendix presents a tabular listing of all the data taken during the test.

### Definitions:

NFC	= Normal force/(Q * A)
PMC	= Pitching moment/(Q * A * D)
YFC	= Side force/(Q * A)
YMC	= Side moment/(Q * A * D)
PXCP	= (Xc.g - Xc.p)/D
YXCP	= (Yc.g - Yc.p)/D
Pressure Coefficient	= Pressure/Q
ST	= $\frac{q}{\rho U C_p (T_a - T_w)}$

where:

Q	= Dynamic pressure
A	= Model base area = 28.27 in. <sup>2</sup>
D	= Model base diameter = 6 in.
Xc.g.	= Axial location of center of gravity = 11.66 in. from nose
Xc.p.	= Axial location of center of pressure
L	= Model length = 19.6 in.
T <sub>a</sub>	= Adiabatic wall temperature
q	= Heat flux
C <sub>p</sub>	= Specific heat

WTP 1365

MA5F PRESSURE AND GADON DATA  
PRESSURE AT INDICATED TAP LOCATION

RUN	1	TYPE UNIFORM																ALPHA - 0.			
		1A	1B	1C	1D	1E	1F	2A	2B	2C	2D	2E	2F	3A	3B	3C	3D	3E	3F	3G	3H
BLOWING RATE 0		.0025	.0028	.0024	.0022	.0025	.0029	.0008	.0009	.0006	.0011	.0012	.0001	.0004	.0001	.0001	.0006	.0002	.0007	.0007	.0007
BLOWING RATE 1		.0025	.0030	.0025	.0024	.0026	.0029	.0014	.0016	.0013	.0016	.0019	.0007	.0014	.0010	.0011	.0015	.0011	.0014	.0014	.0014
BLOWING RATE 2		.0021	.0034	.0024	.0028	.0032	.0034	.0006	.0016	.0008	.0017	.0022	.0008	.0005	.0010	.0004	.0015	.0013	.0015	.0015	.0015
BLOWING RATE 0		* 4A 4B 4C 4D 4E 4F																			
BLOWING RATE 1		.0009	.0006	.0005	.0014	.0005	.0010														
BLOWING RATE 2		.0018	.0015	.0017	.0028	.0010	.0100														
		.0009	.0014	.0009	.0029	.0017	.0124														

WTP 1365

MA5F PRESSURE AND GADON DATA  
PRESSURE COEFFICIENT AT INDICATED TAP LOCATION

RUN	1	TYPE UNIFORM																ALPHA - 0.			
		1A	1B	1C	1D	1E	1F	2A	2B	2C	2D	2E	2F	3A	3B	3C	3D	3E	3F	3G	3H
BLOWING RATE 0		.0387	.0443	.0371	.0345	.0392	.0447	.0131	.0141	.0101	.0170	.0194	.0317	.0064	.0010	.0015	.0099	.0074	.0104	.0104	.0104
BLOWING RATE 1		.0407	.0486	.0402	.0387	.0425	.0467	.0220	.0255	.0212	.0262	.0306	.0109	.0229	.0167	.0182	.0242	.0179	.0230	.0230	.0230
BLOWING RATE 2		.0310	.0486	.0346	.0403	.0457	.0489	.0089	.0230	.0119	.0241	.0322	.0116	.0066	.0146	.0060	.0216	.0184	.0212	.0212	.0212
BLOWING RATE 0		* 4A 4B 4C 4D 4E 4F																			
BLOWING RATE 1		.0139	.0090	.0084	.0222	.0074	.0158														
BLOWING RATE 2		.0296	.0238	.0265	.0456	.0165	.1609														
		.0130	.0208	.0126	.0415	.0243	.1787														

\*BAD GAGE

WTR 1365

HASF PRESSURE AND GARDON DATA  
QDOT AT INDICATED TAP LOCATION

RUN 1	* TYPE UNIFORM												ALPHA = 0.			
	1A	2A	3A	4A	1B	2B	3B	4B	1C	2C	3C	4C				
BLOWING RATE 0	.14	.10	.09	.08	0.00	0.00	0.00	0.00	0.00	0.00	0.00	0.00	4C			
BLOWING RATE 1	.13	.08	.06	.04	0.00	0.00	0.00	0.00	0.00	0.00	0.00	0.00	0.00			
BLOWING RATE 2	.14	.07	.04	.02	0.00	0.00	0.00	0.00	0.00	0.00	0.00	0.00	0.00			
1D	2D	3D	4D	1E	2E	3E	4E	1F	2F	3F	4F					
BLOWING RATE 0	.13	.10	.08	.07	0.00	0.00	0.00	0.00	0.00	0.00	0.00	0.00				
BLOWING RATE 1	.13	.09	.06	.03	0.00	0.00	0.00	0.00	0.00	0.00	0.00	0.00				
BLOWING RATE 2	.13	.07	.04	.02	0.00	0.00	0.00	0.00	0.00	0.00	0.00	0.00				

WTR 1365

HASF PRESSURE AND GARDON DATA  
STANTON NUMBER AT INDICATED TAP LOCATION

* TYPE UNIFORM												
	1A	2A	3A	4A	1B	2B	3B	4B	1C	2C	3C	4C
BLOWING RATE 0	4.32E-03	3.08E-03	2.75E-03	2.37E-03	n.	0.	0.	0.	0.	0.	0.	0.
BLOWING RATE 1	3.41E-03	2.01E-03	1.54E-03	1.01E-03	n.	0.	0.	0.	0.	0.	0.	0.
BLOWING RATE 2	2.98E-03	1.43E-03	9.75E-04	5.39E-04	n.	0.	0.	0.	0.	0.	0.	0.
BLOWING RATE 0	4.02E-03	3.24E-03	2.63E-03	2.19E-03	n.	0.	0.	0.	0.	0.	0.	0.
BLOWING RATE 1	3.21E-03	2.19E-03	1.49E-03	8.64E-04	n.	0.	0.	0.	0.	0.	0.	0.
BLOWING RATE 2	2.78E-03	1.58E-03	8.39E-04	4.68E-04	n.	0.	0.	0.	0.	0.	0.	0.
BLOWING RATE 0	4.02E-03	3.24E-03	2.63E-03	2.19E-03	n.	0.	0.	0.	0.	0.	0.	0.
BLOWING RATE 1	3.21E-03	2.19E-03	1.49E-03	8.64E-04	n.	0.	0.	0.	0.	0.	0.	0.
BLOWING RATE 2	2.78E-03	1.58E-03	8.39E-04	4.68E-04	n.	0.	0.	0.	0.	0.	0.	0.

\*GAGES ONLY ON A AND D RAYS

WTP 1365

HASF PRESSURE AND GARDON DATA  
PRESSURE AT INDICATED TAP LOCATION

HUN 2	TYPE	UNIFORM	ALPHA - 0.															
		1A 1B 1C 1D 1E 1F 2A 2B 2C 2D 2E 2F 3A 3B 3C 3D 3E 3F																
BLOWING RATE 0		.0061 .0058 .0059 .0058 .0058 .0059 .0036 .0037 .0033 .0039 .0037 .0034 .0035 .0033 .0033 .0033 .0034																
BLOWING RATE 1		.0067 .0065 .0064 .0065 .0065 .0065 .0043 .0044 .0040 .0046 .0045 .0040 .0044 .0041 .0041 .0041 .0041																
BLOWING RATE 2		.0070 .0067 .0066 .0066 .0066 .0066 .0044 .0045 .0041 .0046 .0045 .0039 .0044 .0043 .0041 .0044 .0044																
		4A 4B 4C 4D 4E 4F																
BLOWING RATE 0		.0034 .0031 .0033 .0033 .0025 .0027																
BLOWING RATE 1		.0041 .0037 .0041 .0044 .0032 .0112																
BLOWING RATE 2		.0043 .0040 .0042 .0050 .0038 .0155																

A-4

WTP 1365

HASF PRESSURE AND GARDON DATA  
PRESSURE COEFFICIENT AT INDICATED TAP LOCATION

	1A	1B	1C	1D	1E	1F	2A	2B	2C	2D	2E	2F	3A	3B	3C	3D	3E	3F
BLOWING RATE 0	.0462	.0443	.0445	.0444	.0441	.0445	.0271	.0278	.0254	.0297	.0281	.0257	.0267	.0250	.0250	.0251	.0246	.0285
BLOWING RATE 1	.0483	.0464	.0457	.0464	.0468	.0467	.0308	.0316	.0289	.0327	.0322	.0285	.0313	.0295	.0294	.0293	.0245	.0315
BLOWING RATE 2	.0495	.0476	.0468	.0478	.0486	.0478	.0308	.0317	.0293	.0322	.0319	.0278	.0314	.0304	.0291	.0309	.0296	.0314
	4A	4B	4C	4D	4E	4F												
BLOWING RATE 0	.0255	.0238	.0248	.0253	.0193	.0203												
BLOWING RATE 1	.0294	.0267	.0292	.0318	.0230	.0804												
BLOWING RATE 2	.0303	.0280	.0300	.0356	.0270	.1094												

\*BAD GAGE

WTR 1365

MASF PRESSURE AND GARDON DATA  
000T AT INDICATED TAP LOCATION

RUN	2	TYPE	UNIFORM*	ALPHA = 0.											
				1A	2A	3A	4A	1B	2B	3B	4B	1C	2C	3C	4C
BLOWING RATE	0			.35	.23	.20	.18	0.00	0.00	0.00	0.00	0.00	0.00	0.00	0.00
BLOWING RATE	1			.38	.22	.17	.14	0.00	0.00	0.00	0.00	0.00	0.00	0.00	0.00
BLOWING RATE	2			.35	.17	.12	.08	0.00	0.00	0.00	0.00	0.00	0.00	0.00	0.00
BLOWING RATE	0			10	20	30	40	1E	2E	3E	4E	1F	2F	3F	4F
BLOWING RATE	1			.36	.25	.20	.17	0.00	0.00	0.00	0.00	0.00	0.00	0.00	0.00
BLOWING RATE	2			.38	.24	.17	.14	0.00	0.00	0.00	0.00	0.00	0.00	0.00	0.00
BLOWING RATE	2			.35	.19	.12	.08	0.00	0.00	0.00	0.00	0.00	0.00	0.00	0.00

WTR 1365

MASF PRESSURE AND GARDON DATA  
STANTON NUMBER AT INDICATED TAP LOCATION

RUN	2	TYPE	UNIFORM*	ALPHA = 0.											
				1A	2A	3A	4A	1B	2B	3B	4B	1C	2C	3C	4C
BLOWING RATE	0			3.76E-03	2.50E-03	2.16E-03	1.94E-03	0.	0.	0.	0.	0.	0.	0.	0.
BLOWING RATE	1			3.36E-03	1.93E-03	1.53E-03	1.24E-03	0.	0.	0.	0.	0.	0.	0.	0.
BLOWING RATE	2			2.88E-03	1.42E-03	9.74E-04	6.74E-04	0.	0.	0.	0.	0.	0.	0.	0.
BLOWING RATE	0			10	20	30	40	1E	2E	3E	4E	1F	2F	3F	4F
BLOWING RATE	1			3.84E-03	2.66E-03	2.12E-03	1.87E-03	0.	0.	0.	0.	0.	0.	0.	0.
BLOWING RATE	2			3.34E-03	2.08E-03	1.52E-03	1.21E-03	0.	0.	0.	0.	0.	0.	0.	0.
BLOWING RATE	2			2.88E-03	1.56E-03	9.61E-04	6.76E-04	0.	0.	0.	0.	0.	0.	0.	0.

\*GAGES ONLY ON A AND D RAYS

WIP 1365

HASF PRESSURE AND GARDON DATA  
PRESSURE AT INDICATED TAP LOCATION

RUN	3	TYPE UNIFORM																ALPHA - 0.			
		1A	1B	1C	1D	1E	1F	2A	2B	2C	2D	2E	2F	3A	3B	3C	3D	3E	3F	3G	3H
BLOWING RATE 0		.0050	.0048	.0046	.0046	.0047	.0047	.0027	.0026	.0023	.0024	.0028	.0022	.0024	.0021	.0019	.0022	.0020	.0023	.0020	.0023
BLOWING RATE 1		.0069	.0070	.0066	.0067	.0068	.0069	.0053	.0053	.0049	.0054	.0053	.0049	.0052	.0052	.0048	.0052	.0049	.0051	.0048	.0051
BLOWING RATE 2		.0096	.0095	.0093	.0093	.0094	.0094	.0078	.0079	.0077	.0080	.0078	.0076	.0067	.0067	.0063	.0067	.0064	.0065	.0064	.0065
*#																					
BLOWING RATE 0		.0023	.0021	.0019	.0021	.0019	.0019	.0014													
BLOWING RATE 1		.0047	.0047	.0043	.0057	.0046	.0204														
BLOWING RATE 2		.0054	.0054	.0051	.0066	.0057	.0262														

WIP 1365

HASF PRESSURE AND GARDON DATA  
PRESSURE COEFFICIENT AT INDICATED TAP LOCATION

RUN	3	TYPE UNIFORM																ALPHA - 0.			
		1A	1B	1C	1D	1E	1F	2A	2B	2C	2D	2E	2F	3A	3B	3C	3D	3E	3F	3G	3H
BLOWING RATE 0		.0407	.0394	.0376	.0388	.0383	.0388	.0222	.0210	.0185	.0237	.0230	.0182	.0201	.0174	.0161	.0179	.0165	.0193	.0165	.0193
BLOWING RATE 1		.0497	.0505	.0473	.0485	.0490	.0495	.0381	.0384	.0356	.0392	.0383	.0356	.0376	.0376	.0344	.0372	.0353	.0369	.0353	.0369
BLOWING RATE 2		.0675	.0665	.0655	.0656	.0658	.0672	.0551	.0557	.0543	.0560	.0547	.0531	.0470	.0473	.0447	.0468	.0452	.0455	.0452	.0455
*#																					
BLOWING RATE 0		.0192	.0177	.0160	.0175	.0154	.0158														
BLOWING RATE 1		.0342	.0337	.0313	.0409	.0338	.0471														
BLOWING RATE 2		.0380	.0378	.0363	.0465	.0399	.0861														

\*BAD GAGE

W14 1365

HASF PRESSURE AND GARDON DATA  
OUT AT INDICATED TAP LOCATION

RUN	3	TYPE UNIFORM *				ALPHA - 0.			
		1A	2A	3A	4A	1B	2B	3B	4B
BLOWING RATE 0		.33	.23	.20	.18	0.00	0.00	0.00	0.00
BLOWING RATE 1		.19	.04	.02	.01	0.00	0.00	0.00	0.00
BLOWING RATE 2		.06	0.00	0.00	0.00	0.00	0.00	0.00	0.00
BLOWING RATE 0		.34	.25	.19	.16	0.00	0.00	0.00	0.00
BLOWING RATE 1		.18	.06	.01	0.00	0.00	0.00	0.00	0.00
BLOWING RATE 2		.08	.01	0.00	0.00	0.00	0.00	0.00	0.00

W14 1365

HASF PRESSURE AND GARDON DATA  
STANTON NUMBER AT INDICATED TAP LOCATION

RUN	3	TYPE UNIFORM *				ALPHA - 0.			
		1A	2A	3A	4A	1B	2B	3B	4B
BLOWING RATE 0		3.75E-03	2.57E-03	2.23E-03	2.02E-03	n.	0.	0.	0.
BLOWING RATE 1		1.58E-03	3.62E-04	1.51E-04	5.19E-05	n.	0.	0.	0.
BLOWING RATE 2		4.79E-04	2.99E-05	1.15E-05	9.92E-07	n.	0.	0.	0.
BLOWING RATE 0		3.92E-03	2.81E-03	2.18E-03	1.86E-03	n.	0.	0.	0.
BLOWING RATE 1		1.53E-03	5.17E-04	1.01E-04	3.32E-05	n.	0.	0.	0.
BLOWING RATE 2		6.16E-04	9.10E-05	4.22E-06	2.16E-05	n.	0.	0.	0.

\* GAGES ONLY ON A AND D RAYS



WTD 1365

HASF PRESSURE AND GARDON DATA  
PRESSURE AT INDICATED TAP LOCATION

RUN 4	TYPE	UNIFORM												ALPHA - 0.											
		1A	1B	1C	1D	1E	1F	2A	2B	2C	2D	2E	2F	3A	3B	3C	3D	3E	3F	4A	4B	4C	4D	4E	4F
BLOWING RATE 0		.0050	.0050	.0047	.0046	.0046	.0047	.0021	.0021	.0019	.0023	.0022	.0017	.0012	.0012	.0009	.0012	.0009	.0011	.0014	.0014	.0012	.0009	.0012	.0014
BLOWING RATE 1		.0124	.0127	.0120	.0125	.0126	.0127	.0100	.0101	.0100	.0100	.0097	.0097	.0083	.0084	.0081	.0083	.0082	.0081	.0081	.0081	.0084	.0084	.0082	.0081
BLOWING RATE 2		.0155	.0153	.0152	.0153	.0153	.0154	.0120	.0122	.0120	.0114	.0116	.0119	.0100	.0102	.0094	.0100	.0094	.0094	.0094	.0094	.0102	.0094	.0100	.0094
BLOWING RATE 0		.0010	.0009	.0007	.0012	.0013	.0020																		
BLOWING RATE 1		.0062	.0061	.0061	.0080	.0065	.0341																		
BLOWING RATE 2		.0074	.0074	.0075	.0094	.0076	.0367																		

A-8

WTD 1365

HASF PRESSURE AND GARDON DATA  
PRESSURE COEFFICIENT AT INDICATED TAP LOCATION

RUN 4	TYPE	UNIFORM												ALPHA - 0.											
		1A	1B	1C	1D	1E	1F	2A	2B	2C	2D	2E	2F	3A	3B	3C	3D	3E	3F	4A	4B	4C	4D	4E	4F
BLOWING RATE 0		.0399	.0406	.0377	.0369	.0370	.0382	.0171	.0169	.0152	.0184	.0175	.0139	.0097	.0092	.0069	.0094	.0065	.0109	.0109	.0109	.0092	.0069	.0094	.0109
BLOWING RATE 1		.0978	.0962	.0940	.0948	.0955	.0963	.0758	.0766	.0753	.0756	.0736	.0736	.0628	.0638	.0609	.0630	.0610	.0610	.0610	.0610	.0638	.0609	.0630	.0610
BLOWING RATE 2		.1138	.1131	.1117	.1126	.1126	.1132	.0883	.0899	.0886	.0869	.0853	.0874	.0737	.0754	.0725	.0736	.0723	.0723	.0723	.0723	.0754	.0725	.0736	.0723
BLOWING RATE 0		.0083	.0075	.0053	.0093	.0103	.0161																		
BLOWING RATE 1		.0470	.0457	.0458	.0607	.0488	.2581																		
BLOWING RATE 2		.0543	.0542	.0550	.0690	.0561	.2854																		

\*BAD GAGE

WTH 1365

HASF PRESSURE AND GARDON DATA  
COUNT AT INDICATED TAP LOCATION

MUN	4	* TYPE UNIFORM																ALPHA - 0.							
		1A	2A	3A	4A	1B	2B	3B	4B	1C	2C	3C	4C	1D	2D	3D	4D	1E	2E	3E	4E				
FLOWING RATE 0																									
FLOWING RATE 1																									
FLOWING RATE 2																									
FLOWING RATE 0																									
FLOWING RATE 1																									
FLOWING RATE 2																									

WTH 1365

HASF PRESSURE AND GARDON DATA  
STANTON NUMBER AT INDICATED TAP LOCATION

MUN	* TYPE UNIFORM										ALPHA - 0.									
	UNIFORM										UNIFORM									
	UNIFORM										UNIFORM									
	UNIFORM										UNIFORM									
	UNIFORM										UNIFORM									
	UNIFORM										UNIFORM									
	UNIFORM										UNIFORM									
	UNIFORM										UNIFORM									
UNIFORM										UNIFORM										
UNIFORM										UNIFORM										
UNIFORM										UNIFORM										
UNIFORM										UNIFORM										
UNIFORM										UNIFORM										
UNIFORM										UNIFORM										
UNIFORM										UNIFORM										
UNIFORM										UNIFORM										
UNIFORM										UNIFORM										
UNIFORM										UNIFORM										
UNIFORM										UNIFORM										
UNIFORM										UNIFORM										
UNIFORM										UNIFORM										
UNIFORM										UNIFORM										
UNIFORM										UNIFORM										
UNIFORM										UNIFORM										
UNIFORM										UNIFORM										
UNIFORM										UNIFORM										
UNIFORM										UNIFORM										
UNIFORM										UNIFORM										
UNIFORM										UNIFORM										
UNIFORM										UNIFORM										
UNIFORM										UNIFORM										
UNIFORM										UNIFORM										
UNIFORM										UNIFORM										
UNIFORM										UNIFORM										
UNIFORM										UNIFORM										
UNIFORM										UNIFORM										
UNIFORM										UNIFORM										
UNIFORM										UNIFORM										
UNIFORM										UNIFORM										
UNIFORM										UNIFORM										
UNIFORM										UNIFORM										
UNIFORM										UNIFORM										
UNIFORM										UNIFORM										
UNIFORM										UNIFORM										
UNIFORM										UNIFORM										
UNIFORM										UNIFORM										
UNIFORM										UNIFORM										
UNIFORM										UNIFORM										
UNIFORM										UNIFORM										
UNIFORM										UNIFORM										
UNIFORM										UNIFORM										
UNIFORM										UNIFORM										
UNIFORM										UNIFORM										
UNIFORM										UNIFORM										
UNIFORM										UNIFORM										
UNIFORM										UNIFORM										
UNIFORM										UNIFORM										
UNIFORM										UNIFORM										
UNIFORM										UNIFORM										
UNIFORM										UNIFORM										
UNIFORM										UNIFORM										
UNIFORM										UNIFORM										
UNIFORM										UNIFORM										
UNIFORM										UNIFORM										
UNIFORM										UNIFORM										
UNIFORM										UNIFORM										
UNIFORM										UNIFORM										
UNIFORM										UNIFORM										
UNIFORM										UNIFORM										
UNIFORM										UNIFORM										
UNIFORM										UNIFORM										
UNIFORM										UNIFORM										
UNIFORM										UNIFORM										
UNIFORM										UNIFORM										
UNIFORM										UNIFORM										
UNIFORM										UNIFORM										
UNIFORM										UNIFORM										
UNIFORM										UNIFORM										
UNIFORM										UNIFORM										
UNIFORM										UNIFORM										
UNIFORM										UNIFORM										
UNIFORM										UNIFORM										
UNIFORM										UNIFORM										
UNIFORM										UNIFORM										
UNIFORM										UNIFORM										
UNIFORM										UNIFORM										
UNIFORM										UNIFORM										
UNIFORM										UNIFORM										
UNIFORM										UNIFORM										
UNIFORM										UNIFORM										
UNIFORM										UNIFORM										
UNIFORM										UNIFORM										
UNIFORM										UNIFORM										
UNIFORM										UNIFORM										
UNIFORM										UNIFORM										
UNIFORM										UNIFORM										
UNIFORM										UNIFORM										
UNIFORM										UNIFORM										
UNIFORM										UNIFORM										
UNIFORM										UNIFORM										
UNIFORM										UNIFORM										
UNIFORM										UNIFORM										
UNIFORM										UNIFORM										
UNIFORM										UNIFORM										
UNIFORM										UNIFORM										
UNIFORM										UNIFORM										
UNIFORM										UNIFORM										
UNIFORM										UNIFORM										
UNIFORM										UNIFORM										
UNIFORM										UNIFORM										
UNIFORM										UNIFORM										
UNIFORM										UNIFORM										
UNIFORM										UNIFORM										
UNIFORM										UNIFORM										
UNIFORM										UNIFORM										
UNIFORM										UNIFORM										
UNIFORM										UNIFORM										
UNIFORM										UNIFORM										
UNIFORM										UNIFORM										
UNIFORM										UNIFORM										
UNIFORM										UNIFORM										
UNIFORM										UNIFORM										
UNIFORM										UNIFORM										
UNIFORM										UNIFORM										
UNIFORM										UNIFORM										
UNIFORM										UNIFORM										
UNIFORM										UNIFORM										
UNIFORM										UNIFORM										
UNIFORM										UNIFORM										
UNIFORM										UNIFORM										
UNIFORM										UNIFORM										
UNIFORM										UNIFORM										
UNIFORM										UNIFORM										
UNIFORM										UNIFORM										
UNIFORM										UNIFORM										
UNIFORM										UNIFORM										
UNIFORM										UNIFORM										
UNIFORM										UNIFORM										
UNIFORM										UNIFORM										
UNIFORM										UNIFORM										
UNIFORM										UNIFORM										
UNIFORM										UNIFORM										
UNIFORM										UNIFORM										
UNIFORM										UNIFORM										
UNIFORM										UNIFORM										
UNIFORM										UNIFORM										
UNIFORM										UNIFORM										
UNIFORM										UNIFORM										
UNIFORM										UNIFORM										
UNIFORM										UNIFORM										
UNIFORM										UNIFORM										
UNIFORM										UNIFORM										
UNIFORM										UNIFORM										
UNIFORM										UNIFORM										
UNIFORM										UNIFORM										
UNIFORM										UNIFORM										
UNIFORM										UNIFORM										
UNIFORM										UNIFORM										
UNIFORM										UNIFORM										
UNIFORM										UNIFORM										
UNIFORM										UNIFORM										
UNIFORM										UNIFORM										
UNIFORM										UNIFORM										
UNIFORM										UNIFORM										
UNIFORM										UNIFORM										
UNIFORM										UNIFORM										
UNIFORM										UNIFORM										
UNIFORM										UNIFORM										
UNIFORM										UNIFORM										
UNIFORM										UNIFORM										
UNIFORM										UNIFORM										
UNIFORM										UNIFORM										
UNIFORM										UNIFORM										
UNIFORM										UNIFORM										
UNIFORM										UNIFORM										
UNIFORM										UNIFORM										
UNIFORM										UNIFORM										
UNIFORM										UNIFORM										
UNIFORM										UNIFORM										
UNIFORM										UNIFORM										
UNIFORM										UNIFORM										
UNIFORM										UNIFORM										
UNIFORM										UNIFORM</										

\*GAGES ONLY ON A AND D RAYS

WTO 1365	RUN	HASF PRESSURE AND GARDON DATA PRESSURE AT INDICATED TAP LOCATION															
		TYPE UNIFORM															
		ALPHA = 0.															
		1A	1B	1C	1D	1E	1F	1G	1H	1I	1J	1K	1L	1M	1N	1O	1P
FLOWING RATE 0		.0054	.0048	.0045	.0046	.0042	.0051	.0025	.0018	.0025	.0024	.0022	.0023	.0023	.0023	.0023	.0026
FLOWING RATE 1		.0064	.0058	.0064	.0058	.0051	.0060	.0034	.0032	.0026	.0032	.0027	.0035	.0031	.0029	.0030	.0034
FLOWING RATE 2		.0080	.0077	.0067	.0079	.0068	.0073	.0066	.0067	.0059	.0067	.0069	.0064	.0071	.0069	.0069	.0071
		4A	4B	4C	4D	4E	4F										
FLOWING RATE 0		.0021	.0090	.0020	.0021	.0016	.0022										
FLOWING RATE 1		.0034	.0185	.0025	.0031	.0029	.0038										
FLOWING RATE 2		.0054	.0654	.0052	.0061	.0059	.0066										

WTH 1365	RUN	HASF PRESSURE AND GARDON DATA PRESSURE COEFFICIENT AT INDICATED TAP LOCATION															
		TYPE UNIFORM															
		1A	1B	1C	1D	1E	1F	1G	1H	1I	1J	1K	1L	1M	1N	1O	1P
FLOWING RATE 0		.0430	.0384	.0359	.0369	.0337	.0406	.0196	.0198	.0144	.0201	.0194	.0152	.0208	.0194	.0182	.0204
FLOWING RATE 1		.0490	.0441	.0409	.0440	.0389	.0455	.0258	.0246	.0199	.0241	.0245	.0206	.0265	.0234	.0217	.0258
FLOWING RATE 2		.0578	.0558	.0484	.0570	.0495	.0526	.0481	.0484	.0430	.0485	.0500	.0465	.0512	.0502	.0503	.0527
		4A	4B	4C	4D	4E	4F										
FLOWING RATE 0		.0171	.0705	.0157	.0171	.0125	.0178										
FLOWING RATE 1		.0254	.1409	.0188	.0235	.0223	.0286										
FLOWING RATE 2		.0431	.4740	.0378	.0441	.0431	.0495										

\*BAD GAGE

WTU 1365

HASF PRESSURE AND GARDON DATA  
QUOT AT INDICATED TAP LOCATION

RUN	5	* TYPE UNIFORM												ALPHA - 0.			
		1A	2A	3A	4A	1R	2R	3H	4B	1C	2C	3C	4C				
BLOWING RATE	0	.29	.20	.34	.22	0.00	0.00	0.00	0.00	0.00	0.00	0.00	0.00				
BLOWING RATE	1	.26	.13	.20	.10	0.00	0.00	0.00	0.00	0.00	0.00	0.00	0.00				
BLOWING RATE	2	.15	.01	.01	0.00	0.00	0.00	0.00	0.00	0.00	0.00	0.00	0.00				
1D	2D	3D	4D	1E	2E	3E	4E	1F	2F	3F	4F						
BLOWING RATE	0	.29	.21	.12	.13	0.00	0.00	0.00	0.00	0.00	0.00	0.00					
BLOWING RATE	1	.23	.15	.06	.06	0.00	0.00	0.00	0.00	0.00	0.00	0.00					
BLOWING RATE	2	.08	.01	0.00	0.00	0.00	0.00	0.00	0.00	0.00	0.00	0.00					

WTU 1365

HASF PRESSURE AND GARDON DATA  
STANTON NUMBER AT INDICATED TAP LOCATION

RUN	5	1A	2A	3A	4A	1B	2R	3R	4R	1C	2C	3C	4C
		3.36E-03	2.30E-03	3.90E-03	2.51E-03	0.	0.	0.	0.	0.	0.	0.	0.
BLOWING RATE	0	2.49E-03	1.27E-03	1.88E-03	9.18E-04	0.	0.	0.	0.	0.	0.	0.	0.
BLOWING RATE	1	1.20E-03	8.47E-05	1.06E-04	8.04E-06	0.	0.	0.	0.	0.	0.	0.	0.
BLOWING RATE	0	3.34E-03	2.44E-03	1.33E-03	1.49E-03	0.	0.	0.	0.	0.	0.	0.	0.
BLOWING RATE	1	2.19E-03	1.44E-03	5.75E-04	5.56E-04	0.	0.	0.	0.	0.	0.	0.	0.
BLOWING RATE	2	6.82E-04	7.78E-05	-3.04E-05	3.98E-05	0.	0.	0.	0.	0.	0.	0.	0.

\*GAGES ONLY ON A AND D RAYS

WIR 1365

HASF PRESSURE AND GARDON DATA  
PRESSURE AT INDICATED TAP LOCATION

RUN	6	TYPE UNIFORM																ALPHA - 0.			
		1A	1B	1C	1D	1E	1F	2A	2B	2C	2D	2E	2F	3A	3B	3C	3D	3E	3F	3G	3H
BLOWING RATE 0		.0053	.0049	.0048	.0051	.0045	.0050	.0029	.0031	.0027	.0031	.0031	.0024	.0021	.0020	.0021	.0022	.0017	.0022	.0017	.0022
BLOWING RATE 1		.0083	.0092	.0081	.0096	.0088	.0087	.0074	.0084	.0076	.0086	.0090	.0082	.0064	.0074	.0067	.0075	.0077	.0075	.0077	.0075
BLOWING RATE 2		.0140	.0135	.0130	.0137	.0129	.0132	.0118	.0116	.0113	.0116	.0117	.0115	.0102	.0099	.0096	.0094	.0100	.0098	.0100	.0098
BLOWING RATE 0		.0025	.0153	.0027	.0029	.0021	.0015														
BLOWING RATE 1		.0060	.0286	.0064	.0072	.0063	.0065														
BLOWING RATE 2		.0091	.0156	.0086	.0088	.0080	.0083														

WIR 1365

HASF PRESSURE AND GARDON DATA  
PRESSURE COEFFICIENT AT INDICATED TAP LOCATION

RUN	6	TYPE UNIFORM																ALPHA - 0.			
		1A	1B	1C	1D	1E	1F	2A	2B	2C	2D	2E	2F	3A	3B	3C	3D	3E	3F	3G	3H
BLOWING RATE 0		.0432	.0400	.0394	.0417	.0370	.0404	.0233	.0251	.0219	.0267	.0254	.0199	.0172	.0164	.0168	.0175	.0175	.0177	.0177	.0177
BLOWING RATE 1		.0674	.0745	.0652	.0775	.0715	.0704	.0596	.0682	.0616	.0696	.0727	.0665	.0519	.0596	.0541	.0405	.0430	.0404	.0430	.0404
BLOWING RATE 2		.1159	.1115	.1075	.1135	.1067	.1091	.0976	.0957	.0938	.0960	.0969	.0949	.0844	.0816	.0796	.0811	.0827	.0811	.0827	.0811
BLOWING RATE 0		.0206	.1251	.0223	.0236	.0170	.0121														
BLOWING RATE 1		.0486	.2309	.0519	.0578	.0511	.0524														
BLOWING RATE 2		.0757	.1290	.0716	.0730	.0659	.0687														

\*BAD GAGE

WTP 1365

MAST PRESSURE AND GARDON DATA  
 QUOT AT INDICATED TAP LOCATION

HUN 6	TYPE UNIFORM *	ALPHA - 0.											
		1A	2A	3A	4A	1B	2B	3B	4B	1C	2C	3C	4C
FLOWING RATE 0	.26	.19	.30	.00	.19	0.00	0.00	0.00	0.00	0.00	0.00	0.00	0.00
FLOWING RATE 1	.01	0.00	0.00	0.00	.01	0.00	0.00	0.00	0.00	0.00	0.00	0.00	0.00
FLOWING RATE 2	0.00	.01	.01	.01	.01	0.00	0.00	0.00	0.00	0.00	0.00	0.00	0.00
FLOWING RATE 0	.28	.22	.12	.14	.14	0.00	0.00	0.00	0.00	0.00	0.00	0.00	0.00
FLOWING RATE 1	-.01	-.01	0.00	0.00	0.00	0.00	0.00	0.00	0.00	0.00	0.00	0.00	0.00
FLOWING RATE 2	-.01	0.00	0.00	.01	.01	0.00	0.00	0.00	0.00	0.00	0.00	0.00	0.00

WTP 1365

MAST PRESSURE AND GARDON DATA  
 STANTON NUMBER AT INDICATED TAP LOCATION

HUN 6	TYPE UNIFORM *	ALPHA - 0.											
		1A	2A	3A	4A	1B	2B	3B	4B	1C	2C	3C	4C
FLOWING RATE 0	3.05E-03	4.26E-03	3.52E-03	2.24E-03	0.	0.	0.	0.	0.	0.	0.	0.	0.
FLOWING RATE 1	9.67E-05	-7.91E-06	3.88E-05	7.99E-05	0.	0.	0.	0.	0.	0.	0.	0.	0.
FLOWING RATE 2	-7.56E-05	6.09E-05	1.36E-04	1.37E-04	0.	0.	0.	0.	0.	0.	0.	0.	0.
FLOWING RATE 0	3.33E-03	4.60E-03	1.46E-03	1.66E-03	0.	0.	0.	0.	0.	0.	0.	0.	0.
FLOWING RATE 1	-7.81E-05	-1.01E-04	-6.65E-05	4.19E-05	0.	0.	0.	0.	0.	0.	0.	0.	0.
FLOWING RATE 2	-1.18E-04	-3.19E-05	3.10E-06	9.45E-05	0.	0.	0.	0.	0.	0.	0.	0.	0.

\*GAGES ONLY ON A AND D RAYS

WTR 1365      FORCE DATA

     RUN 7      TYPE III      ALPHA = 10.

BLOWING RATE 0	NFC	PMC	YMC	PXCP	YXCP
BLOWING RATE 1	.2984	-.0651	.0061	-.2181	-.2969
BLOWING RATE 2	.2723	-.0582	.0031	-.2136	.2301
	.2457	-.0510	.0191	-.2075	.3574

WTR 1365      FORCE DATA

     RUN 8      TYPE III      ALPHA = 20.

BLOWING RATE 0	NFC	PMC	YMC	PXCP	YXCP
BLOWING RATE 1	.7339	-.0855	.0010	-.1164	-.1523
BLOWING RATE 2	.7214	-.0820	.0116	-.1137	.0201
	.7182	-.0786	.0177	-.1094	.0759

WTR 1365      FORCE DATA

     RUN 9      TYPE III      ALPHA = 5.

BLOWING RATE 0	NFC	PMC	YMC	PXCP	YXCP
BLOWING RATE 1	.1104	-.0332	-.0015	-.3012	2.7482
BLOWING RATE 2	.0891	-.0177	.0047	-.1991	.6956
	.0718	-.0086	.0094	-.1201	1.0981

WTR 1365      FORCE DATA

RUN 10

TYPE	NOMINAL	ALPHA = 10.	YFC	YMC	PXCP	YXCP
BLOWING RATE 0	NFC					
BLOWING RATE 1	.3001		-.0036	.0138	-.2200	-.2372
BLOWING RATE 2	.2803		.0020	.0038	-.2196	4.8487
	.2661		.0045	.0063	-.2217	2.6430

WTR 1365      FORCE DATA

RUN 11

TYPE	NOMINAL	ALPHA = 20.	YFC	YMC	PXCP	YXCP
BLOWING RATE 0	NFC					
BLOWING RATE 1	.7057		-.0036	-.0006	-.1391	.2087
BLOWING RATE 2	.6922		.0030	.0026	-.1381	1.2500
	.6897		.0067	.0035	-.1314	.6851

WTR 1365      FORCE DATA

RUN 12

TYPE	NOMINAL	ALPHA = 10.	YFC	YMC	PXCP	YXCP
BLOWING RATE 0	NFC					
BLOWING RATE 1	.3015		-.0038	.0042	-.2129	-.A305
BLOWING RATE 2	.2821		-.0127	-.0045	-.2133	.4400
	.2699		-.0173	-.0090	-.2159	.6894

WTR 1365      FORCE DATA

RUN 13

TYPE	NOMINAL	ALPHA = 35.	YFC	YMC	PXCP	YXCP
BLOWING RATE 0	NFC					
BLOWING RATE 1	1.4160		.0018	-.0037	-.1021	-1.5315
BLOWING RATE 2	1.3992		.0094	-.0011	-.0992	-.1142
	1.3880		.0140	.0002	-.0952	.0413



WTR 1365      FORCE DATA

RUN 14      TYPE II      ALPHA = 10.

BLOWING RATE 0	NFC	PMC	YFC	YMC	PKCP	YKCP
BLOWING RATE 1	.2756	-.0619	-.0012	-.0005	-.2248	-1.2751
BLOWING RATE 2	.2550	-.0615	.0014	.0031	-.2413	-1.9362
	.2395	-.0612	.0028	.0051	-.2555	11.2593

WTR 1365      FORCE DATA

RUN 15      TYPE II      ALPHA = 20.

BLOWING RATE 0	NFC	PMC	YFC	YMC	PKCP	YKCP
BLOWING RATE 1	.6732	-.0767	-.0114	-.0010	-.1139	.1084
BLOWING RATE 2	.6607	-.0787	-.0078	.0017	-.1190	-.2190
	.6554	-.0784	-.0055	.0033	-.1197	-.6067

WTR 1365      FORCE DATA

RUN 16      TYPE II      ALPHA = 35.

BLOWING RATE 0	NFC	PMC	YFC	YMC	PKCP	YKCP
BLOWING RATE 1	1.4012	-.1431	-.0454	.0028	-.1021	-.0617
BLOWING RATE 2	1.3931	-.1448	-.0410	.0060	-.1039	-.1456
	1.3971	-.1423	-.0387	.0075	-.1018	-.1925

RUN	WTR 1365	FORCE DATA					
		TYPE 4	PMC	YFC	YMC	PKCP	YKCP
RUN 17	WTR 1365	TYPE 4	ALPHA = 10.				$\phi = +60^0$
			NFC				
			.2361	.0006	-.0004	-.1309	
			.2251	.0021	.0015	-.1405	
BLOWING RATE 0							YKCP
BLOWING RATE 1							-.2336
BLOWING RATE 2							2.1242
							.7003
RUN 18	WTR 1365	TYPE 4	ALPHA = 10.				$\phi = -60^0$
			NFC				
			.2869	-.0011	.0002	-.1365	
			.2729	-.0027	-.0016	-.1420	
BLOWING RATE 0							YKCP
BLOWING RATE 1							7.5736
BLOWING RATE 2							.7621
							.4935
RUN 19	WTR 1365	TYPE 4	ALPHA = 20.				
			NFC				
			.6298	.0080	-.0019	-.1171	
			.6189	.0111	-.0003	-.1175	
BLOWING RATE 0							YKCP
BLOWING RATE 1							-.2336
BLOWING RATE 2							-.0283
							.0160
RUN 20	WTR 1365	TYPE 4	ALPHA = 35.				
			NFC				
			1.2089	-.0114	.0004	-.1024	
			1.1979	-.0082	.0019	-.1015	
BLOWING RATE 0							YKCP
BLOWING RATE 1							-.0324
BLOWING RATE 2							-.2257
							-.3214

WTP 1365

MAF PRESSURE AND GARDON DATA  
PRESSURE AT INDICATED TAP LOCATION

RUN 21	TYPE	NOMINAL																ALPHA = 5.			
		1A	1B	1C	1D	1E	1F	2A	2B	2C	2D	2E	2F	3A	3B	3C	3D	3E	3F	3G	3H
FLOWING RATE 0		.0037	.0033	.0036	.0050	.0068	.0057	.0010	.0009	.0010	.0032	.0076	.0031	.0006	.0000	.0004	.0032	.0050	.0030	.0035	.0035
FLOWING RATE 1		.0044	.0043	.0050	.0075	.0078	.0062	.0025	.0027	.0030	.0056	.0116	.0043	.0021	.0018	.0018	.0039	.0050	.0035	.0035	.0035
FLOWING RATE 2		.0059	.0066	.0076	.0104	.0100	.0075	.0045	.0046	.0049	.0073	.0148	.0060	.0037	.0035	.0035	.0052	.0052	.0052	.0052	.0052
FLOWING RATE 0		.0022	.0003	.0001	.0036	.0077	.0000														
FLOWING RATE 1		.0016	.0011	.0013	.0036	.0077	.0000														
FLOWING RATE 2		.0027	.0023	.0024	.0042	.0073	.0000														

WTP 1365

MAF PRESSURE AND GARDON DATA  
PRESSURE COEFFICIENT AT INDICATED TAP LOCATION

RUN 21	TYPE	NOMINAL																ALPHA = 5.			
		1A	1B	1C	1D	1E	1F	2A	2B	2C	2D	2E	2F	3A	3B	3C	3D	3E	3F	3G	3H
FLOWING RATE 0		.0268	.0242	.0258	.0434	.0489	.0411	.0071	.0064	.0069	.0229	.0266	.0223	.0043	.0003	.0070	.0230	.0419	.0218	.0218	.0218
FLOWING RATE 1		.0311	.0306	.0357	.0530	.0555	.0443	.0180	.0193	.0210	.0397	.0623	.0307	.0149	.0126	.0129	.0279	.0420	.0249	.0249	.0249
FLOWING RATE 2		.0405	.0452	.0522	.0712	.0685	.0516	.0310	.0314	.0334	.0501	.1020	.0409	.0257	.0240	.0278	.0359	.0454	.0314	.0314	.0314
FLOWING RATE 0		.0016	.0023	.0005	.0259	.0556	.0000														
FLOWING RATE 1		.0112	.0080	.0093	.0258	.0507	.0000														
FLOWING RATE 2		.0184	.0156	.0166	.0287	.0500	.0000														

\*BAD GAGE

WTR 1365

MASF PRESSURE AND GARDON DATA  
QUOT AT INDICATED TAP LOCATION

RUN 21	TYPE	ALPHA - 5.											
		* NOMINAL				*							
	1A	2A	3A	4A	1H	2H	3H	4H	1C	2C	3C	4C	
BLOWING RATE 0	0.00	.24	.14	.17	.27	0.00	.11	.04	.34	.21	.20	.17	
BLOWING RATE 1	0.00	.04	.04	.05	.12	0.00	.01	0.00	.07	.01	.02	.01	
BLOWING RATE 2	0.00	.02	0.00	.01	.03	0.00	0.00	0.00	.01	0.00	0.00	0.00	
	1D	2D	3D	4D	1E	2E	3E	4E	1F	2F	3F	4F	
BLOWING RATE 0	.47	.39	.40	.38	0.00	.50	0.00	0.00	.49	.37	.37	.40	
BLOWING RATE 1	.16	.04	.09	.10	0.00	.15	0.00	0.00	.36	.17	.20	.21	
BLOWING RATE 2	.02	0.00	.01	.02	0.00	.02	0.00	0.00	.18	.04	.07	.07	

WTR 1365

MASF PRESSURE AND GARDON DATA  
STANTON NUMBER AT INDICATED TAP LOCATION

* * *													
		1A	2A	3A	4A	1B	2B	3B	4B	1C	2C	3C	4C
BLOWING RATE	0	0.	2.14E-03	1.27E-03	1.46E-03	2.36E-03	0.	9.59E-04	6.85E-04	2.09E-03	1.41E-03	1.75E-03	1.47E-03
BLOWING RATE	1	0.	7.84E-04	3.20E-04	4.15E-04	1.00E-03	0.	6.76E-05	4.09E-05	5.76E-04	7.69E-05	1.64E-04	8.44E-04
BLOWING RATE	2	0.	1.80E-04	3.24E-05	6.51E-05	2.52E-04	0.	-1.39E-06	7.55E-06	9.82E-05	-1.87E-05	3.01E-06	-2.49E-05
* * *													
		1D	2D	3D	4D	1E	2E	3E	4E	1F	2F	3F	4F
BLOWING RATE	0	4.10E-03	3.43E-03	3.52E-03	3.37E-03	0.	4.44E-03	0.	0.	4.29E-03	3.70E-03	3.24E-03	3.44E-03
BLOWING RATE	1	1.28E-03	3.40E-04	7.76E-04	8.27E-04	0.	1.20E-03	0.	0.	2.92E-03	1.34E-03	1.60E-03	1.74E-03
BLOWING RATE	2	2.06E-04	-2.94E-05	1.20E-04	1.60E-04	0.	1.72E-04	0.	0.	1.62E-03	3.54E-04	6.07E-04	6.74E-04

\*BAD GAGE

WTR 1365	HUN 22	HASF PRESSURE AND GARDON DATA PRESSURE AT INDICATED TAP LOCATION															
		TYPE NOMINAL ALPHA = 10.															
		1A	1B	1C	1D	1E	1F	2A	2B	2C	2D	2E	2F	3A	3B	3C	3F
BLOWING RATE 0		.0032	.0024	.0030	.0081	.0125	.0042	.0003	.0003	.0003	.0063	.0139	.0067	.0002	.0003	.0079	.0103
BLOWING RATE 1		.0029	.0030	.0037	.0089	.0125	.0081	.0017	.0018	.0019	.0084	.0150	.0076	.0014	.0009	.0007	.0100
BLOWING RATE 2		.0051	.0055	.0064	.0116	.0145	.0096	.0032	.0031	.0034	.0101	.0193	.0088	.0022	.0020	.0020	.0179
		4A	4B	4C	4D	4E	4F										
BLOWING RATE 0		-.0009	-.0010	-.0011	.0088	.02000	.0000										
BLOWING RATE 1		.0004	.0002	.0003	.0087	.02020	.0000										
BLOWING RATE 2		.0013	.0011	.0012	.0089	.02110	.0000										

WTR 1365	HUN 22	HASF PRESSURE AND GARDON DATA PRESSURE COEFFICIENT AT INDICATED TAP LOCATION															
		TYPE NOMINAL ALPHA = 10.															
		1A	1B	1C	1D	1E	1F	2A	2B	2C	2D	2E	2F	3A	3B	3C	3F
BLOWING RATE 0		.0232	.0174	.0213	.0578	.0897	.0585	.0022	.0022	.0022	.0453	.0978	.0483	.0015	.0023	.0039	.0570
BLOWING RATE 1		.0203	.0208	.0264	.0624	.0882	.0573	.0121	.0127	.0137	.0592	.1057	.0535	.0072	.0061	.0046	.0533
BLOWING RATE 2		.0349	.0374	.0435	.0788	.0985	.0648	.0217	.0211	.0228	.0683	.1312	.0599	.0148	.0138	.0114	.0546
		4A	4B	4C	4D	4E	4F										
BLOWING RATE 0		-.0063	-.0069	-.0080	.0633	.14340	.0000										
BLOWING RATE 1		.0027	.0014	.0024	.0615	.14210	.0000										
BLOWING RATE 2		.0091	.0072	.0083	.0604	.14300	.0000										

\*BAD GAGE

WTN 1365

HASF PRESSURE AND GARDON DATA  
QUOT AT INDICATED TAP LOCATION

RUN 22	TYPE	NOMINAL										ALPHA = 10.			
		1A	2A	3A	4A	1B	2B	3B	4B	1C	2C	3C	4C		
BLOWING RATE 0	0.00	0.00	.22	.13	.14	.20	0.00	.07	.05	.31	.19	.18	.14		
BLOWING RATE 1	0.00	.10	.05	.06	.06	.07	0.00	0.00	0.00	.06	.01	.03	.02		
BLOWING RATE 2	0.00	.03	.01	.02	.02	.01	0.00	0.00	0.00	0.00	0.00	0.00	0.00		
BLOWING RATE 0	0.00	0.00	0.00	0.00	0.00	0.00	0.00	0.00	0.00	0.00	0.00	0.00	0.00		
BLOWING RATE 1	0.00	.19	.16	.30	.30	.57	0.00	0.00	0.00	.50	.36	.45	.48		
BLOWING RATE 2	0.04	.05	.10	.13	.13	.23	0.00	0.00	0.00	.29	.16	.25	.29		

WTN 1365

HASF PRESSURE AND GARDON DATA  
STANTON NUMBER AT INDICATED TAP LOCATION

RUN 22	TYPE	NOMINAL										ALPHA = 10.			
		1A	2A	3A	4A	1B	2B	3B	4B	1C	2C	3C	4C		
BLOWING RATE 0	0.00	0.00	0.00	0.00	0.00	0.00	0.00	0.00	0.00	0.00	0.00	0.00	0.00		
BLOWING RATE 1	0.00	0.00	0.00	0.00	0.00	0.00	0.00	0.00	0.00	0.00	0.00	0.00	0.00		
BLOWING RATE 2	0.00	0.00	0.00	0.00	0.00	0.00	0.00	0.00	0.00	0.00	0.00	0.00	0.00		
BLOWING RATE 0	0.00	0.00	0.00	0.00	0.00	0.00	0.00	0.00	0.00	0.00	0.00	0.00	0.00		
BLOWING RATE 1	0.00	0.00	0.00	0.00	0.00	0.00	0.00	0.00	0.00	0.00	0.00	0.00	0.00		
BLOWING RATE 2	0.00	0.00	0.00	0.00	0.00	0.00	0.00	0.00	0.00	0.00	0.00	0.00	0.00		

\*BAD GAGE

WTP 1365

HASF PRESSURE AND GARDON DATA  
PRESSURE AT INDICATED TAP LOCATION

HUN 23	TYPE	NOMINAL																ALPHA = 2.0			
		1A	1B	1C	1D	1E	1F	2A	2B	2C	2D	2E	2F	3A	3B	3C	3D	3E	3F	3G	3H
FLOWING RATE 0		.0010	.0011	.0010	.0139	.0401	.0164	.0010	.0003	.0012	.0180	.1421	.0192	.0009	.0012	.0014	.0181	.0429	.0179		
FLOWING RATE 1		.0010	.0016	.0018	.0141	.0399	.0163	.0001	.0003	.0001	.0197	.1320	.0196	.0001	.0005	.0005	.0187	.0431	.0184		
FLOWING RATE 2		.0027	.0032	.0038	.0159	.0414	.0176	.0010	.0011	.0012	.0224	.0625	.0208	.0006	.0001	.0003	.0197	.0445	.0190		
FLOWING RATE 0		.0009	.0018	.0012	.0167	.0455	.0000														
FLOWING RATE 1		.0000	.0008	.0001	.0178	.0462	.0000														
FLOWING RATE 2		.0006	.0003	.0006	.0187	.0477	.0000														

A-22

WTP 1365

HASF PRESSURE AND GARDON DATA  
PRESSURE COEFFICIENT AT INDICATED TAP LOCATION

HUN 23	TYPE	NOMINAL																ALPHA = 2.0			
		1A	1B	1C	1D	1E	1F	2A	2B	2C	2D	2E	2F	3A	3B	3C	3D	3E	3F	3G	3H
FLOWING RATE 0		.0076	.0084	.0074	.1032	.2972	.1215	.0072	.0020	.0009	.1390	.0000	.1423	.0064	.0091	.0100	.1341	.3174	.1325		
FLOWING RATE 1		.0069	.0118	.0132	.1015	.2877	.1179	.0010	.0022	.0006	.1420	.9520	.1413	.0009	.0033	.0017	.1347	.3113	.1325		
FLOWING RATE 2		.0191	.0221	.0264	.1113	.2904	.1234	.0073	.0077	.0087	.1572	.4383	.1455	.0044	.0010	.0022	.1379	.3099	.1330		
FLOWING RATE 0		.0064	.0134	.0086	.1240	.3374	.0000														
FLOWING RATE 1		.0002	.0055	.0007	.1284	.3330	.0000														
FLOWING RATE 2		.0042	.0020	.0041	.1312	.3341	.0000														

\*BAD GAGE

WTP 1365

HASF PRESSURE AND GARDON DATA  
OUT AT INDICATED TAP LOCATION

RUN 23	TYPE	NOMINAL	ALPHA = 20. *											
			1A	2A	3A	4A	1B	2B	3B	4B	1C	2C	3C	4C
FLOWING RATE 0	0		0.00	.16	.13	.13	.12	0.00	.08	.06	.22	.14	.15	.13
FLOWING RATE 1	0		0.00	.11	.07	.07	.02	0.00	0.00	0.00	.04	.02	.05	.02
FLOWING RATE 2	0		0.00	.05	.02	.03	0.00	0.00	0.00	0.00	0.00	0.00	.01	-.01
							*		*					
FLOWING RATE 0	0		1D	2D	3D	4D	1E	2E	3E	4E	1F	2F	3F	4F
FLOWING RATE 1	0		1.02	1.07	.90	.76	0.00	1.74	0.00	0.00	1.11	1.06	.86	.80
FLOWING RATE 2	0		.67	.52	.58	.48	0.00	1.39	0.00	0.00	1.00	.85	.74	.71
FLOWING RATE 1	1		.17	.26	.29	.27	0.00	.84	0.00	0.00	.69	.52	.50	.44

WTP 1365

HASF PRESSURE AND GARDON DATA  
STANTON NUMBER AT INDICATED TAP LOCATION

ALPHA = 20. *													
		1A	2A	3A	4A	1B	2B*	3B	4B	1C	2C	3C	4C
FLOWING RATE	0	0.	1.44E-03	1.16E-03	1.12E-03	1.08E-03	0.	6.68E-04	5.11E-04	1.98E-03	1.25E-03	1.35E-03	1.13E-03
FLOWING RATE	1	0.	8.79E-04	5.57E-04	5.81E-04	2.03E-04	0.	3.74E-05	7.78E-07	3.68E-04	2.04E-04	4.07E-04	2.01E-04
FLOWING RATE	2	0.	4.71E-04	1.92E-04	2.59E-04	4.21E-06	0.	-4.01E-05	-4.43E-05	7.54E-06	-3.27E-05	6.72E-05	-6.44E-05
		1D	2D	3D	4D	1E*	2E	3E*	4E	1F	2F	3F	4F
FLOWING RATE	0	9.02E-03	9.54E-03	8.02E-03	6.75E-03	0.	1.55E-02	0.	0.	9.83E-03	9.40E-03	7.67E-03	7.07E-03
FLOWING RATE	1	5.51E-03	4.29E-03	4.82E-03	3.94E-03	0.	1.15E-02	0.	0.	8.28E-03	7.00E-03	6.10E-03	5.43E-03
FLOWING RATE	2	1.55E-03	2.39E-03	2.65E-03	2.46E-03	0.	7.74E-03	0.	0.	6.44E-03	4.79E-03	4.62E-03	4.13E-03

\*BAD GAGE



\*Tp 1365

HASF PRESSURE AND GARDON DATA  
PRESSURE AT INDICATED TAP LOCATION

RUN 24	TYPE III	ALPHA - 0.															
		1A	1B	1C	1D	1E	1F	1G	1H	1I	1J	1K	1L	1M	1N	1O	1P
BLOWING RATE 0		.0041	.0043	.0039	.0046	.0039	.0039	.0015	.0019	.0021	.0022	.0017	.0042	.0031	.0036	.0012	.0011
BLOWING RATE 1		.0047	.0050	.0052	.0043	.0062	.0051	.0027	.0035	.0046	.0051	.0042	.0042	.0028	.0031	.0036	.0040
BLOWING RATE 2		.0055	.0061	.0076	.0398	.0079	.0068	.0054	.0059	.0069	.0074	.0062	.0070	.0049	.0052	.0055	.0056
BLOWING RATE 0		.0011	.0013	.0016	.0011	.0011	.0014	.0016									
BLOWING RATE 1		.0025	.0029	.0031	.0029	.0034	.0030										
BLOWING RATE 2		.0038	.0041	.0044	.0040	.0044	.0041										

\*Tp 1365

HASF PRESSURE AND GARDON DATA  
PRESSURE COEFFICIENT AT INDICATED TAP LOCATION

RUN 24	TYPE III	ALPHA - 0.															
		1A	1B	1C	1D	1E	1F	1G	1H	1I	1J	1K	1L	1M	1N	1O	1P
BLOWING RATE 0		.0303	.0320	.0285	.0224	.0289	.0288	.0113	.0142	.0159	.0162	.0123	.0166	.0073	.0093	.0089	.0089
BLOWING RATE 1		.0337	.0355	.0369	.0268	.0441	.0360	.0189	.0245	.0329	.0362	.0296	.0299	.0200	.0223	.0252	.0244
BLOWING RATE 2		.0376	.0421	.0522	.2724	.0543	.0469	.0369	.0405	.0477	.0511	.0426	.0478	.0334	.0358	.0376	.0352
BLOWING RATE 0		.0081	.0096	.0114	.0082	.0106	.0117										
BLOWING RATE 1		.0180	.0203	.0222	.0203	.0239	.0214										
BLOWING RATE 2		.0259	.0278	.0302	.0273	.0305	.0283										

\*BAD GAGE

WTH 136S

MASF PRESSURE AND GARDON DATA  
OUT AT INDICATED TAP LOCATION

MUN 24	TYPE III	ALPHA - U.											
		1A	2A	3A	4A	1B	2B	3B	4B	1C	2C	3C	4C
FLOWING RATE 0	.43	.30	.25	.23	.45	.28	.28	.24	0.00	.32	.25	.20	
FLOWING RATE 1	.34	.15	.08	.07	.32	.10	.07	.04	0.00	.02	.02	.01	
FLOWING RATE 2	.14	.04	.01	.01	.16	.01	.01	0.00	0.00	0.00	0.00	0.00	
	*	10	20	30	40	1F	2E	3F	4E	1F	2F	3F	4F
FLOWING RATE 0	0.00	.31	.27	.24	.46	.46	.35	.24	.21	.41	.27	.18	.22
FLOWING RATE 1	0.00	0.00	.03	.02	.13	.13	0.00	0.00	.02	.28	.04	.03	.04
FLOWING RATE 2	0.00	0.00	0.00	0.00	.05	.05	0.00	0.00	0.00	.12	.01	.01	0.00

WTH 136S

MASF PRESSURE AND GARDON DATA  
STANTON NUMBER AT INDICATED TAP LOCATION

ALPHA - U.													
	1A	2A	3A	4A	1B	2B	3B	4B	1C	2C	3C	4C	
FLOWING RATE 0	3.75E-03	4.66E-03	2.18E-03	2.07E-03	2.46E-03	2.46E-03	2.42E-03	2.11E-03	0.	2.78E-03	2.21E-03	1.74E-03	
FLOWING RATE 1	2.72E-03	1.22E-03	6.53E-04	5.54E-04	2.61E-03	8.17E-04	5.85E-04	3.30E-04	0.	1.65E-04	1.47E-04	1.10E-04	
FLOWING RATE 2	1.66E-03	3.17E-04	1.04E-04	1.24E-04	1.37E-03	1.21E-04	6.18E-05	3.09E-05	0.	-2.44E-05	6.54E-06	-1.04E-05	
	★												
	1D	2D	3D	4D	1E	2E	3E	4E	1F	2F	3F	4F	
FLOWING RATE 0	0.	2.74E-03	2.35E-03	2.14E-03	4.07E-03	3.12E-03	2.11E-03	1.83E-03	3.62E-03	2.41E-03	1.59E-03	1.49E-03	
FLOWING RATE 1	0.	3.46E-05	2.22E-04	1.29E-04	1.02E-03	3.54E-05	2.56E-05	1.58E-04	2.27E-03	6.74E-04	2.22E-04	3.44E-04	
FLOWING RATE 2	0.	2.18E-06	1.10E-05	1.08E-05	4.35E-04	1.12E-05	8.32E-06	-3.25E-05	1.08E-03	7.29E-05	5.57E-05	3.43E-05	

\*BAD GAGE

MTR 1365

MAF PRESSURE AND GARDON DATA  
PRESSURE AT INDICATED TAP LOCATION

RUN 25	TYPE III															
	ALPHA - 5.															
	1A	1B	1C	1U*	1F	1F	2A	2A	2C	2C	2D	2E	2F	3A	3B	3F
BLOWING RATE 0	.0030	.0035	.0037	.0487	.0071	.0056	.0011	.0011	.0011	.0011	.0031	.0053	.0033	.0008	.0003	.0035
BLOWING RATE 1	.0044	.0049	.0051	.0107	.0087	.0065	.0028	.0033	.0034	.0034	.0054	.0073	.0042	.0028	.0027	.0069
BLOWING RATE 2	.0061	.0068	.0079	.0133	.0111	.0080	.0051	.0055	.0057	.0057	.0076	.0090	.0062	.0046	.0046	.0066
BLOWING RATE 0	.0008	.0004	.0008	.0046	.0083	.0041										
BLOWING RATE 1	.0023	.0023	.0024	.0052	.0079	.0043										
BLOWING RATE 2	.0036	.0036	.0037	.0062	.0084	.0050										

MTR 1365

MAF PRESSURE AND GARDON DATA  
PRESSURE COEFFICIENT AT INDICATED TAP LOCATION

RUN 25	TYPE III															
	ALPHA - 5.															
	1A	1B	1C	1U*	1F	1F	2A	2A	2C	2C	2D	2E	2F	3A	3B	3F
BLOWING RATE 0	.0290	.0267	.0281	.0368	.0533	.0426	.0082	.0081	.0081	.0081	.0232	.0401	.0245	.0057	.0025	.0055
BLOWING RATE 1	.0324	.0321	.0377	.0795	.0646	.0481	.0205	.0243	.0254	.0254	.0399	.0541	.0313	.0206	.0198	.0241
BLOWING RATE 2	.0433	.0486	.0561	.0949	.0791	.0568	.0366	.0394	.0402	.0402	.0540	.0639	.0440	.0324	.0325	.0337
BLOWING RATE 0	.0057	.0033	.0064	.0350	.0624	.0310										
BLOWING RATE 1	.0171	.0169	.0179	.0384	.0584	.0320										
BLOWING RATE 2	.0258	.0256	.0263	.0442	.0597	.0356										

\*BAD GAGE

WTR 1365

MASK PRESSURE AND GASKON DATA  
QUOT AT INDICATED TAP LOCATION

RUN 25

TYPE III

ALPHA = 5.

	1A	2A	3A	4A	1H	2H	3H	4H	1C	2C	3C	4C
BLOWING RATE 0	.34	.23	.18	.17	.29	.15	.12	.08	0.00	.24	.18	.14
BLOWING RATE 1	.24	.09	.04	.04	.16	.02	.01	0.00	0.00	0.00	.01	0.00
BLOWING RATE 2	.11	.01	0.00	.01	.04	0.00	0.00	0.00	0.00	0.00	0.00	0.00
*												
BLOWING RATE 0	1D	2D	3D	4D	1F	2F	3F	4F	1F	2F	3F	4F
BLOWING RATE 1	0.00	.42	.41	.40	.66	.63	.53	.54	.43	.38	.27	.37
BLOWING RATE 2	0.00	.03	.06	.08	.30	.10	.20	.24	.28	.17	.12	.19
	0.00	0.00	0.00	.01	.12	.02	.06	.08	.13	.04	.03	.06

WTR 1365

MASK PRESSURE AND GASKON DATA  
STATION NUMBER AT INDICATED TAP LOCATION

	1A	2A	3A	4A	1B	2B	3B	4B	1C	2C	3C	4C
BLOWING RATE 0	1.13E-03	2.09E-03	1.68E-03	1.57E-03	2.68E-03	1.38E-03	1.09E-03	7.76E-04	0.	2.18E-03	1.67E-03	1.31E-03
BLOWING RATE 1	2.07E-03	6.44E-04	3.50E-04	3.37E-04	1.41E-03	1.47E-04	4.78E-05	1.59E-05	0.	7.87E-06	5.21E-05	3.54E-05
BLOWING RATE 2	1.07E-03	1.02E-04	4.26E-05	5.40E-05	4.15E-04	4.49E-05	1.68E-05	-2.21E-06	0.	-3.18E-05	-5.44E-06	-1.54E-05
*												
BLOWING RATE 0	1D	2D	3D	4D	1F	2F	3F	4F	1F	2F	3F	4F
BLOWING RATE 1	0.	3.87E-03	3.77E-03	3.73E-03	4.10E-03	5.83E-03	4.91E-03	4.95E-03	3.97E-03	3.53E-03	2.49E-03	3.43E-03
BLOWING RATE 2	0.	2.45E-04	5.24E-04	6.48E-04	2.58E-03	8.57E-04	1.72E-04	2.05E-03	2.44E-03	1.44E-03	1.00E-03	1.51E-03
	0.	-8.64E-06	3.93E-05	5.91E-05	1.09E-03	1.91E-04	5.70E-04	7.88E-04	1.22E-03	4.07E-04	2.44E-04	5.11E-04

\*BAD GAGE

WTR 1365

HASF PRESSURE AND GARDON DATA  
PRESSURE AT INDICATED TAP LOCATION

RUN 26	TYPE 111	ALPHA - 10.															
		1A	1B	1C	1D	1E	1F	2A	2B	2C	2D	2E	2F	3A	3B	3C	3F
FLOWING RATE 0		.0029	.0025	.0028	-.0719	.0125	.0078	.0002	.0003	.0002	.0063	.0144	.0068	.0002	.0002	.0004	.0210
FLOWING RATE 1		.0035	.0035	.0041	-.0546	.0148	.0086	.0018	.0022	.0021	.0078	.0151	.0072	.0014	.0015	.0014	.0206
FLOWING RATE 2		.0051	.0056	.0066	-.0460	.0166	.0095	.0034	.0037	.0038	.0095	.0162	.0078	.0026	.0027	.0026	.0209
FLOWING RATE 0		.0000	.0006	.0007	.0098	.0206	.0097										
FLOWING RATE 1		.0007	.0008	.0009	.0099	.0206	.0094										
FLOWING RATE 2		.0016	.0016	.0017	.0101	.0210	.0094										

A-28

WTR 1365

HASF PRESSURE AND GARDON DATA  
PRESSURE COEFFICIENT AT INDICATED TAP LOCATION

RUN 26	TYPE 111	ALPHA - 10.															
		1A	1B	1C	1D	1E	1F	2A	2B	2C	2D	2E	2F	3A	3B	3C	3F
FLOWING RATE 0		.0209	.0179	.0198	-.5132	.0889	.0555	.0011	.0023	.0014	.0451	.1025	.0481	.0016	.0012	.0026	.0595
FLOWING RATE 1		.0245	.0245	.0288	-.3835	.1036	.0604	.0123	.0152	.0150	.0548	.1056	.0505	.0100	.0104	.0098	.0631
FLOWING RATE 2		.0355	.0389	.0457	-.3214	.1161	.0665	.0239	.0260	.0268	.0662	.1130	.0543	.0184	.0187	.0183	.0655
FLOWING RATE 0		.0055	.0040	.0053	.0700	.1472	.0691										
FLOWING RATE 1		.0048	.0056	.0064	.0696	.1445	.0659										
FLOWING RATE 2		.0112	.0114	.0120	.0706	.1464	.0660										

\*BAD GAGE



WTR 1365

HASF PRESSURE AND GARDON DATA  
PRESSURE AT INDICATED TAP LOCATION

RUN 27	TYPE III																ALPHA - 20.			
	1A	1B	1C	1D	1E	1F	2A	2B	2C	2D	2E	2F	3A	3B	3C	3D	3E	3F	3G	3H
FLOWING RATE 0	.0011	.0012	.0009	.0354	.0487	.0172	.0013	.0003	.0014	.0188	.0430	.0207	.0009	.0011	.0010	.0179	.0454	.0181		
FLOWING RATE 1	.0025	.0029	.0027	.0048	.0437	.0177	.0001	.0007	.0004	.0185	.0425	.0201	.0003	.0002	.0001	.0190	.0449	.0182		
FLOWING RATE 2	.0035	.0038	.0042	.0006	.0452	.0182	.0011	.0016	.0016	.0195	.0431	.0200	.0004	.0005	.0008	.0201	.0455	.0191		
FLOWING RATE 0	.0004	.0013	.0006	.0180	.0467	.0179														
FLOWING RATE 1	.0004	.0008	.0001	.0182	.0457	.0178														
FLOWING RATE 2	.0001	.0002	.0006	.0189	.0456	.0178														

WTR 1365

HASF PRESSURE AND GARDON DATA  
PRESSURE COEFFICIENT AT INDICATED TAP LOCATION

RUN 27	TYPE III																ALPHA - 20.			
	1A	1B	1C	1D	1E	1F	2A	2B	2C	2D	2E	2F	3A	3B	3C	3D	3E	3F	3G	3H
FLOWING RATE 0	.0082	.0089	.0067	.2635	.2994	.1266	.0099	.0025	.0102	.1382	.3167	.1520	.0067	.0079	.0076	.1317	.3355	.1331		
FLOWING RATE 1	.0181	.0201	.0198	.0352	.3208	.1297	.0010	.0053	.0026	.1358	.3121	.1476	.0024	.0016	.0004	.1390	.3207	.1334		
FLOWING RATE 2	.0256	.0279	.0305	.0041	.3311	.1331	.0079	.0114	.0117	.1427	.3152	.1465	.0032	.0033	.0058	.1474	.3114	.1397		
FLOWING RATE 0	.0004	.0008	.0006	.1329	.3440	.1317														
FLOWING RATE 1	.0029	.0057	.0008	.1336	.3352	.1305														
FLOWING RATE 2	.0007	.0017	.0041	.1384	.3338	.1301														

\*BAD GAGE

WTR 1365

MASF PRESSURE AND GARDON DATA  
QUOT AT INDICATED TAP LOCATION

RUN 27

TYPE III

ALPHA = 20.

	1A	2A	3A	4A	1B	2B	3B	4B	1C	2C	3C	4C
BLOWING RATE 0	.24	.16	.14	.14	.14	.09	.09	.07	0.00	.17	.15	.12
BLOWING RATE 1	.17	.09	.06	.06	.05	.01	.01	0.00	0.00	.01	.00	.02
BLOWING RATE 2	.09	.04	.02	.02	.01	0.00	0.00	-.01	0.00	-.01	0.00	0.00
	*											
BLOWING RATE 0	10	20	30	40	1E	2E	3E	4E	1F	2F	3F	4F
BLOWING RATE 1	0.00	1.14	.95	.80	2.21	1.99	1.51	1.40	1.16	1.03	.75	.77
BLOWING RATE 2	0.00	.53	.52	.45	1.32	1.32	1.16	1.13	.97	.81	.62	.63
	0.00	.24	.24	.20	.62	1.12	.70	.71	.67	.53	.39	.42

WTR 1365

MASF PRESSURE AND GARDON DATA  
STANTON NUMBER AT INDICATED TAP LOCATION

	1A	2A	3A	4A	1B	2B	3B	4B	1C	2C	3C	4C
BLOWING RATE 0	1.98E-03	1.39E-03	1.19E-03	1.14E-03	1.17E-03	7.24E-04	7.34E-04	5.78E-04	0.	1.45E-03	1.30E-03	1.01E-03
BLOWING RATE 1	1.36E-03	7.56E-04	4.97E-04	4.68E-04	3.94E-04	4.44E-05	4.94E-05	-3.25E-05	0.	9.17E-05	1.96E-04	1.16E-04
BLOWING RATE 2	7.95E-04	3.55E-04	1.38E-04	1.42E-04	8.31E-05	-4.47E-05	-1.84E-05	-7.14E-05	0.	-1.09E-04	-3.73E-05	-2.12E-05
	*											
BLOWING RATE 0	10	20	30	40	1E	2E	3E	4E	1F	2F	3F	4F
BLOWING RATE 1	0.	9.59E-03	7.98E-03	6.71E-03	1.86E-02	1.64E-02	1.27E-02	1.18E-02	9.75E-03	8.49E-03	6.33E-03	6.44E-03
BLOWING RATE 2	0.	4.32E-03	4.26E-03	3.66E-03	1.08E-02	1.04E-02	9.51E-03	9.20E-03	7.90E-03	6.44E-03	5.04E-03	5.11E-03
	0.	2.17E-03	2.18E-03	1.83E-03	5.65E-03	1.02E-02	6.39E-03	6.43E-03	6.09E-03	4.90E-03	3.51E-03	3.74E-03

\*BAD GAGE



MAF PRESSURE AND GARDON DATA  
PRESSURE AT INDICATED TAP LOCATION

TYPE II

	1A	1B	1C	1D	1E	1F	2A	2B	2C	2D	2E	2F	3A	3B	3C	3D	3E	3F
FLOWING RATE 0	.0034	.0028	.0031	.0078	.0131	.0079	.0008	.0011	.0006	.006A	.0154	.0064	.0000	.0000	-.0001	.000H2	.010A	.000A1
FLOWING RATE 1	.0045	.0044	.0050	.0092	.0138	.0089	.0022	.0025	.0020	.0071	.0148	.0067	.0012	.0042	.0011	.0079	.01P7	.007A
FLOWING RATE 2	.006A	.0065	.0074	.0120	.0162	.0108	.0037	.0038	.0036	.0080	.0154	.0075	.0023	.0023	.0022	.0080	.01A2	.007A

	4A	4B	4C	4D	4E	4F
BLUING RATE 0	-.0002	.0000	-.0003	.0100	.0197	.0099
BLUING RATE 1	.0004	.0008	.0007	.0096	.0202	.0094
BLUING RATE 2	.0017	.0015	.0015	.0095	.0210	.0097

WASF PRESSURE AND GARDON DATA  
PRESSURE COEFFICIENT AT INDICATED TAP LOCATION

[illegible]

	4A	4B	4C	4D	4E	4F
BLOWING RATE 0	-.0016	.0001	-.0025	.0736	.1447	.0728
BLOWING RATE 1	.0064	.0059	.0087	.0693	.1454	.0677
BLOWING RATE 2	.0118	.0104	.0105	.0669	.1477	.0680

**#BAD GAGE**

WTR 1365

HASF PRESSURE AND GARDON DATA  
QUOT AT INDICATED TAP LOCATION

HUN 28	IYF II	ALPHA - 10.											
		1A	2A	3A	4A	1B	2B	3B	4B	1C	2C	3C	4C
BLOWING RATE 0		.29	.20	.16	.14	.21	.10	.07	.05	.29	.21	.16	.11
BLOWING RATE 1		.10	.05	.07	.05	.02	0.00	.01	0.00	.02	.03	.05	.04
BLOWING RATE 2		.02	0.00	.01	0.00	0.00	0.00	0.00	0.00	0.00	0.00	0.00	-.01
BLOWING RATE 0		.63	.59	.61	.60	1E	2E	3E	4E	1F	2F	3F	4F
BLOWING RATE 1		.14	.24	.35	.42	0.00	1.04	1.02	.77	.61	.55	.64	.60
BLOWING RATE 2		0.00	.05	.15	.23	0.00	.64	.41	.67	.34	.33	.47	.47

WTR 1365

HASF PRESSURE AND GARDON DATA  
STANTON NUMBER AT INDICATED TAP LOCATION

ALPHA - 10.													
		1A	2A	3A	4A	1B	2B	3B	4B	1C	2C	3C	4C
BLOWING RATE 0		2.66E-03	1.85E-03	1.46E-03	1.29E-03	1.92E-03	9.11E-04	6.25E-04	4.90E-04	2.59E-03	1.91E-03	1.44E-03	9.40E-04
BLOWING RATE 1		8.91E-04	4.40E-04	5.47E-04	3.89E-04	2.06E-04	3.23E-05	5.22E-05	3.13E-05	1.98E-04	2.28E-04	3.85E-04	3.07E-04
BLOWING RATE 2		1.64E-04	1.84E-05	1.16E-04	3.87E-05	-1.94E-05	-2.29E-05	1.15E-05	-1.01E-05	-2.14E-05	-9.29E-06	3.35E-05	-9.44E-05
*													
		1D	2D	3D	4D	1E	2E	3E	4E	1F	2F	3F	4F
BLOWING RATE 0		5.66E-03	5.30E-03	5.55E-03	5.40E-03	4.43E-06	9.41E-03	9.25E-03	7.00E-03	5.54E-03	4.94E-03	5.77E-03	5.40E-03
BLOWING RATE 1		1.17E-03	2.00E-03	2.91E-03	3.54E-03	2.66E-06	5.40E-03	6.85E-03	5.67E-03	2.83E-03	2.76E-03	3.92E-03	3.49E-03
BLOWING RATE 2		4.54E-06	4.96E-04	1.38E-03	2.11E-03	3.04E-07	2.54E-03	4.65E-03	4.29E-03	9.95E-04	1.24E-03	2.39E-03	2.74E-03

\*BAD GAGE

WTP 1365

MAF PRESSURE AND GARDON DATA  
PRESSURE AT INDICATED TAP LOCATION

RUN 29	TYPE II	ALPHA - 20.																	
		1A	1B	1C	1D	1E	1F	2A	2B	2C	2D	2E	2F	3A	3B	3C	3D	3E	3F
BLOWING RATE 0		.0014	.0015	.0013	.0158	.0436	.0173	.0014	.0004	.0011	.0202	.0463	.0207	.0005	.0004	.0004	.0188	.0467	.0193
BLOWING RATE 1		.0026	.0028	.0032	.0161	.0409	.0172	.0002	.0004	.0002	.0195	.0454	.0199	.0001	.0002	.0001	.0187	.0444	.0190
BLOWING RATE 2		.0044	.0041	.0050	.0180	.0403	.0175	.0011	.0013	.0014	.0197	.0460	.0197	.0005	.0004	.0005	.0193	.0444	.0190
		4A	4B	4C	4D	4E	4F												
BLOWING RATE 0		-.0007	-.0014	-.0008	.0187	.0482	.0186												
BLOWING RATE 1		.0000	-.0008	-.0001	.0186	.0472	.0184												
BLOWING RATE 2		.0005	-.0005	.0002	.0188	.0476	.0187												

A-34

WTH 1365

MAF PRESSURE AND GARDON DATA  
PRESSURE COEFFICIENT AT INDICATED TAP LOCATION

	1A	1B	1C	1D	1F	1F	2A	2B	2C	2D	2E	2F	3A	3B	3C	3D	3F
BLOWING RATE 0	.0100	.0106	.0091	.1117	.3076	.1219	.0098	.0025	.0075	.1426	.3271	.1459	.0037	.0056	.0043	.1330	.3271
BLOWING RATE 1	.0182	.0198	.0229	.1150	.2920	.1224	.0014	.0030	.0017	.1390	.3236	.1420	.0009	.0017	.0010	.1333	.3197
BLOWING RATE 2	.0311	.0293	.0355	.1279	.2867	.1242	.0076	.0091	.0102	.1400	.3266	.1401	.0039	.0027	.0015	.1371	.3176

\*BAD GAGE

WTP 1365 MASF PRESSURE AND GARDON DATA  
 QUOT AT INDICATED TAP LOCATION

NUM 29	TYPE II	ALPHA - 20.											
		1A	2A	3A	4A	1B	2B	3B	4B	1C	2C	3C	4C
BLOWING RATE 0		.24	.16	.15	.14	.14	.10	.09	.07	.23	.16	.15	.12
BLOWING RATE 1		.09	.07	.08	.05	.01	0.00	0.00	0.00	.03	.03	.01	.06
BLOWING RATE 2		.02	.01	.03	.01	-.01	-.01	-.01	0.00	0.00	0.00	.02	.02
BLOWING RATE 0		1D	2D	3D	4D	1E*	2E	3E	4E	1F	2F	3F	4F
BLOWING RATE 1		1.17	1.09	.86	.78	0.00	1.87	1.56	1.27	1.20	.99	.92	.78
BLOWING RATE 2		.58	.74	.63	.62	0.00	1.56	1.17	1.14	.87	.79	.78	.67
BLOWING RATE 2		.24	.40	.38	.40	0.00	1.08	.99	.84	.50	.51	.54	.47

WTH 1365 MASF PRESSURE AND GARDON DATA  
 STANTON NUMBER AT INDICATED TAP LOCATION

ALPHA - 20.													
		1A	2A	3A	4A	1B	2B	3B	4B	1C	2C	3C	4C
BLOWING RATE 0		2.04E-03	1.33E-03	1.26E-03	1.16E-03	1.23E-03	8.27E-04	7.20E-04	6.17E-04	1.98E-03	1.77E-03	1.24E-03	9.47E-04
BLOWING RATE 1		7.70E-04	5.50E-04	6.68E-04	4.41E-04	4.04E-05	2.46E-05	2.70E-05	1.97E-05	2.52E-04	2.74E-04	5.54E-04	4.41E-04
BLOWING RATE 2		1.66E-04	9.54E-05	2.76E-04	8.10E-05	-5.16E-05	-5.07E-05	-4.98E-05	-4.20E-05	-3.47E-05	-2.50E-05	1.74E-04	1.04E-04
*													
		1D	2D	3D	4D	1E	2E	3E	4E	1F	2F	3F	4F
BLOWING RATE 0		9.49E-03	9.29E-03	7.38E-03	6.68E-03	1.18E-06	1.60E-02	1.33E-02	1.08E-02	1.03E-02	8.45E-03	7.91E-03	6.71E-03
BLOWING RATE 1		4.48E-03	6.17E-03	5.24E-03	5.15E-03	1.85E-06	1.31E-02	1.14E-02	9.50E-03	7.27E-03	6.40E-03	6.55E-03	5.71E-03
BLOWING RATE 2		2.16E-03	3.65E-03	3.54E-03	3.72E-03	2.11E-06	9.90E-03	9.09E-03	7.76E-03	4.62E-03	4.69E-03	4.97E-03	4.34E-03

\*BAD GAGE

WTR 1365	RUN 30	MASF PRESSURE AND GAPDOOR DATA PRESSURE AT INDICATED TAP LOCATION															
		TYPE II															
		ALPHA = 35.															
		1A	1B	1C	1D	1E	1F	2A	2B	2C	2D	2E	2F	3A	3B	3C	3F
BLOWING RATE 0		-.0006	-.0004	-.0009	.0365	.1090	.0385	-.0013	-.0019	-.0011	.0381	.1019	.0383	-.0010	-.0020	-.0012	.0360
BLOWING RATE 1		.0005	.0008	.0008	.0370	.1094	.0389	-.0010	-.0002	.0391	.1036	.0390	-.0006	-.0045	-.0007	.0369	.1036
BLOWING RATE 2		.0019	.0016	.0026	.0392	.1138	.0405	.0004	-.0002	.0010	.0415	.1086	.0409	-.0001	-.0010	.0000	.0391
		4A	4B	4C	4D	4E	4F										
BLOWING RATE 0		-.0009	-.0021	-.0011	.0361	.1048	.0353										
BLOWING RATE 1		-.0007	-.0020	-.0010	.0366	.1064	.0363										
BLOWING RATE 2		-.0001	-.0018	-.0006	.0384	.1116	.0381										

WTR 1365	RUN 30	MASF PRESSURE AND GAPDOOR DATA PRESSURE COEFFICIENT AT INDICATED TAP LOCATION															
		TYPE II															
		1A	1B	1C	1D	1E	1F	2A	2B	2C	2D	2E	2F	3A	3B	3C	3F
BLOWING RATE 0		-.0046	-.0028	-.0066	.2597	.7747	.2735	-.0042	-.0137	-.0077	.2708	.7249	.2720	-.0070	-.0144	-.0086	.2559
BLOWING RATE 1		.0032	.0038	.0053	.2575	.7614	.2709	.0042	-.0070	-.0012	.2722	.7210	.2717	-.0045	-.0103	-.0046	.2568
BLOWING RATE 2		.0126	.0110	.0175	.2632	.7639	.2718	.0025	-.0014	.0048	.2784	.7289	.2745	-.0005	-.0065	-.0001	.2622
		4A	4B	4C	4D	4E	4F										
BLOWING RATE 0		-.0066	-.0151	-.0079	.2566	.7452	.2513										
BLOWING RATE 1		-.0051	-.0137	-.0068	.2547	.7405	.2525										
BLOWING RATE 2		-.0007	-.0119	-.0038	.2579	.7486	.2555										

\*BAD GAGE

WTK 1365

MASF PRESSURE AND GARDON DATA  
QUOT AT INDICATED TAP LOCATION

RUN JO	TYPE II										ALPHA = 35.			
	1A	2A	3A	4A	1B	2B	3B	4B	1C	2C	3C	4C		
BLOWING RATE 0	.19	.17	.15	.13	.12	.08	.06	.05	.18	.18	.15	.11		
BLOWING RATE 1	.10	.10	.10	.07	0.00	0.00	0.00	0.00	.05	.07	.09	.07		
BLOWING RATE 2	.03	.04	.05	.02	-.01	-.01	-.01	-.01	0.00	.01	.04	.03		
BLOWING RATE 0	1.94	1.40	1.21	1.12	0.00	2.92	2.43	1.95	2.01	1.31	1.33	1.10		
BLOWING RATE 1	1.46	1.14	1.05	1.04	0.00	2.73	2.40	1.94	1.83	1.19	1.28	1.07		
BLOWING RATE 2	.93	.73	.74	.76	0.00	2.05	1.82	1.48	1.31	.85	.95	.81		

WTK 1365

MASF PRESSURE AND GARDON DATA  
STANTON NUMBER AT INDICATED TAP LOCATION

TYPE II													ALPHA = 35.
	1A	2A	3A	4A	1B	2B	3B	4B	1C	2C	3C	4C	
BLOWING RATE 0	1.63E-03	1.46E-03	1.25E-03	1.13E-03	1.06E-03	7.06E-04	5.39E-04	4.66E-04	1.53E-03	1.53E-03	1.53E-03	1.53E-03	
BLOWING RATE 1	8.04E-04	8.11E-04	7.69E-04	5.57E-04	1.66E-05	3.02E-05	4.88E-06	1.35E-05	3.99E-04	5.86E-04	6.96E-04	5.86E-04	
BLOWING RATE 2	2.82E-04	3.66E-04	3.93E-04	1.92E-04	-0.61E-05	-5.40E-05	-5.38E-05	-5.47E-05	1.51E-05	1.01E-04	3.12E-04	2.74E-04	
	1D	2D	3D	4D	1E	2E	3E	4E	1F	2F	3F	4F	
BLOWING RATE 0	1.67E-02	1.21E-02	1.04E-02	9.60E-03	7.48E-06	2.51E-02	2.09E-02	1.68E-02	1.73E-02	1.13E-02	1.13E-02	9.50E-03	
BLOWING RATE 1	1.17E-02	9.13E-03	8.44E-03	8.33E-03	6.52E-07	2.19E-02	1.92E-02	1.55E-02	1.46E-02	9.50E-03	1.02E-02	9.50E-03	
BLOWING RATE 2	8.10E-03	6.35E-03	6.41E-03	6.64E-03	7.77E-06	1.78E-02	1.59E-02	1.29E-02	1.14E-02	7.79E-03	8.24E-03	7.07E-03	

\*BAD GAGE

WTR 1365

MASF PRESSURE AND GARDON DATA  
PRESSURE AT INDICATED TAP LOCATION

RUN 31	TYPE 4	ALPHA - 0.																	
		1A	1B	1C	1D	1E	1F	2A	2B	2C	2D	2E	2F	3A	3B	3C	3D	3E	3F
BLOWING RATE 0		.0035	.0037	.0040	.0029	.0030	.0935	.0039	.0044	.0025	.003A	.0021	.0037	.0047	.0048	.0044	.0049	.0055	.0046
BLOWING RATE 1		.0054	.0054	.0058	.0055	.0057	.0008	.0049	.0053	.0038	.0051	.0035	.0048	.0049	.0050	.0044	.0050	.0054	.0044
BLOWING RATE 2		.0071	.0071	.0077	.0076	.0079	.0080	.0065	.0070	.0059	.0070	.0056	.0065	.0058	.0059	.0055	.0061	.0064	.0057
BLOWING RATE 0		.0050	.0053	.0057	.0056	.0052	.0049												
BLOWING RATE 1		.0047	.0050	.0053	.0054	.0052	.0051												
BLOWING RATE 2		.0053	.0055	.0059	.0060	.0059	.0060												

A-38

WTR 1365

MASF PRESSURE AND GARDON DATA  
PRESSURE COEFFICIENT AT INDICATED TAP LOCATION

	* ALPHA - 0.																	
	1A	1B	1C	1D	1E	1F	2A	2B	2C	2D	2E	2F	3A	3B	3C	3D	3E	3F
BLOWING RATE 0	.0265	.0279	.0299	.0215	.0222	.7002	.0294	.0328	.0185	.0281	.0154	.0277	.0353	.0357	.0329	.0364	.0418	.0344
BLOWING RATE 1	.0394	.0401	.0424	.0408	.0420	.0045	.0360	.0392	.0280	.0379	.0260	.0352	.0357	.0370	.0326	.0364	.0411	.0353
BLOWING RATE 2	.0502	.0502	.0543	.0535	.0560	.0589	.0459	.0493	.0415	.0495	.0396	.0458	.0411	.0419	.0392	.0434	.0448	.0404
BLOWING RATE 0	.0371	.0395	.0426	.0422	.0390	.0365												
BLOWING RATE 1	.0349	.0371	.0391	.0397	.0381	.0377												
BLOWING RATE 2	.0375	.0391	.0416	.0422	.0415	.0424												

\*BAD GAGE

WTH 1365  
MASF PRESSURE AND GARDON DATA  
QUOT AT INDICATED TAP LOCATION

KUN 31	TYPE 4	ALPHA - 0.											
		1A	2A	3A	4A	1B	2B	3B	4B	1C	2C	3C	4C
BLOWING RATE 0	.57	.43	.39	.38	.52	.49		.42	.41	.54	.48	.43	.40
BLOWING RATE 1	.28	.26	.23	.23	.28	.26		.23	.22	.22	.20	.14	.18
BLOWING RATE 2	.11	.09	.08	.08	.09	.08		.07	.07	.05	.04	.04	.04
BLOWING RATE 0	1D	2D	3D	4D	1E	2E		3E	4E	1F	2F	3F	4F
BLOWING RATE 1	.48	.35	.44	.40	.52	.46		.45	.42	.47	.45	.45	.39
BLOWING RATE 2	.14	.01	.16	.15	.22	.19		.19	.14	.26	.23	.25	.22
	.02	-.13	.03	.03	.05	.04		.04	.04	.09	.07	.07	.07

WTH 1365  
MASF PRESSURE AND GARDON DATA  
STANTON NUMBER AT INDICATED TAP LOCATION

KUN 31	TYPE 4	ALPHA - 0.											
		1A	2A	3A	4A	1B	2B	3B	4B	1C	2C	3C	4C
BLOWING RATE 0	4.28E-03	3.94E-03	3.56E-03	3.44E-03	4.73E-03	4.46E-03		4.46E-03	3.84E-03	3.71E-03	4.43E-03	4.43E-03	4.43E-03
BLOWING RATE 1	2.40E-03	2.19E-03	1.94E-03	1.94E-03	2.40E-03	2.24E-03		2.24E-03	1.93E-03	1.88E-03	1.86E-03	1.86E-03	1.86E-03
BLOWING RATE 2	9.88E-04	8.35E-04	7.36E-04	7.35E-04	8.49E-04	7.28E-04		7.28E-04	6.41E-04	6.31E-04	6.45E-04	6.45E-04	6.45E-04
BLOWING RATE 0	4.40E-03	3.20E-03	4.00E-03	3.67E-03	4.75E-03	4.22E-03		4.22E-03	4.15E-03	3.81E-03	4.30E-03	4.30E-03	4.30E-03
BLOWING RATE 1	1.20E-03	1.11E-03	1.34E-03	1.31E-03	1.86E-03	1.61E-03		1.61E-03	1.65E-03	1.53E-03	2.23E-03	2.23E-03	2.23E-03
BLOWING RATE 2	7.00E-04	1.21E-03	2.67E-04	2.86E-04	4.57E-04	3.50E-04		3.50E-04	3.79E-04	3.72E-04	8.11E-04	8.11E-04	8.11E-04

\*BAD GAGE



WTP 1365

HASF PRESSURE AND GARDON DATA  
PRESSURE AT INDICATED TAP LOCATION

RUN 32	TYPE 4	ALPHA - 10.															
		1A	1B	1C	1D	1E	1F	2A	2B	2C	2D	2E	2F	3A	3B	3C	3F
FLOWING RATE 0		.0005	.0005	.0008	.0138	.0239	.2463	.0003	.0002	.0005	.0139	.0225	.0118	.0001	.0007	.000A	.0133
FLOWING RATE 1		.0013	.0017	.0016	.0126	.0227	.2189	.0007	.0011	.0012	.0138	.0222	.0118	.0008	.0007	.0014	.0135
FLOWING RATE 2		.0029	.0033	.0032	.0130	.0229	.1580	.0021	.0027	.0026	.0144	.0227	.0118	.0014	.0017	.0020	.0136
																	.0229
																	.0113
FLOWING RATE 0		.0000	.0008	.0009	.0125	.0234	.0111										
FLOWING RATE 1		.0010	.0068	.0017	.0128	.0233	.0110										
FLOWING RATE 2		.0012	.0015	.0020	.0130	.0237	.0113										

WTP 1365

HASF PRESSURE AND GARDON DATA  
PRESSURE COEFFICIENT AT INDICATED TAP LOCATION

RUN 32	TYPE 4	ALPHA - 10.															
		1A	1B	1C	1D	1E	1F	2A	2B	2C	2D	2E	2F	3A	3B	3C	3F
FLOWING RATE 0		.0039	.0037	.0059	.1004	.1745	.0000	.0019	.0012	.0038	.1014	.1641	.0864	.0005	.0054	.0057	.1654
FLOWING RATE 1		.0095	.0122	.0114	.0915	.1647	.0000	.0054	.0080	.0088	.1002	.1606	.0854	.0059	.0054	.0104	.0978
FLOWING RATE 2		.0213	.0242	.0234	.0941	.1652	.0000	.0154	.0192	.0188	.1043	.1643	.0856	.0104	.0125	.0146	.0986
																	.1657
																	.0819
FLOWING RATE 0		.0002	.0056	.0063	.0912	.1709	.0807										
FLOWING RATE 1		.0070	.0057	.0124	.0930	.1690	.0794										
FLOWING RATE 2		.0087	.0105	.0145	.0938	.1711	.0820										

\*BAD GAGE

WTP 1365

HASF PRESSURE AND GARDON DATA  
QUOT AT INDICATED TAP LOCATION

RUN 32	TYPE 4	ALPHA - 10.											
		1A	2A	3A	4A	1B	2B	3B	4B	1C	2C	3C	4C
BLOWING RATE 0		.28	.25	.23	.21	.13	.10	.08	.07	.36	.32	.28	.25
BLOWING RATE 1		.17	.16	.14	.14	.02	.01	.01	.01	.14	.13	.12	.12
BLOWING RATE 2		.07	.06	.07	.07	0.00	0.00	0.00	0.00	.03	.04	.02	.05
BLOWING RATE 0		.97	.65	.77	.69	1.42	1.23	1.14	1.05	.96	.81	.78	.66
BLOWING RATE 1		.60	.27	.56	.50	1.13	.99	.97	.91	.74	.63	.63	.55
BLOWING RATE 2		.29	-.07	.32	.29	.72	.64	.65	.60	.46	.40	.41	.35
BLOWING RATE 0		.97	.65	.77	.69	1.42	1.23	1.14	1.05	.96	.81	.78	.66
BLOWING RATE 1		.60	.27	.56	.50	1.13	.99	.97	.91	.74	.63	.63	.55
BLOWING RATE 2		.29	-.07	.32	.29	.72	.64	.65	.60	.46	.40	.41	.35

WTP 1365

HASF PRESSURE AND GARDON DATA  
STANTON NUMBER AT INDICATED TAP LOCATION

ALPHA - 10.													
	1A	2A	3A	4A	1B	2B	3B	4B	1C	2C	3C	4C	
BLOWING RATE 0	2.49E-03	2.24E-03	2.01E-03	1.85E-03	1.13E-03	9.27E-04	6.46E-04	6.21E-04	3.17E-03	2.45E-03	2.04E-03	2.14E-03	
BLOWING RATE 1	1.44E-03	1.33E-03	1.22E-03	1.17E-03	1.48E-04	1.07E-04	9.42E-05	8.25E-05	1.17E-03	1.13E-03	1.10E-03	1.01E-03	
BLOWING RATE 2	6.47E-04	6.13E-04	6.42E-04	6.32E-04	-1.10E-05	-1.10E-06	2.04E-05	2.04E-06	3.27E-04	3.49E-04	4.16E-04	4.44E-04	
	1D	2D	3D	4D	1E	2E	3E	4E	1F	2F	3F	4F	
BLOWING RATE 0	8.61E-03	5.75E-03	6.83E-03	6.12E-03	1.27E-02	1.09E-02	1.02E-02	9.32E-03	8.49E-03	7.40E-03	6.89E-03	5.44E-03	
BLOWING RATE 1	5.04E-03	2.27E-03	4.75E-03	4.23E-03	6.57E-03	8.41E-03	4.24E-03	7.47E-03	6.23E-03	5.38E-03	5.35E-03	4.64E-03	
BLOWING RATE 2	2.80E-03	-6.36E-04	3.09E-03	2.76E-03	6.66E-03	6.04E-03	6.23E-03	5.73E-03	4.38E-03	3.78E-03	3.97E-03	3.34E-03	

\*BAD GAGE

WTR 1365

HASF PRESSURE AND GARDON DATA  
PRESSURE AT INDICATED TAP LOCATION

RUN 33	TYPE 4	ALPHA - 20.															
		1A	1B	1C	1D	1E	1F	2A	2B	2C	2D	2E	2F	3A	3B	3C	3F
BLOWING RATE 0		.0002	.0007	.0006	.0555	.0562	.0112	.0010	.0013	.0002	.0400	.0537	.0222	.0005	.0015	.0000	.0213
BLOWING RATE 1		.0002	.0001	.0010	.0561	.0561	.0214	.0006	.0003	.0004	.0410	.0539	.0224	.0003	.0004	.0004	.0217
BLOWING RATE 2		.0010	.0010	.0018	.0574	.0569	.0146	.0001	.0005	.0012	.0423	.0546	.0228	.0001	.0002	.0004	.0221
BLOWING RATE 0		.0004	.0013	.0000	.0473	.0556	.0214										
BLOWING RATE 1		.0002	.0007	.0005	.0479	.0558	.0218										
BLOWING RATE 2		.0000	.0003	.0007	.0485	.0565	.0223										

WTR 1365

HASF PRESSURE AND GARDON DATA  
PRESSURE COEFFICIENT AT INDICATED TAP LOCATION

RUN 33	TYPE 4	ALPHA - 20.															
		1A	1B	1C	1D	1E	1F	2A	2B	2C	2D	2E	2F	3A	3B	3C	3F
BLOWING RATE 0		.0011	.0049	.0041	.3907	.3959	.0786	.0074	.0093	.0014	.2816	.3779	.1565	.0037	.0106	.0002	.3760
BLOWING RATE 1		.0017	.0006	.0072	.3889	.3895	.1508	.0040	.0024	.0030	.2843	.3737	.1557	.0018	.0054	.0029	.3760
BLOWING RATE 2		.0065	.0066	.0123	.3942	.3904	.1000	.0003	.0036	.0082	.2903	.3746	.1567	.0008	.0015	.0054	.3760
BLOWING RATE 0		.0027	.0095	.0001	.3331	.3915	.1506										
BLOWING RATE 1		.0013	.0047	.0033	.3324	.3872	.1513										
BLOWING RATE 2		.0000	.0022	.0049	.3332	.3879	.1531										

\*BAD GAGE

MAST PRESSURE AND GARDON DATA  
QUOT AT INDICATED TAP LOCATION

ALPHA - 20.

ALPHA - 20.

18  
10  
10  
10

1E	2.32	2.07
2.17		1.94

HASF PRESSURE AND GAKOON DATA  
STANTON NUMBER AT INDICATED TAP LOCATION

40-104  
CO-1  
A1

DD	IE
-03	1.95E-
-03	1.72E-
-03	1.40E-

WTH 1365

HASF PRESSURE AND GARDON DATA  
PRESSURE AT INDICATED TAP LOCATION

RUN 34	TYPE 4	ALPHA - 35.																	
		1A	1B	1C	1D	1E	1F	2A	2B	2C	2D	2E	2F	3A	3B	3C	3D	3E	3F
BLOWING RATE 0		.0007	-.0004	-.0010	.0406	.1110	-.0207	-.0002	-.0007	.0422	.1066	.0379	-.0003	-.0016	.0003	.0426	.1059	.0349	
BLOWING RATE 1		.0003	-.0003	-.0010	.0415	.1115	-.0131	-.0001	-.0003	.0437	.1077	.0386	.0000	-.0010	.0007	.0438	.1072	.0175	
BLOWING RATE 2		.0009	.0006	.0018	.0437	.1160	.0033	.0005	.0004	.0463	.1121	.0401	.0001	-.0006	.0000	.0454	.1105	.0390	
BLOWING RATE 0	4A		4B	4C	4D	4E	4F												
BLOWING RATE 1		-.0005	-.0018	-.0001	.0403	.1070	.0374												
BLOWING RATE 2		.0002	-.0009	.0009	.0417	.1088	.0379												

WTH 1365

HASF PRESSURE AND GARDON DATA  
PRESSURE COEFFICIENT AT INDICATED TAP LOCATION

WTH 1365	TYPE 4	ALPHA - 35.																	
		1A	1B	1C	1D	1E	1F	2A	2B	2C	2D	2E	2F	3A	3B	3C	3D	3E	3F
BLOWING RATE 0		.0049	-.0030	.0075	.3025	.8273	-.1564	-.0012	-.0054	.0016	.7946	.2827	-.0023	-.0120	.0020	.3180	.7894	.2744	
BLOWING RATE 1		.0025	-.0022	.0075	.3040	.8161	-.0947	-.0005	-.0022	.0031	.3199	.7888	.2823	-.0002	-.0072	.0052	.3208	.7845	.2743
BLOWING RATE 2		.0067	.0039	.0130	.3120	.8286	.0238	.0033	.0026	.0079	.3307	.8003	.2861	.0005	-.0044	.0060	.3240	.7811	.2785
BLOWING RATE 0	4A		4B	4C	4D	4E	4F												
BLOWING RATE 1		-.0034	-.0135	-.0009	.3003	.7981	.2792												
BLOWING RATE 2		.0016	-.0064	.0064	.3053	.7965	.2777												

\*BAD GAGE

WIR 1365

MASF PRESSURE AND GARDON DATA  
QDOT AT INDICATED TAP LOCATION

RUN 34	TYPE 4	ALPHA - 35.											
		1A	2A	3A	4A	1B	2B	3B	4B	1C	2C	3C	4C
BLOWING RATE 0	.22	.18	.15	.13	.07	.06	.05	.05	.05	.26	.22	.17	.15
BLOWING RATE 1	.17	.14	.11	.01	0.00	0.00	0.00	0.00	0.00	.15	.13	.11	.10
BLOWING RATE 2	.11	.08	.07	.06	0.00	0.00	0.00	0.00	0.00	.07	.06	.05	.05
BLOWING RATE 0	1.62	1.06	1.37	1.22	3.23	2.86	2.76	2.63	2.63	1.71	1.4A	1.44	1.22
BLOWING RATE 1	1.45	.80	1.29	1.16	3.28	2.87	2.83	2.70	2.70	1.69	1.43	1.43	1.24
BLOWING RATE 2	1.01	.33	.95	.86	2.54	2.18	2.20	2.08	2.08	1.31	1.10	1.11	.95

A-45

WIR 1365

MASF PRESSURE AND GARDON DATA  
STANTON NUMBER AT INDICATED TAP LOCATION

RUN 34	TYPE 4	ALPHA - 35.											
		1A	2A	3A	4A	1B	2B	3B	4B	1C	2C	3C	4C
BLOWING RATE 0	1.98E-03	1.64E-03	1.34E-03	1.23E-03	4.89E-04	5.97E-04	4.67E-04	4.43E-04	4.43E-04	2.39E-03	1.90E-03	1.60E-03	1.34E-03
BLOWING RATE 1	1.45E-03	1.18E-03	9.62E-04	9.19E-04	5.16E-05	3.47E-05	3.50E-05	3.25E-05	3.25E-05	1.28E-03	1.14E-03	9.55E-04	8.60E-04
BLOWING RATE 2	9.94E-04	7.74E-04	6.37E-04	6.08E-04	-7.29E-05	-3.37E-05	-2.21E-05	-2.43E-05	-2.43E-05	6.20E-04	5.73E-04	5.05E-04	4.44E-04
BLOWING RATE 0	1.50E-02	9.76E-03	1.26E-02	1.13E-02	2.94E-02	2.64E-02	2.54E-02	2.43E-02	2.43E-02	1.59E-02	1.36E-02	1.32E-02	1.13E-02
BLOWING RATE 1	1.24E-02	6.82E-03	1.11E-02	9.94E-03	2.80E-02	2.44E-02	2.42E-02	2.31E-02	2.31E-02	1.44E-02	1.22E-02	1.23E-02	1.07E-02
BLOWING RATE 2	9.59E-03	3.07E-03	9.00E-03	8.13E-03	2.40E-02	2.04E-02	2.04E-02	1.96E-02	1.96E-02	1.23E-02	1.04E-02	1.05E-02	8.94E-03

\*BAD GAGE

## DISTRIBUTION

	<u>Copies</u>		<u>Copies</u>
Director		Internal Distribution:	
Strategic Systems Project Office		K24 (M. Roberts)	25
Attn: SP-2722	5	E35	1
Department of the Navy		E431	9
Washington, D.C. 20390		E432	3
Defense Technical Information Center			
Cameron Station			
Alexandria, VA 22314	12		
Lockheed Missiles and Space Co.			
Attn: G. T. Chrusciel	1		
R. Nelson	1		
C. Louis	1		
W. Colman	1		
C. Lee	1		
L. Hull	1		
J. Mandeville	1		
P. O. Box 504			
Sunnyvale, CA 94806			
Lockheed Missiles and Space Co.			
Attn: Technical Information Center			
Center	1		
3251 Hanover St.			
Palo Alto, CA 94304			
Kaman Sciences Corp.			
Attn: Library	1		
Mr. F. Barbera	1		
Mr. P. Wells	1		
Mr. D. Foxwell	1		
Mr. J. Forkois	1		
1500 Garden of the Gods Road			
Colorado Springs, CO 80907			
Library of Congress			
Attn: Gift and Exchange Division	4		
Washington, DC 20540			